REGULATION OF EPITHELIAL-MESENCHYMAL TRANSITION AND DNA DAMAGE RESPONSES BY SINGLEMINDED-2s

A Dissertation

by

BRIAN LAFFIN

Submitted to the Office of Graduate Studies of
Texas A&M University
in partial fulfillment of the requirements for the degree of

DOCTOR OF PHILOSOPHY

August 2008

Major Subject: Toxicology

REGULATION OF EPITHELIAL-MESENCHYMAL TRANSITION AND DNA DAMAGE RESPONSES BY SINGLEMINDED-2s

A Dissertation

by

BRIAN LAFFIN

Submitted to the Office of Graduate Studies of
Texas A&M University
in partial fulfillment of the requirements for the degree of

DOCTOR OF PHILOSOPHY

Approved by:

Chair of Committee,	Weston W. Porter
Committee Members,	Robert C. Burghardt
	Stephen H. Safe
	Timothy D. Phillips
Intercollegiate Faculty Chair,	Robert Burghardt

August 2008

Major Subject: Toxicology

ABSTRACT

Regulation of Epithelial-Mesenchymal Transition and DNA Damage Responses by Singleminded-2s.

(August 2008)

Brian Laffin, B.S., Texas A&M University

Chair of Advisory Committee: Dr. Weston W. Porter

Virtually all signaling pathways that play key roles in development such as the transfroming growth factor (TGF)-beta, notch, and wnt pathways also influence tumor formation, implying that cancer is in a sense development gone awry. Therefore, identification and elucidation of developmental pathways has great potential for generating new diagnostic tools and molecular therapy targets. Singleminded-2s (SIM2s), a splice variant of the basic helilx-loop-helix / PER-ARNT-SIM (bHLH/PAS) transcriptional repressor Singleminded-2, is lost or repressed in approximately 70% of human breast tumors and has a profound influence on normal mammary development. In order to gain a better understanding of the mechanisms by which SIM2s restricts malignant transformation and progression in breast cancer, we depleted SIM2 RNA in MCF-7 cells using a retroviral shRNA system and examined gene expression and functional abilities of the SIM2-depleted MCF-7 cells (SIM2*i*) relative to a control MCF line expressing a non-specific "scrambled" shRNA (SCR). Depletion of SIM2 resulted in an epithelial-mesenchymal transition (EMT)-like effect characterized by increased

migration and invasion, altered morphology, and loss of epithelial markers concomitant with gain of mesenchymal markers. The root of this effect may be loss of SIM2-mediated repression of the E-cadherin repressor slug, as SIM2 is able to bind and repress transcription from the slug promoter, and slug expression is dramatically elevated in SIM2*i* MCF-7 cells. Consistent with the previously established role of slug in resistance to various cancer therapies, SIM2*i* cells are resistant to the radiomimetic doxorubicin and appear to have elevated self-renewal capacity under certain conditions. Intriguingly, SIM2 protein levels are elevated by treatment with DNA damaging agents, and SIM2 interacts with the p53 complex via co-regulation of specific p53- target gene such as p21/WAF1/CIP1. These results provide a plausible mechanism for the tumor suppressor activity of SIM2, and provide insight into a novel tumor suppressive transcriptional circuit that may have utility as a therapeutic target.

I dedicate this work to my son, Nathaniel W. Laffin, who brings me happiness in any situation

ACKNOWLEDGEMENTS

I would like to thank my advisor, Dr. Weston Porter, for his support, guidance and willingness to allow me to test my ideas. I would like to thank my committee members, Dr. Robert Burghardt, Dr. Stephen Safe and Dr. Timothy Phillips for doing whatever they could to assist me and giving generously of their time. I also thank Dr. Rick Metz and Elizabeth Wellberg for being the absolute best co-workers I can conceive of having. I appreciate the advice and hard work of our collaborators, Dr. Pepper Schedin, Dr. Mike Lewis, and Dr. Jeffrey Rosen. Finally, I would like to thank my wife, Teresa, and all my extended family, without whose support I could not have achieved the completion of this work.

NOMENCLATURE

AP-1	Activator protein-1
AHR	Aryl hydrocarbon receptor
ARNT	Aryl hydrocarbon receptor nuclear translocator
bHLH	Basic helix-loop-helix
C/EBPβ	CCAAT/enhancer binding protein, beta
ChIP	Chromatin immunoprecipitation
CME	Central midline element
DMBA	7,12-dimethylbenz[a]anthracene
DMEM	Dulbecco's modified Eagle's medium
DOX	Doxorubicin
DS	DS
DSL	Delta/Serrate/lag-2
E	Embryonic day
EGF	Epidermal growth factor
EGFR	Epidermal growth factor receptor
EMT	Epithelial-mesenchymal transition
ETS2	V-ets erythroblastosis virus E26 oncogene homolog 2
HIF1-α	Hypoxia-inducible factor 1 alpha
HIF2-α	Hypoxia-inducible factor 2 alpha
HRE	Hypoxia response element

IκB	Inhibitor of kappaB
IKK	Inhibitor of kappaB kinase
MAPK	Mitogen-activated protein kinase
NFκB	Nuclear factor-kappaB
NICD	Notch intracellular domain
PAS	Per-Arnt-Sim
PI3K	Phosphatidylinositol 3′-kinase
SIM1	Single-minded 1
SIM2	Single-minded 2
SIM2s	Single-minded 2, short isoform
TEB	Terminal end bud
TGFβ	Transforming growth factor beta
XRE	Xenobiotic response element

TABLE OF CONTENTS

CHAPTER Page

LIST OF FIGURES

FIGURE Page

LIST OF TABLES

CHAPTER I

INTRODUCTION

Breast cancer is the second most common malignancy in women and the second leading cause of cancer death in women, with an estimated 178,480 new cases of invasive disease and 62,030 cases of *in situ* disease along with approximately 40,460 deaths from breast cancer in 2007 American Cancer Society. Breast cancer retains its position as the second most common malignancy despite introduction of improved estimation methods, which have resulted in new case figures dramatically lower than the 2005 estimate. Early detection and new treatments have significantly improved the mortality rate of breast cancer patients, however, it is becoming increasingly clear that many current treatments simply diminish the bulk of the tumor without destroying the so-called tumor initiating cells the that are primarily responsible for tumor growth, invasion, angiogenesis, metastasis, and recurrence (1-5). This makes understanding the developmental pathways that are hijacked or dismantled by tumor-initiating cells to acquire de-differentiated stem cell-like properties critical to development of therapies that can truly destroy tumors. Understanding how these pathways function in normal development and the adult organism is also of great importance for creating targeted therapies that will cause the least of amount of suffering possible for the patient while delivering the maximum therapeutic effect.

This dissertation follows the style of *Cancer Research*.

1.1 Normal mammary gland development

The first morphological descriptions of mammary gland development were undertaken in the 1900s, proceeding through investigations of tissue interaction in the mammary placodes and young virgins glands in the 1960s up to the molecular studies of the present day (6, 7). The mammary gland has evolved in egg-laying synapsids during the Pennsylvanian epoch as a means of hydrating and nourishing thin-shelled eggs that would otherwise dry out (8, 9). In mammals, the ectoderm-derived mammary gland functions primarily to provide nutrients to offspring, but also confers immune protection through transfer of maternal antibodies to the young. The mammary gland develops in three distinct stages (Fig. 1), embryonic, pubertal, and adult, the latter two of which are under the control of circulating hormones and growth factors.

The embryonic stage of mouse mammary development begins with the formation of mammary placodes along the so-called “milk line”, which is defined by expression of Wnt10b (10). In female mice, the epithelium then condenses into bulb-like mammary buds at distinct locations on the milk line, while in male mice androgen acting on the mammary mesenchyme causes bud regression (11-13). The bulb elongates under control of interaction between parathyroid hormone related protein (PTHrP) and bone morphogenetic protein (BMP) signaling, invades into the fat pad beneath the skin, and forms a nipple with a lumen that opens to the skin (14). This PTHrP – BMP interaction also functions to suppress hair follicle development in the vicinity of the nascent gland, via induction of MSX2 (14). Invasion into the fat pad is led by dense epithelial structures called terminal end buds, or TEBs. TEBs, which appear at the tips of elongating mammary ducts in young virgin animals, consist of multiple layers of body cells

surrounded by a cap cell layer. Proliferation occurs exclusively in the cap cell layer, which expresses enzymes that facilitate fat pad invasion, leaving the elongating duct behind (15-17). Interaction between the TEB and the surrounding stroma guides invasion into the fat pad, and may also instruct clefting events that result in bifurcation ands trifurcations that in concert with side branching events give rise to the ductal tree.

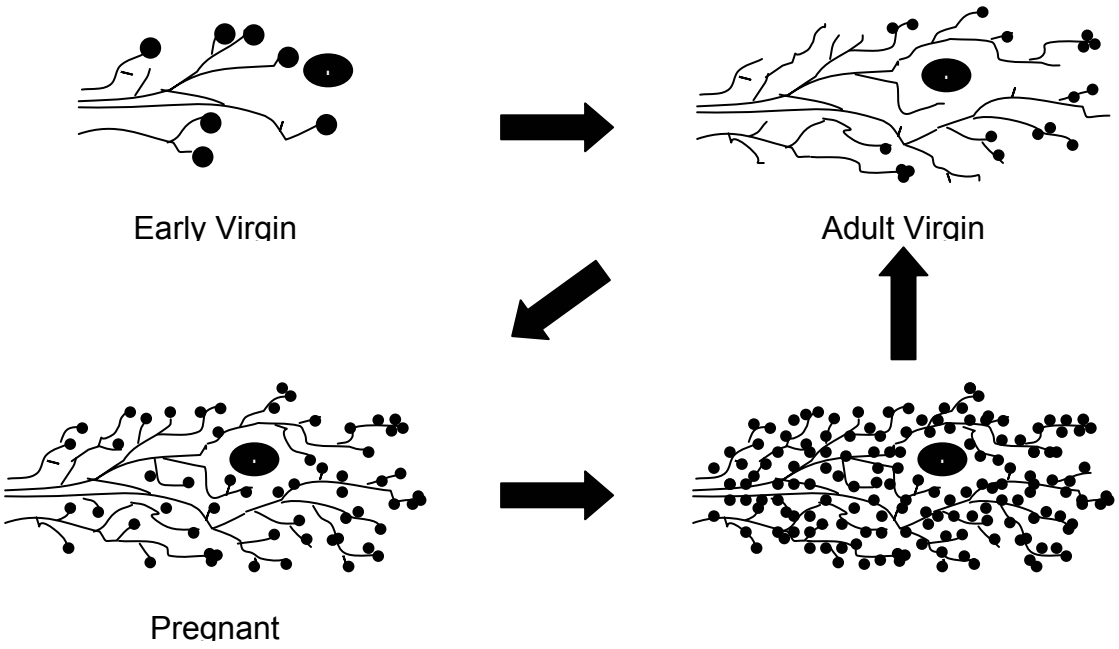

Figure 1 Post-natal mammary ductal tree morphology. TEB outgrowth in early virgin glands along with side branching events results in a ductal tree that reaches to the end of the fat pad in the adult virgin. Hormonal changes during pregnancy initiate the formation of lobuloalveolar units for milk production, which by the time of lactation have almost completely filled the fat pad. After pups are weaned, the gland returns to the pre-pregnant state via the process of involution.

This process, termed branching morphogenesis, occurs in many organs such as the lungs and kidneys (18, 19), suggesting that a conserved branching transcriptional module exists and is heavily involved in the execution of all developmental branching

processes. This branching module orchestrates expression of the tissue remodeling factors such as matrix metalloproteases (MMPs) that drive ductal extension and branching (15-17). Broad inhibition of MMPs does not block initial formation of lateral branches, but ductal extension appears to require MMP activity (15). MMP2 null mice display impaired ductal extension as expected (15), and extensive lateral branching in MMP2-/- glands suggests that MMP2 supresses lateral branching. Surprisingly, these effects appear to be mediated through effects on cell survival and proliferation within the TEB, despite localization of the MMP2 activator MMP14 at the tips of TEBs (15). MMP3 acts antagonistically to MMP2 and promotes lateral branching, as MMP3 null mice had greatly reduced numbers of branch points (15). However, the number of TEBs and duct length in MMP3 null mice was unchanged, implying that MMP3 is not involved in TEB invasion or bifurcation (15). Other factors can compensate for MMP3, as MMP3 null mice eventually catch up to wild type controls in ductal development (ref). Additionally, there is evidence that as the tree penetrates into the fat pad, morphogen gradients created by the geometry of the extending tree have a strong influence on branch point selection and the frequency of side branching (20). Growth of the mammary ductal tree slows or ceases altogether with the reaching of the end of the fat pad and puberty-associated rises in estrogen. Although elevated estrogen levels contribute to stopping ductal tree outgrowth, estrogen signaling is critical to virgin mammary development, as estrogen receptor-α (ERα) null mice lack TEBs and are deficient in ductal invasion into the fat pad (21, 22). This phenotype appears to be due in part to a lack of ERα -driven expression of the estrogen-responsive EGFR ligand amphiregulin, as the ductal phenotype of ERα, amphiregulin, and EGFR null mice are highly similar (23-26).

Amphiregulin function requires proteolytic release from the cell membrane by ADAM17/TACE, consistent with the phenotypic similarity of ADAM17-/- mice to ERα, amphiregulin, and EGFR null mice (27). Consistent with all of these observations, lack of mammary gland development in ovariectomized mice can be rescued by EGF or TGFα pellets, but not by insulin or albumin containing pellets (28). This demonstrates that circulating hormones exert their effects by driving expression of paracrine-acting growth factors. Apoptosis within the body cells left behind by invading TEBs has been proposed as the mechanism by which lumen formation occurs, and indeed, deletion of the pro-apoptotic protein Bim delays lumen formation significantly (29, 30). The ducts in Bim null mice eventually form lumens, demonstrating that functionally redundant apoptotic processes ensure eventual lumen formation. After puberty, estrogen cycling gives rise to waves of side-branch formation and apoptotic dieback, mimicking on a small scale the dramatic changes that occur during pregnancy, lactation, and involution. The amount of this estrous-related side branching that occurs varies widely between mouse strains, but can be quite extensive.

During pregnancy, the hormones progesterone and prolactin drive the gene expression and morphologic changes necessary to effect lactation, namely the formation and differentiation of alveolar subunits, where milk production occurs. Progesterone, through the action of its receptor, is a prime mover in the formation of side branches and alveolar units during pregnancy (31). Progesterone also acts in concert with prolactin (PRL) signaling through the prolactin receptor to promote differentiation of the alveolar cells, which produce the large quantities milk needed during lactation (31, 32). During

lactation, PRL-induced phosphorylation of STAT-5 and subsequent milk protein mRNA transcription interact with translational control mechanisms to generate elevated amounts of caseins and other milk proteins, resulting in production of up to 5 mL of milk per day (33-39). As the offspring grow and are weaned, milk accumulation triggers involution, a cell death and fatty tissue regeneration process that returns the gland to its pre-pregnant state. Involution occurs in two distinct stages which are defined by the point at which suckling is no longer able to reverse the involution process (40). The first, reversible stage lasts roughly 48 hrs and characterized by decreased expression of pro-survival proteins and increased expression of pro-apoptotic proteins (41). The second, irreversible stage starts with clearance of apoptotic cells and excess milk by the epithelium followed by macrophage and MMP-mediated tissue remodeling that reverses the pregnancy-associated epithelial expansion as the animal resumes estrous cycling (40, 42). In addition to the radical changes in the epithelium of the mammary gland during pregnancy and lactation, the extracellular matrix (ECM) simultaneously undergoes dynamic changes that contribute to mammary gland function and affect the phenotype of pregnancy-associated breast cancer (43, 44).

1.2 The history of breast cancer and chemotherapy

Breast cancer was one of the first tumors to be described in ancient medical writings. The Edwin Smith Papyrus, which is the earliest known medical writing of any kind, was written around 1600 BC and describes 8 cases of breast ulcers or tumors in humans, one of whom was a man. While Egyptian doctors were sometimes able to remove the tumors by cauterizing them with an instrument called a “fire drill”, the

disease was essentially incurable at that time. This state of knowledge and care for breast cancer patients remained largely unchanged for centuries, until the work of Jean Louis Petit and Benjamin Bell in the early 18th century. Bell and Petit were the first to advocate removal of surrounding tissue, lymph nodes, and muscle in addition to the tumor mass itself to combat recurrence and metastasis. Their work was continued and expanded upon by Dr. William Halsted, who performed the first complete mastectomy in 1882. The procedure that bears his name, the Halsted radical mastectomy, is still performed to this day. Breast cancer treatment took its next major step forward in 1946. The port-mortem observation of lymphoid and myeloid depletion in persons exposed to nitrogen mustard gas led to seminal work by Goodman, Gilman, and Linskog which demonstrated that lymphomas could be shrunk by injection of nitrogen mustard compounds and established the feasibility of cancer chemotherapy (45, 46). In 1952 the first major contribution to improving the mental well being of breast cancer patients and survivors was made by Terese Lasser when she founded the Reach to Recovery program (47). Reach to Recovery employs trained volunteers, many of whom are mastectomy patients and cancer survivors, to provide emotional support and guidance to breast cancer patients and help them to maintain their feeling of personal dignity. This program and others like it have raised awareness of the devastating impact cancer has on a patient's entire life and had a profound positive impact on the quality of life had by breast cancer patients and survivors.

Additional steps forward in cancer therapy such as the discovery of the anticancer activity of antifolates, 6-mercaptopurine, and vinca alkaloids led congress to establish the

National Cancer Chemotherapy Service Center (NCCSC) at the National Cancer Institute (NCI) in 1955. The NCCSC was the first federal program promoting cancer drug discovery, and generated numerous animal models and cell lines in its pioneering drug development efforts, leading to the relatively rapid development of additional chemotherapeutic drugs such as the taxanes in 1964 and camptothecins in 1966. Cisplatin and Tamoxifen were also discovered during this time, but were not approved for use in human cancers until the 1970s. 1965 saw a major paradigm shift in cancer chemotherapy: contemplating the problem of mutation-induced drug resistance in tumors, James Holland, Emil Freireich, and Emil Frei extrapolated the multi-drug treatment regimens used to treat tuberculosis to treatment of leukemias by simultaneously administering methotrexate, vincristine, 6-mercaptopurine (6-MP) and prednisone— together referred to as the POMP regimen — and induced long-term remissions in children with acute lymphoblastic leukaemia (ALL). Bernard Fisher and Gianni Bonadonna independently followed this and additional work by Dr. Frei in osteosarcomas by showing that adjuvant chemotherapy after complete surgical resection of breast tumours significantly extended survival — particularly in more advanced cancer (48, 49).

From the 1970s to the 1990s, several other classes of drugs were developed such as the anthracyclines, nitrosoureas, and epipodophyllotoxins, as well as supporting therapies such as anti-nausea drugs. With the advent of genomics, proteomics, and other high-throughput techniques, knowledge of tumor signaling networks has exploded to the point that therapies that target specific weak points of tumors with greatly reduced damage to normal tissue are now possible. Examples of this are tyrosine kinase inhibitors

such as imatinib, which specifically targets the oncogenic fusion protein BCR-ABL, and humanized antibodies such trastuzumab, which inactivates the product of the HER2/neu oncogene in breast tumors (50, 51). The promise of these targeted therapies makes understanding tumor signaling networks of the utmost importance, so as to elucidate new targets and create the most possibilities for combination therapies in the infinitely heterogeneous tumor signaling networks encountered in patients.

1.3 Types and subtypes of breast cancer

Breast cancer is a remarkably heterogeneous disease, with well over 50 types and subtypes of invasive disease currently recognized by the World Health Organization (52), a summary of which appears in Table 1(53-102) (103). Invasive ductal carcinomas represent the vast majority of breast tumors (52). While these tumors fall into the same category histologically, they are quite variable in clinical behavior, underscoring that these tumors cannot be broadly treated in the same way as might be warranted in rarer subtypes that have a more uniform set of genetic abnormalities. Groundbreaking work by Perou et al (104) and Sorlie et al (105) has provided a new approach to the problem posed by the morphologic similarity and behavioral heterogeneity of invasive ductal carcinomas. These studies demonstrated that gene expression profiling could sort invasive ductal carcinomas into 5-6 molecular subtypes - luminal A, luminal B, luminal C, normal breast-like, HER2 overexpressing, and basal-like – and that these groupings had significant predictive value for patient outcome. Luminal subtype may be viewed as a subset of luminal B tumors. Abbreviated molecular definitions of these subtypes and their relative prognosis is presented in table 2.

Table 1. Types and subtypes of invasive breast carcinomas.

Type / Subtype	Frequency	Prognosis	Description / characteristics
Invasive ductal carcinoma (not otherwise specified)	35-50%	—	Generally ER-positive, Epithelioid
Basal-like carcinoma	7-20%	Poor	Expression of high-molecular weight cytokeratins 5, 14 and 17, Triple negative (ER, PR, p53)
Mixed type carcinoma	<1%	Varies	Varies widely
Pleomorphic carcinoma	<1%	Poor	Frequent E-cadherin gene inactivation / LOH
Carcinoma with osteoclastic giant cells	<1%	Good	Osteoclastic giant cells present in stroma surrounding tumor
Carcinoma with choriocarcinomatous features	<1%	Poor	Elevated human chorionic gonadotropin-β expression, presence of multinucleated syncytiotrophoblast-like giant cells
Invasive lobular carcinoma	10%	Similar	Small, "lens-like" nuclei, mucin-filled acini. Rows of cells sandwiched between collagen fascicles, poorly defined margins
Tubular carcinoma	5%	Good	Highly differentiated, Low recurrence rate, low potential for metastasis, Generally ER positive
Invasive cribriform carcinoma	<1%	Good	Mucin positive, laminin negative cystic appearance. Luminal epithelial ultrastructural appearance.
Medullary carcinoma / Atypical medullary carcinoma	6%	Good	Predominant syncytial growth pattern, featuring broad anastamosing sheets, microscopically complete circumscription, marked mononuclear stromal infiltrate, nuclear grade II or III.
Mucinous carcinoma	<5%	Good	Monomorphic ductal epithelial tumor cells "floating" in abundant background mucin pool, comprising more than 90% of tumor. Low rate of metastatis, generally hormone receptor positive.
Cystadenocarcinoma and columnar cell mucinous carcinoma	<1%	Good	Predominantly tall, columnar mucinous epithelium. Presence of both intracellular and extracellular mucin
Signet ring cell carcinoma	<1%	Poor	Abundant intracellular mucin. Metastasis to the peritoneum, gastrointestinal tract, lung, and gynecologic organs.
Neuroendocrine tumors	<1%	Varies	Positive IHC for neuroendocrine markers. Small cell / oat cell carcinoma is the most agressive type.
Invasive papillary carcinoma	<1%	Good	Fibrovascular stromal core lined by epithelial and myoepithelial cells, attached to the wall of the duct and extending into the duct lumen
Invasive micropapillary carcinoma	<1%	Poor	Micropapillary epithelial architecture surrounded by lymphatic duct–like empty space. Aggressive behavior with frequent lymph node metastasis
Apocrine carcinoma	<1%	Good	ER, PR negative. Elevated expression of Androgen Receptor, psoriasin, S100A9, and p53. Low proliferative index.
Metaplastic carcinomas	<1%	Poor	Tumor cells display differentiation along multiple lineages. Generally aggressive clinical course, haematogenous metastasis pattern (lung and bone).
Squamous cell carcinoma	<1%	Poor	Presence of cells with squamous differentiation forming a keratinizing tissue, frequent lymph node metastasis, rapid growth

All WHO-recognized histological types and subtypes for which there is sufficient published data to make statements about prognosis are shown. Prognosis shown is relative to not otherwise listed invasive ductal carcinomas.

Table 1, Continued.

Type / Subtype	Frequency	Prognosis	Description / characteristics
Adenosquamous carcinoma	<1%	Similar	Combination of glandular and squamous differentiation
Mucoepidermoid carcinoma	<1%	Good	Nesting pattern with multiple well-circumscribed squamous nests containing numerous clear cells. Prominent mucin-secreting component frequently present. Myoepithelial differentiation common.
Mixed epithelial/mesenchymal metaplastic carcinomas	<1%	Poor	Tumor cells display epithelial (carcinoma) and mesenchymal (sarcoma) differentiation. Generally agrgressive clinical course.
Secretory carcinoma	<1%	Good	Frequent presence of oncogenic ETV6-NTRK3 fusion kinase. Most common in children.
Glycogen-rich clear cell carcinoma	<1%	Poor	Finely granular eosinophilic cytoplasm or foamy to clear cytoplasm with well-defined cytoplasmic membranes, moderate to marked nuclear pleomorphism with prominent nucleoli
Inflammatory carcinoma	<10%	Poor	Presence of skin erythema and oedema. Rapidly growing tumors that are highly angiogenic, angio-invasive, numerous tumour emboli filling the dermal lymphatics causing inflammatory signs
Myofibroblastoma	<1%	Good	Densely packed large cells with a solid or trabecular growth pattern, focally arranged in nests, with abundant eosinophilic glassy cytoplasm and sharp cellular borders. Large and round nuclei, prominent nucleoli. P63 and vimentin positive.
Inflammatory myofibroblastic tumor	<1%	Good	Large cohesive sheets of histiocytes intermingled with clusters of spindle cells and mixed inflammatory cells. Lack of granulomas and ductal epithelial cells.
Granular cell tumor	<1%	Good	Granular cytoplasm. Fat necrosis, duct ectasia.
Neurofibroma	<1%	Good	Schwann cell origin. Composed of spindle cells with thin, often wavy nuclei. S100 positive, generally well-circumscribed.
Schwannoma	<1%	Good	S100 positive. Compact and spongy biphasic pattern, nuclear palisading, interlacing bundles of numerous elongated spindle shaped cells.
Angiosarcoma	<1%	Poor	Rapid growth. Malignant endothelial cells lining vascular channels are flat, and most nuclei are pale and small. Contains anastomosing vascular channels that surround and invade lobules.
Liposarcoma	<1%	Variable	Mature adipocytic proliferation, variable cell size, focal nuclear atypia of adipocytes and stromal cells.
Osteosarcoma	<1%	Poor	Osteoid production present. Broad eosinophilic seams were that may display mature bone formation. Frequent mitoses, early recurrence, haematogenous metastasis pattern (lung and bone).
Leiomysarcoma	<1%	Similar	Pleomorphic spindle cells, hyperchromatism and elongated nuclei, eosinophilic cytoplasm, large nucleoli and numerous mitoses.

In addition to their prognostic value, these classifications have implications for targeted therapies that will grow more important as understanding of tumor signaling pathways increases. Indeed, larger, more refined gene expression profiling studies centered around analysis of kinase gene expression can not only differentiate the subtypes previously described, but predict prognosis within the luminal A subtype (106). Many of these kinases, which were selected in an unbiased fashion for their ability to discriminate between the subtypes, are already therapeutic targets under investigation while others are potential targets.

Table 2. Molecular subtypes of invasive ductal carcinoma.

IDC subtype:	**Highly expressed genes:**	**Weakly expressed genes:**	**Average relative prognosis**
Normal breast-like	Adipose tissue genes Basal epithelial genes	Luminal epithelial genes	Good
Luminal A	ERα Gata-3 TFF3 Keratin 8/18 Luminal epithelial genes	Basal epithelial genes Non-epithelial genes	Best
Luminal B	Luminal epithelial genes	ER cluster (moderate expression)	Average
Luminal C	Luminal epithelial genes Subset of basal epithelial genes of unknown function	ER cluster (moderate expression)	Poor
Basal-like	Keratin 5 Keratin 17 FABP7 Laminin	ER cluster PR ERBB2 cluster	Worst
ERBB2+	ERBB2 Others in ERBB2 amplicon	ER cluster	Poor

1.4 Basal-like carcinomas

Basal-like carcinomas are a subset of invasive ductal carcinomas that consistently have the poorest prognosis of all breast carcinomas whether grouped by histological appearance or molecular signature (104, 106-108). Basal-like carcinomas are also more aggressively metastatic than other invasive ductal carcinomas (109, 110). While recent studies have provided a fairly robust molecular definition for basal-like carcinomas, tumors displaying basal / myoepithelial differentiation were first described in the 1970s (111, 112). The basal phenotype is defined histologically by pushing margins, frequent central necrosis and lymphatic infiltrate, expression of high molecular weight keratins such as 5, 14 and 17, overexpression of EGFR / HER1, and frequently triple negative status for ER, PR, and ERBB2 / HER2 (113, 114). On the molecular level, basal-like breast carcinomas frequently feature inactivation of the Rb tumor suppressor pathway, up-regulation of slug and other EMT-like changes (113-117). These abnormalities are frequently present in the *in situ* lesion (118-120), and may explain why basal-like carcinomas are highly sensitive to some treatments despite their poor prognosis (121, 122). It has been proposed that basal-like carcinoma may have a more stem-cell-like phenotype, due to the significant overlap in their respective gene expression profiles (114, 123, 124). However, there is no published evidence that basal-like carcinomas have functionally greater stem cell capacity than luminal tumors, and the basal phenotype has an inverse correlation with some stem cell markers (108). Basal-like tumors have a more consistent pheontype in terms of metaplastic EMT-like elements. While the relevance of strictly-defined EMT to human breast carcinogenesis remains controversial (125), evidence is mounting that transient EMTs or EMT-like events are real phenomena that

are associated with metastasis, invasion, disease progression (114, 117, 126-132). These findings challenge assumptions made about the biology of basal-like carcinomas, and demonstrate the need for additional study into their molecular origins to develop targeted therapies and animal models for basal-like tumors, which are thus far confined to BRCA1 models (133, 134).

1.5 Epithelial-mesenchymal transition

The importance of epithelial-mesenchymal transitions in embryonic development has been appreciated since work done in the laboratory of Elizabeth Hay in 1967 (135), when the role of EMT in gastrulation was established. Since that time, multiple studies have revealed a crucial role for EMT in the patterning of multiple mature and embryonic tissues including the heart, palate, and neural crest (136-139). During gastrulation, epiblast cells ingressing through the primitive groove undergo EMT and migrate into the blastocoel to form the mesoderm (140), until Noggin-mediated suppression of BMP signaling halts gastrulation (138). Blockage of EMT via disruption of BMP signaling leads to failure in either mesoderm or neural crest formation (141-143), demonstrating the centrality of EMT to these processes. During heart development, endocardial cushion mesenchyme formation occurs via EMT in cells residing in the atrioventicular (AV) canal, which invade into the underlying cardiac jelly and form the septal and valvular primordia via process dependent upon cross talk between the TGF-beta and Notch pathways (144-149). TGF-beta3 induced EMT is necessary for palate fusion, and involves induction of a LEF1-Smad2-Smad4 transcriptional complex that represses E-cadherin and up-regulates vimentin and fibronectin in a beta-catenin independent fashion

(137, 150-153). A central feature of EMT during gastrulation and other developmental events, as well as in pathological EMTs, is loss or suppression of E-cadherin and other epithelial adhesion molecules (127-130, 137, 139, 154-158) and acquisition of mesenchymal markers such as vimentin and N-cadherin (131, 159-162). These gene expression changes have functional consequences as in the case of cadherins, which have different adhesion strengths that can affect invasion and metastasis (163).

EMT is thought to be associated with the most aggressive cancers (117), and is likely to be more heterogenous in manifestation than EMTs in developmental settings, leading to the proposal that EMT-like events in tumor cells generate "metastable" cells that are an abnormal blending of epithelial and mesenchymal phenoypes and transcriptomes (164). This hypothesis is supported by the involvement of EMT-related factors in the metastasis of epithelioid cancers (126, 127, 162, 165-170), the similarity in phenotype of metastatic nodules to the parent tumor (171), and the dynamic EMT-MET processes known to be involved in bladder and colorectal cancer metastasis (172-175). These observations suggest that metastatic cells must shed enough of their epithelial nature to escape their tissue of origin, but retain the abilty to become epithelioid once again to facilitate extravasation and survival in the new tissue.

Transcriptional control of EMT is complex, and in developmental settings typically begins with receipt of local molecular signals such as TGF-beta receptor ligands (141-143, 147) Wnts (176, 177), FGFs (178-181), and Notch ligands (149). TGF-beta and BMP signaling results both in broad chromatin remodeling via HMGA2 (182, 183)

and the assembly of numerous transcriptional complexes on pro-EMT gene promoter regions. These complexes include, but are not limited to Smad/LEF, Ets1, FoxC2, and MRTF-containing complexes, which drive expression of genes that suppress E-cadherin and other epithelial proteins while upregulating those associated with mesenchyme (137, 152, 184-187). The list of E-cadherin repressors is long and includes Snail family members, Twist, Zeb proteins, EZH2, and E47 proteins, as well as many others, which are thought to act in concert *in vivo* to effect E-cadherin repression (127-129, 161, 182, 188). One or more of these proteins are the eventual targets of all EMT-promoting signaling pathways.

1.6 Transforming growth factor (TGF)-beta signaling

TGF-β signaling (Fig. 2) begins with the synthesis of one of 30 or more TGF-β superfamily preprotein dimers, all of which must be proteolytically processed to be secreted (189). The TGF-β superfamily includes bone morphogenetic proteins (BMPs), TGF-β s, activin beta-chains, growth and differentiation factors (GDFs), and the protein nodal of which are typically secreted as homodimers, although some members can form heterodimers (190, 191). While most TGF-β superfamily members can be proteolytically processed after secretion, only GDF8, GDF11, and the TGF-β s require post-secretion processing to initiate signal transduction, which is performed by proteases such as BMP1, MMP2, MMP14, plasmin, or elastase (192-195). TGF-β s are secreted in a form known as the large latent complex, in which TGF-β and its prodomain are bound by latent TGF-β binding proteins (LTBPs) and subsequently targeted to the ECM (193). After secretion

and in some cases proteolytic release of the mature, active ligand, TGF-β superfamily members bind their cognate receptors and induce formation of heterotetrameric

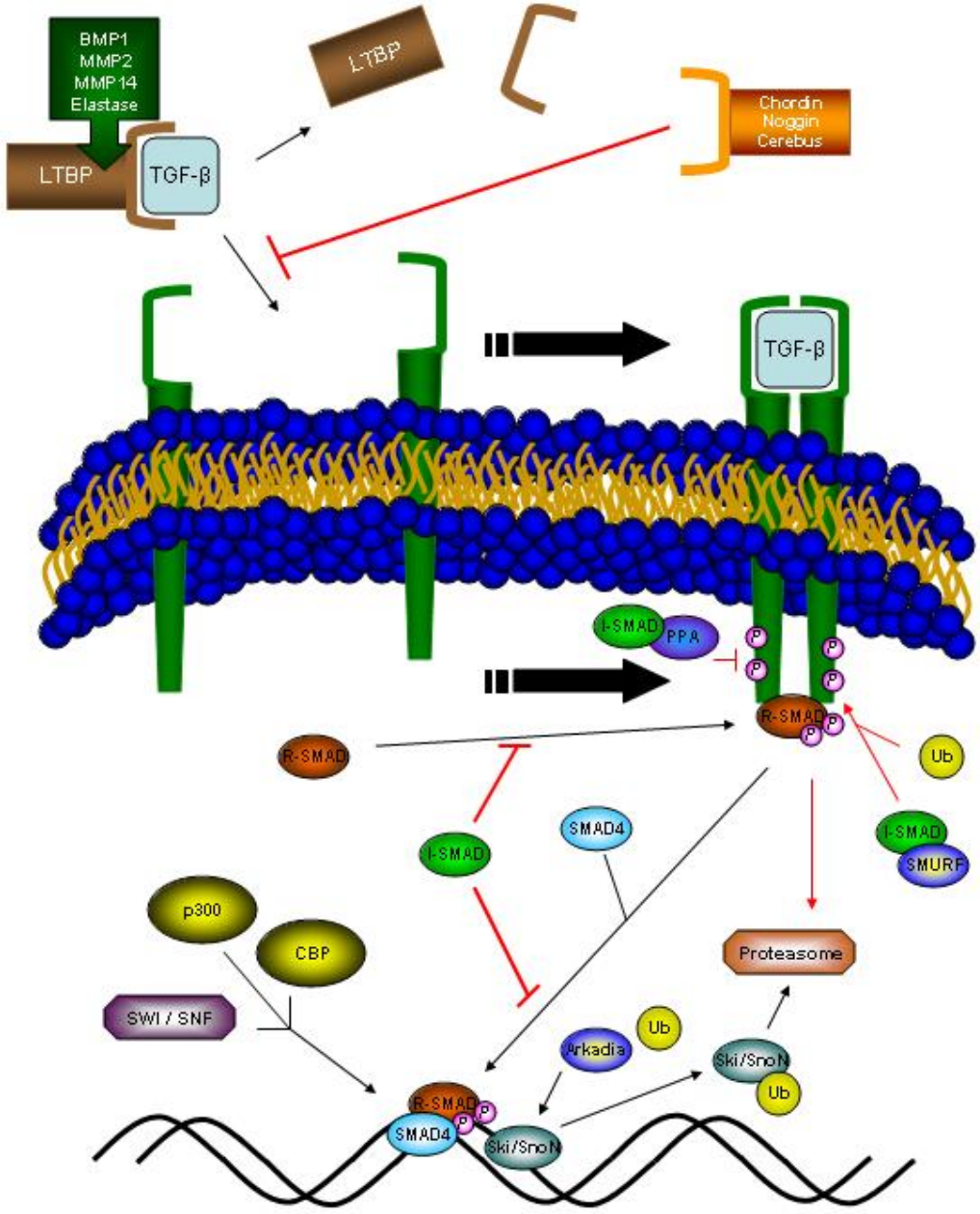

Figure 2. TGF-β - SMAD signaling. TGF-β in its latent form is proteolytically cleaved and released for receptor binding by one of several proteases, and can be sequestered by ligand binding antagonists such as Noggin. Receptor-bound TGF-β triggers clustering and auto-phosphorylation of type I and type II TGF-β receptors, which phosphorylate and activate R-SMADs causing interaction with SMAD4 and nuclear translocation. Activate SMAD complexes displace the Ski/SnoN repressors, which are targeted to the prpteasome by the ubiquitin ligase Arkadia. The SMAD complex then recruits co-regulatory proteins such as SWI/SNF, p300, and CBP to effect target gene activation and repression. I-SMADs inhibit the TGF-β at multiple points, including blocking association of R-SMADs with active TGF-β receptors and target gene promoters, promotion of receptor de-phosphorylation via recruitment of phosphatases, and targeting of active R-SMADs and receptors for degradation via the ubiquitin ligase SMURF.

complexes that then activate through autophosphorylation (196-198). These tetrameric complexes form from preexisting dimers of type I and type II TGF-β receptors, whereupon the constitutively active type II receptor dimer activates the type I receptor via phosphorylation (197, 198). TGF-β pathway activation can be stifled at this level by ligand-sequestering antagonists such as Chordin, Noggin, and Cerebus, which can either modulate the TGF-β signal strength or block it altogether. Activated receptor complexes recruit and activate members of the SMAD family of transcription factors (SMADs 1, 2, 3, 5 and 8), which upon phosphorylation by the receptor complex are able to interact with SMAD4, the common binding partner of all receptor-regulated SMADs. Individual SMADs are recruited by specific type I TGF-β receptors; SMADs 1, 5, and 8 are phosphorylated by ALK1, 2, 3, and 6, while SMADs 2 and 3 are phosphorylated by ALK4, 5, and 7. SMAD complexes can act as transcriptional activators or repressors, depending upon phosphorylations and other modifications to SMADs that determine which proteins are recruited to target promoters. All SMADs with the exception of SMAD2 directly bind DNA, but are unable to recruit the basal transcriptional machinery, and act via chromatin remodeling enzymes such as SWI-SNF, p300, and CBP. In the absence of TGF-β pathway activation, SMAD response elements are often occupied by the transcriptional repressors SKI and SNON, which are rapidly degraded by the ubiquitin ligase Arkadia to allow for SMAD binding.

In addition to the receptor associated SMADs and the co-SMAD, SMAD4, the inhibitory SMADS (I-SMADs) SMAD6 and SMAD7 provide feedback inhibition for TGF-β signaling. I-SMADs are induced by R-SMAD transcriptional activity and

attenuate TGF-β pathway activation through several mechanisms such as competition with R-SMADs for receptor binding, recruitment of SMURF ubiquitin ligases to activated TGF-β receptors resulting in their degreadation, recruitment of phosphatases to active receptors causing their deactivation, and competition R-SMADs for binding to SMAD response elements in target promoters. In addition to targeting genes involved in EMT such as E-cadherin and Vimentin, TGF-β receptor stimulation in untransformed cells elicits cell cycle arrest via SMAD/Sp mediated induction p15(Ink4b)(199, 200). This cytostatic induction of p15 is mediated by the transcription factor C/EBP-β and is required for the tumor suppressive effects of intact TGF-β pathway function (201, 202).

1.7 The Wnt / β-catenin pathway

Wnt glycoproteins are the ligands for Frizzled receptor complexes, which consist of frizzled receptors and low density lipoprotein receptors. While Wnt/Frizzled signal transduction (Fig. 3) has numerous downstream effectors that contribute to EMT, the majority of its output proceeds through either the canonical (β-catenin) or planar cell polarity (PCP) pathway. β-catenin normally resides at cell-cell junctions in a dynamic complex with other catenins and cadherins. When β-catenin is freed from these membrane-associated complexes, it ordinarily resides in a cytoplasmic pool that is targeted for destruction by a complex containing the scaffolding protein Axin and the Adenomatous polyposis coli (APC) tumor suppressor (203). Upon receipt of Wnt signals, β-catenin residing in this pool is stabilized by a mechanism that is poorly understood but appears to involve all 3 human homologs of the *drosophila* protein dishevelled in non-overlapping roles (204).

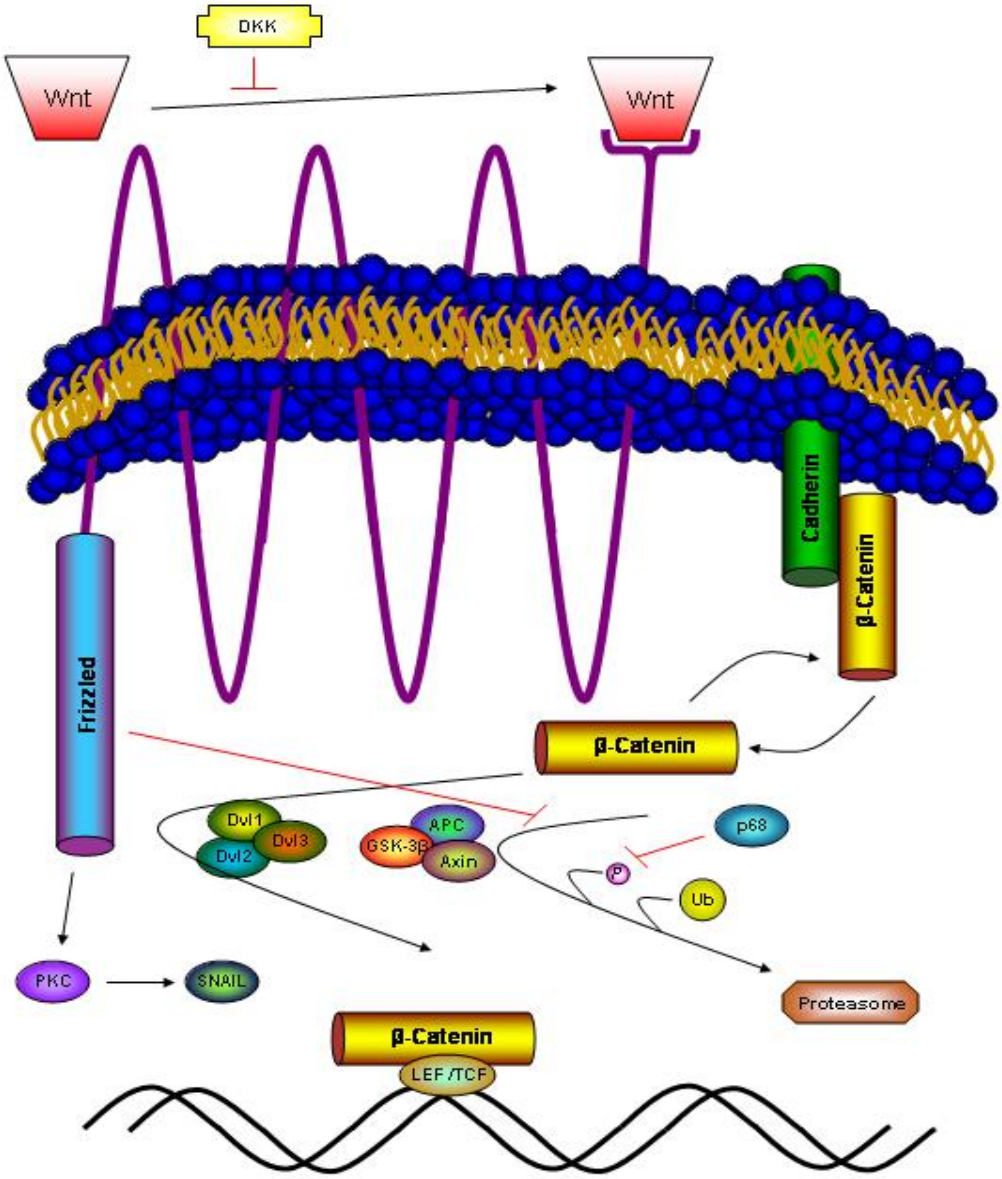

Figure 3. Wnt-frizzled signaling. Engagement of the Wnt ligand by Frizzled receptors results in stabilization of cytoplasmic β-catenin, which is a potent co-activator of LEF/TCF transcription factors. β-catenin normally exists in dynamic membrane -bound complexes with other catenins and cadherins, with some exiting to form a cytoplasmic pool that is targeted for proteosomal degradation by the Axin / APC / GSK-3β complex, which phosphorylates β-catenin priming it for ubiquitination. p68 RNA helicase promotes β-catenin stabilization by blocking this phosphorylation event. Wnt/Frizzled signaling also acts in β-catenin-independent signaling modes such as through promotion of PKC-mediated phosphorylation and activation of Snail.

The RNA helicase p68, which blocks phosphorylation of β-catenin in response to PDGF to promote EMT, may also play a role in Wnt-induced EMT or similar proteins may act in the fashion or p68 (205). Stabilized β-catenin translocates to the nucleus, where it acts as a potent co-activator for the LEF/ TCF family of transcription factors, leading to EMT (206-210). Wnt signaling can also lead to EMT through β-catenin-independent pathways. Wnt5A induces EMT via PKC-dependent induction of Snail, even in the presence of dominant-negative TCF4, demonstrating that Wnt signaling promotes EMT via several pathways besides β-catenin (211). Similar to the action of the BMP antagonist Noggin in the TGF-β pathway, secreted inhibitors such as the Dickkopf proteins attenuate and modulate Wnt signal strength in both β-catenin-dependent and independent Wnt signaling modes (212-214). Wnt signaling also exhibits extensive cross-talk with other EMT-promoting pathways, most notably the Notch pathway (215-217).

1.8 Notch and EMT

Notch signaling (Fig. 4) is relatively simple compared to other EMT-related pathways such as TGF-β and Wnt / Frizzled signaling, and has considerable cross-talk with both, being required for TGF-β-induced EMT in some cases (218). Notch signaling, similar to the TGF-β and Wnt / Frizzled pathways, begins with engagement of a ligand - Delta, Lag, or Serrate - by the Notch receptor, triggering cleavage of Notch and release of its intracellular domain (219). Cleavage of membrane-bound Notch occurs in two steps, the first step is catalyzed by ADAMs family metalloproteases and results in release of the extracellular domain of Notch (220-222). Step two is carried out by the activity of the

presenilin-nicastrin-Aph1-Pen2 protein complex, which is more commonly referred to as γ-secretase, and releases the intracellular domain of Notch (NICD) which translocates to the nucleus (223). Freed NICD displaces co-repressors such as NcoR, SMRT and SHARP from their interaction with Notch target-gene bound CSL, clearing the way for recruitment of co-activators such as Mastermind (224-230). During EMT, the most important Notch targets appear to be the E-cadherin reprssors snail and slug. Snail and slug are up-regulated directly via association of the NICD with their promoters and Snail indirectly via induction of lysyl oxidase, which stabilizes Snail via phosphorylation (149, 231, 232).

1.9 Snail

Snail promotes EMT in response to all the major pathways known to elicit EMT, such as the Wnt, Notch, TGF-β, and FGF signaling pathways (176, 182, 208, 211, 231, 233). Snail's function in EMT is centered around its role as a repressor of E-cadherin gene expression (234, 235), although it also targets other epithelial genes such as ERα, MUC1 and tight junction proteins (236-238). Snail effects repression of these genes by recruitment of the Sin3A/histone deacetylase 1 (HDAC1)/HDAC2 complex and C-terminal binding protein (CtBP) (239-241). Snail also promotes cell survival via induction of cell cycle arrest (242-244), and suppression of the PTEN phosphatase (245). Consistent with the aggressive, metaplastic nature of many ERα- tumors, Snail expression is restricted by estrogen signaling (246), suggesting the existence of a Snail-ERα regulatory loop that governs cellular plasticity. ERα signaling represses Snail indirectly by activating transcription of MTA3, a component of the Mi-2 / NuRD

transcriptional repressor, which then targets Snail (246). Like many other factors involved in EMT, Snail is associated with metastasis, recurrence, and poor prognosis (247-249).

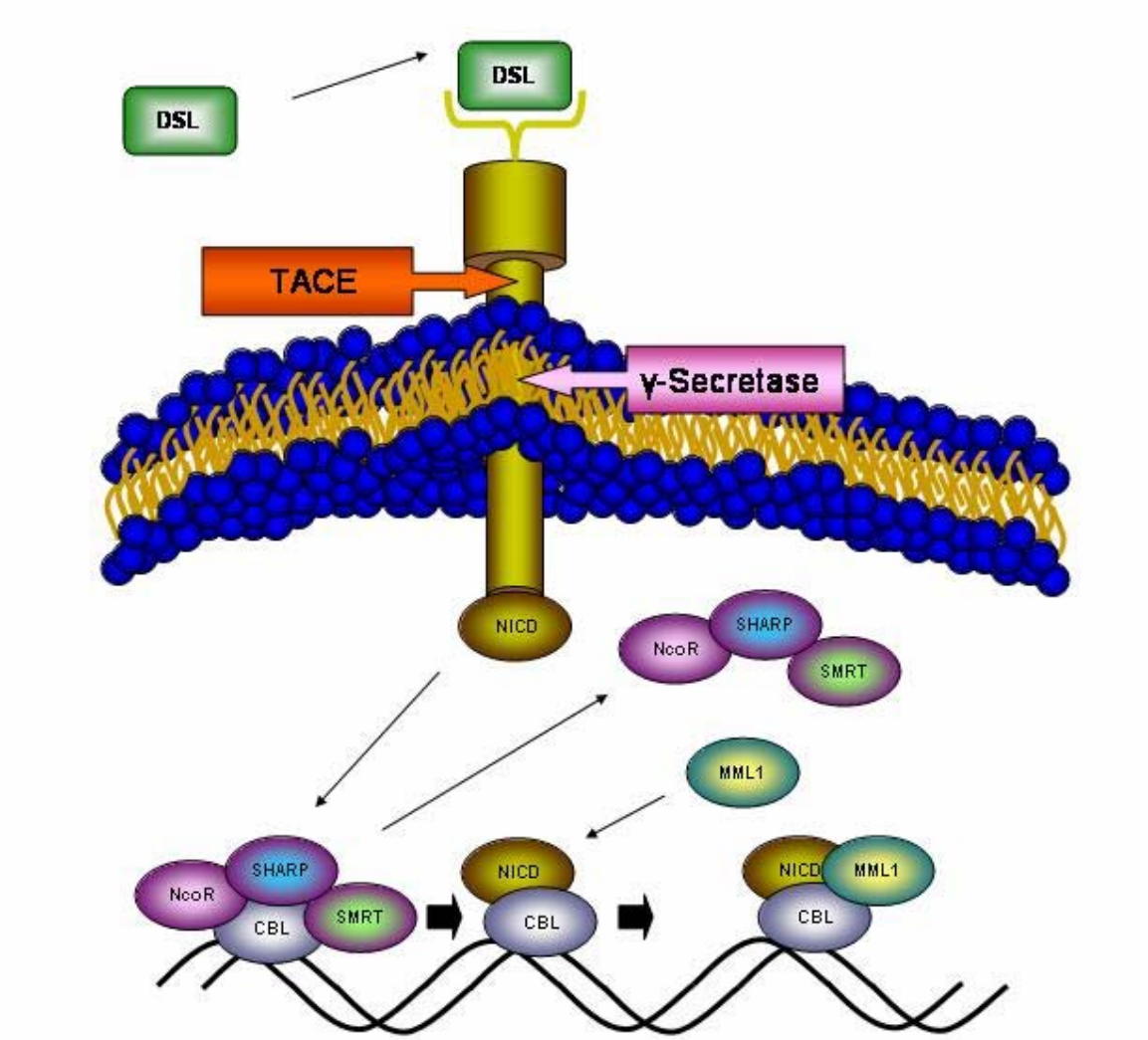

Figure 4. Notch signaling. Binding of a Delta - Serrate - Lag2 family ligand by the Notch receptor triggers cleavage of the receptor and releases of the intracellular domain of Notch (NICD). Cleavage takes place in two steps, the first is an extracellular cleavage event mediated by TACE that primes the receptor for the second cleavage event in the transmembrane domain performed by the γ-secretase complex. Once released, the NICD translocates to the nucleus where it disrupts interactions between the transcription factor CBL and co-repressors such as NcoR and SMRT. Co-activators such as Mastermind and then free to bind to CBL, which constitutively resides on the promoter regions of Notch target genes.

1.10 Twist

Similar to Snail proteins (Fig. 5), Twist has been reported to promote EMT via suppression of E-cadherin (161, 182, 250, 251), and up-regulation of genes associated with mesenchyme such as N-cadherin, FGFR2, and cadherin 11 (187, 252, 253). While the mechanisms by which Twist activates or represses transcription has not been solved fully, it is clear that dimerization partner selection is the major determinant of Twist activity (252, 254). Twist homodimerization or dimerization with E2A E12 results in transactivation (252, 254), while partnering with Id proteins and other bHLH repressors results in repression (252). In addition to targets associated with EMT, twist has profound effects on cell survival and genome integrity (255, 256). Twist represses expression of p14 (ARF) while upregulating AKT2, leading to checkpoint failure, drug resistance, and genomic instability (257, 258). Twist is also a key mediator of drug resistance induced by NF-kB activation, and appears to regulate phosphorylation of Bcl-2 proteins (259). Regulation of twist occurs mainly at the transcriptional level. Twist can be induced by Wnt, hypoxia, Notch, TGF-β, NF-kB, and VEGF, amongst other pro-EMT pathways and stimuli (162, 182, 259-261). Twist is a direct target of HIF1α and HIF2α and is associated with tumor vascularity, suggesting that Twist participates in angiogenesis and may promote metastasis via enabling access to the bloodstream as well as through EMT (162, 165, 262). In additon to its role in EMT and angiogenesis, Twist is associated with distant metastasis, recurrence, poor prognosis, and tumor vascularity (162, 165, 263-267), a common finding with transcription factors related to EMT.

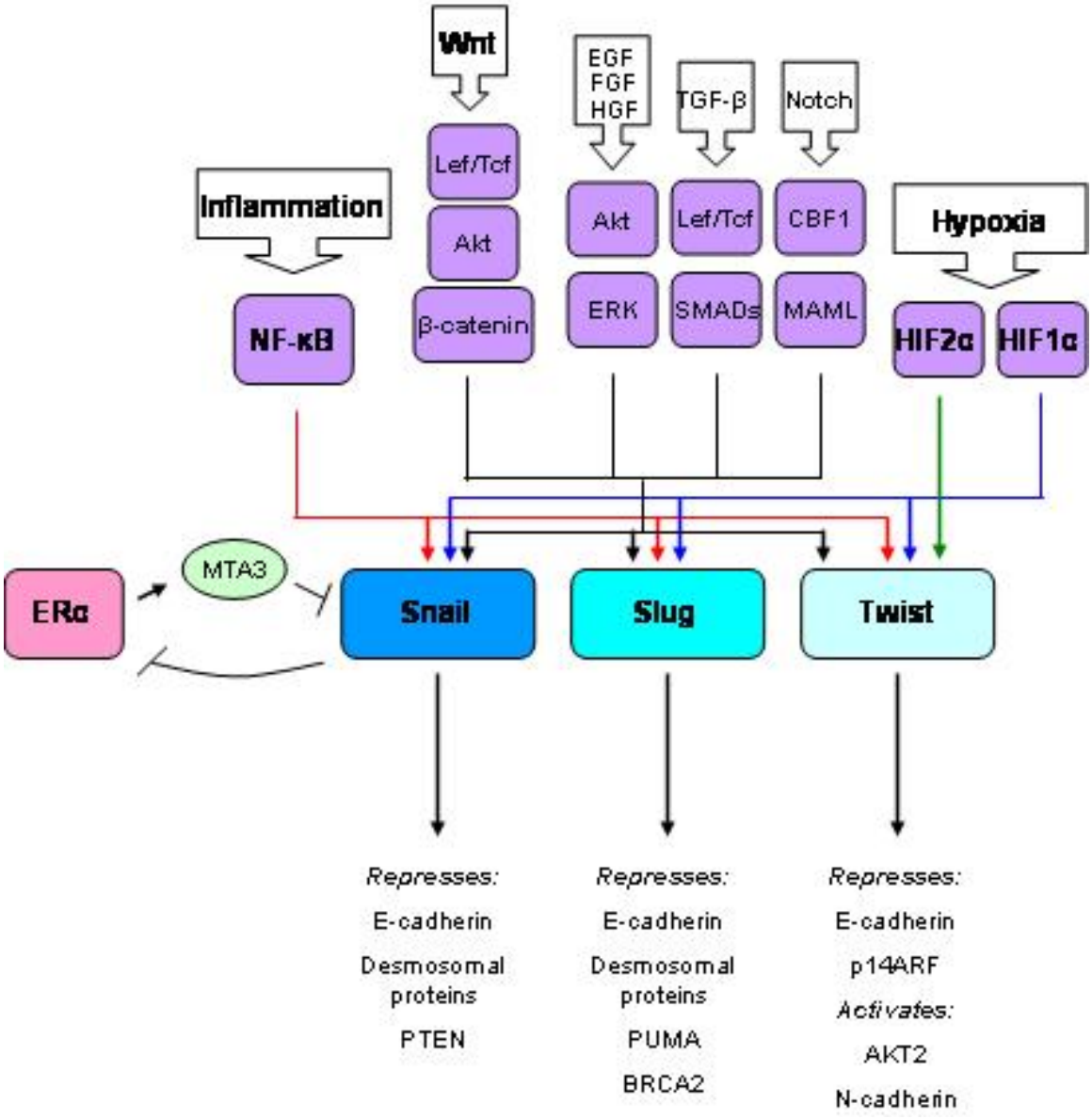

Figure 5. Regulation of the E-cadherin repressors snail, slug, and twist in breast cancer. Snail, slug, and twist are induced by activation of multiple signaling pathways such as the Wnt / β-catenin, TGF-β, and notch pathways (black arrows), as well as by microenvironmental stimuli (hypoxia and inflammation, blue and red arrows, respectively). In breast tissue, estrogen signaling represses snail via MTA3 and is repressed by snail, consistent with the agressive nature of ERα-negative tumors. The output that procedes from these pro-emt factors promotes motility and invasiveness through repression of cadherins and desmosomal proteins, as well as survival via repression of p14ARF and PTEN and up-regulation of AKT2.

1.11 Slug

The zinc finger transcriptional repressor slug (SNAI2) provides a link between EMT and acquisition of stem-cell like properties by tumor-initiating cells. Slug facilitates EMT downstream of multiple pathways such as the TGF-beta, notch, Wnt, and FGF pathways (182, 232, 268, 269), which promote maintenance of stem cell identity (270-276). Additionally, slug is a key player in stem cell biology, with important transcriptional targets unrelated to EMT such as PUMA and BRCA2 (124, 277-283). Consistent with the current thought on stem-cell like properties of tumors cells in basal-like carcinomas, slug is a driving force behind the basal phenotype (114). Slug also predicts poor prognosis and recurrence in multiple tumor types including breast cancer, which further suggests that slug is at the heart of the aggressive nature of basal-like carcinomas (127, 168, 169, 248). In the context of EMT, slug is best known as a repressor of E-cadherin expression (129). However, slug targets multiple epithelial genes such as high molecular weight keratins and desmosomal proteins to promoter cellular motility and suppression of the epithelial phenotype (158, 268, 284). Multiple studies have implicated slug in DNA damage responses, particularly those of stem/progenitor cells and transformed cells (124, 278, 279, 282, 283, 285). Slug promotes survival in the face of genotoxic stress, centered on its ability to stifle p53-mediated induction of the pro-apoptotic protein PUMA (278). This fact may explain the frequency of recurrence in basal-like carcinomas of the breast, which frequently display initial sensitivity to treatment but have high recurrence rates (122). Structurally, slug consists of a SNAG domain that effects transcriptional repression and five DNA-binding ZNF domains, and is the most conserved of all mammalian snail homologs (286). The SNAG domain, which is

common to all snail family proteins and multiple other oncogenes, functions as an interaction domain with scaffolding proteins to recruit macromolecular repression complexes to slug target genes (287). Examples of this include recruitment of Ajuba LIM proteins, which in turn recruit protein arginine methyltransferase 5 (PRMT5) to repress transcription (287-289), and recruitment of the Sin3A/Histone Deacetylase 1 (HDAC1)/HDAC2 repressor complex (239), both to the E-cadherin promoter. Several studies have shed light on the regulation of slug expression. The promoter region of SLUG contains multiple regulatory elements, including MyoD, TCF/LEF, AhR, E2A-HLF, and SMAD-responsive regions (184, 290-293), all of which facilitate transactivation of the SLUG gene. However, the factors that restrict inappropriate slug expression have thus far remained unidentified.

1.12 Comparison of pathological and developmental EMT

EMT in developmental contexts is tightly controlled in space and time (294). Often, likely always, multiple pathways associated with EMT induction are simultaneously activated, and crosstalk between them confers the precision needed for proper development of embryonic and mature tissues. An example of this precision can be found during gastrulation, which is tightly controlled by the BMP antagonist Noggin (138). Spatially and temporally controlled NOG expression brings gastrulation to an end in an appropriate time frame, while still allowing for EMT-like events to shape the tailbud. Mice mutant for NOG fail to bring a halt to the ingressive cell movements of gastrulation, and NOG null mice have severe skeletal defects and mesenchymal hyperplasias by the time of lethality on embryonic day 18.5 (295, 296). Additionally,

mice and humans haploinsufficient for NOG suffer from skeletal defects such as carpal and tarsal fusions, which highlights the necessity for an "off-switch" for non-pathologic EMT processes to function normally (296). In the developing heart, defects in NOG or the EMT "on-switch" BMP2 leads to defects in the endocardial cushions and derived structures, and proper functioning of both switches requires input from the notch, leptin, Wnt, and HGF signaling pathways to ensure appropriate expression of the downstream targets slug and snail (136, 148, 149, 296-298). This implies that one of the ways that EMT is suppressed in mature tissues is a requirement for convergence of mulitple EMT-promoting pathways to initiate and sustain EMT, and may explain the rarity of EMT events observed in solid tumors, since activation of an EMT promoting pathway could be sufficient to drive tumor growth without reaching the signal threshold for EMT. That is, pro-EMT signals must hit a specific pitch before the anti-EMT signals are overridden and EMT occurs. Thus it appears one of three phenomena drive pathologic EMT: a relentless on-switch, a malfunctioning or absent off-switch, or the creation of new on-switches which results in enough "on" signal to drive EMT (Fig. 6).

Overexpression of EMT-promoting factors and loss of antagonistic factors has been reported in many cancers (173). An important example of a malfunctioning switch was recently elucidated by Gomis et al, when they discovered that loss of the LIP isoform of the transcription factor C/EBPβ eliminated the cytostatic effects of TGFβ in human breast tumors (202). This malfunctioning switch allows the cancer cells to receive the benefit of the pro-invasive properties of TGFβ and explains the biphasic action of TGFβ in tumors. As more intrinsic breaks and feedback loops on the EMT process are

uncovered, the apparently contradictory tissue specific roles of other EMT-related factors such as Notch may be understood more fully (299).

1.13 Pathologic vs. non-pathologic EMT: role of hypoxia

Two major EMT-promoting switches are present under pathologic conditions that are absent in developmental EMT: hypoxia and inflammation. Hypoxia is present even in microscopic tumors, and contributes to tumor progression, angiogenesis, and radioresistance (300-302). Hypoxia results in prolylhydroxylase-dependent stabilization, dissociation from the VHL ubiquitin ligase, and activation of hypoxia-inducible factor 1-α (HIF1α), as well as activation of HIF2α, both of which activate genes involved in angiogenesis as well as those involved in EMT (162, 303). HIF1α directly binds the hypoxia response element (HRE) in the Twist1 proximal promoter region in response to hypoxia and induces EMT, an effect reversible by siRNA directed to Twist (162). HIF2α has also been reported to transactivate Twist in response to hypoxia, but intriguingly HIF2α targets intronic HREs that are not responsive to HIF1α (262). This is particularly interesting in light of previous reports that HIF1α and HIF2α are differentially activated during acute and prolonged hypoxia in tumors, where high HIF2α expression correlated with VEGF expression, advanced clinical stage, and poor prognosis (304). This would suggest that during initial acute hypoxia HIF1α expression triggers angiogenesis and pro-survival Twist expression, while continued low-level hypoxia causes continued expression of Twist via HIF2α and promotes EMT and metastasis. As HIF-driven EMT appears to be dependent upon Twist, arrival in a mature, oxygenated tissue may decrease Twist expression sufficiently to allow for MET and establishment of metastatic colonies.

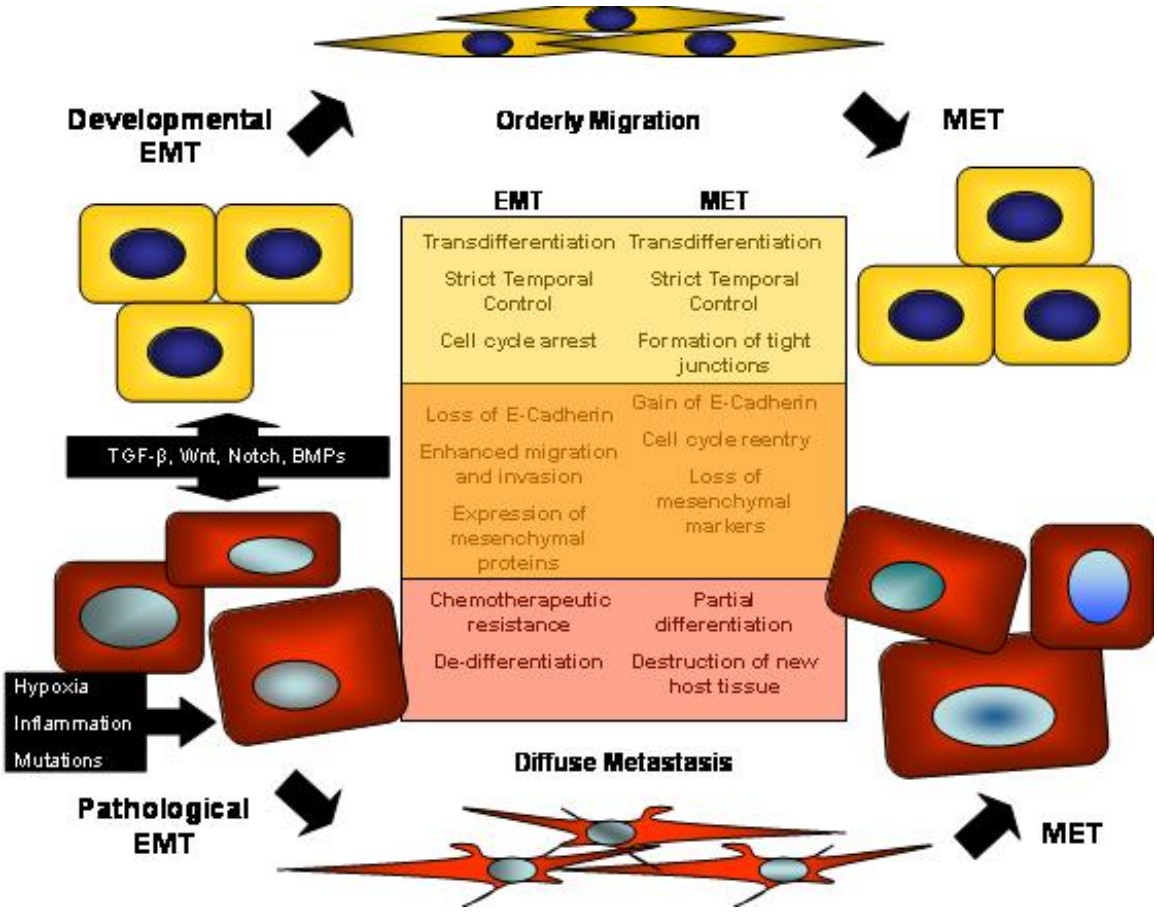

Figure 6. Pathological and developmental EMT. Developmental and pathological EMTs and METs share many common features such as loss of E-cadherin in EMT, as shown in the orange panel. Developmental EMT (orange and yellow panels) is characterized by strict spatial and temporal control, while pathological EMTs such as those occurring during metastasis and fibrosis have lost or eluded the molecular brakes on the EMT process. Pathological EMTs also occur in microenviroments rife with EMT-promoting hypoxic and inflammatory stimuli, which may disappear during extravasation thereby facilitating MET. The metastatic colony soon generates hypoxic and inflammatory stimuli of its own, maintaining the plasticity of the cells to spread further even if the original tumor is removed.

Several other factors appear to be required for hypoxia driven EMT. The Notch signaling pathway is necessary to convert the hypoxic stimulus into a pro-EMT signal and promote Snail expression directly and via lysyl oxidase mediated phosphorylation of Snail (231). Additionally, increased expression of the urokinase-type plasminogen activator receptor (uPAR) and activation of cell signaling factors downstream of uPAR

such as Akt and Rac1 have been shown to be required for full manifestation of the EMT phenotype in response to hypoxia (305). Blockage of either Notch or uPAR signaling in these studies was sufficient to halt hypoxia-induced EMT, and activation of Notch or overexpression of uPAR could substitute for hypoxia in EMT promotion. This is further evidence that EMT signaling must reach a threshold before EMT is initiated, and that tumor-associated hypoxia represents a pro-EMT signal that tilts the balances in favor of EMT but is not sufficient to initiate it alone, else nearly all solid tumors would display EMT. Hypoxia also contributes to pathogenic EMT in non-transformed cells, such as during kidney fibrosis (306, 307), suggesting that EMT and transformation are separate processes that can employ many of the same effectors.

1.14 Pathologic vs. non-pathologic EMT: role of inflammation

The most well known link between inflammation and cancer is the transcription factor NF-κB, which activates transcription of genes that promote inflammation, cell survival, EMT, and cellular transformation, both initiating and feeding forward in these repsonses (308). NF-κB mediates EMTs initiated by the pro-inflammatory cytokine Tumor Necrosis Factor-α (TNFα) via induction of the E-cadherin repressors ZEB-1 and ZEB-2, and up-regulates Twist and Snail (259, 309, 310). In addition to activation by inflammatory stimuli, NF-κB-driven EMT can be activated by genotoxicants such as 7,12-dimethylbenz(a)anthracene (DMBA), and by hypoxia (311, 312). NF-κB can also be activated by loss of E-cadherin via p38 MAPK, providing a feed-forward mechanism for sustained EMT signaling (313). NF-κB can also feed forward on itself (314), suggesting another possible mechanism by which NF-κB signaling can sustain EMT. Ectopic

expression of supraphysiological levels of active NF-κB is also capable of inducing EMT (309), indicating that NF-κB activity represents another EMT on-switch that initiates EMT upon reaching of a threshold signal. Physiological levels of cancer-related NF-κB activity do appear to be sufficient to drive EMT on their own, given the prevalence of aberrant NF-κB activation and rarity of EMT in breast cancers (116, 132, 315). EMT in breast cancer is often associated with ERα negative tumors, which have poorer progonosis than ERα positive tumors (117). Therefore, it is not surprising that ERα represses expression of the RelB subunit of NF-κB (316). ERα is in turn suppressed by the NF-κB target Snail (238), which is itself a target of suppression by MTA3, a downstream effector of ERα (246).

Inflammtory NF-κB-mediated signialing pathways also have extensive cross-talk with other EMT-promoting factors such as Wnt, Notch, HIF1α, and TGF-β (317-323). NF-κB transactivates the HIF1α promoter, and is required for hypoxia-induced HIF1α accumulation (321). HIF1α returns the favor by promoting NF-κB activation via phosphorylation of IKK and NF-κB itself, suggesting cooperation between hypoxia and inflammation in pathogenic EMT (324). Inflammatory signaling pathways can also crosstalk with HIF1α in an NF-κB-independent fashion, as LPS-induced HIF1α activation appears to be NF-κB-independent but is sensitive to antioxidants (325), and processes that generate reactive nitrogen species can stabilize HIF1α through S-nitrosylation of HIF1α's oxygen-dependent degradation domain, preventing interaction with VHL (326). Knowledge of the extensive entanglements between the various EMT-promoting pathways has provided numerous potential therapeutic targets, however,

relatively little work has been done to elucidate the factors that restrain EMT in normal tissues and less advanced cancers.

1.15 SIM2

In the developing *Drosophila* CNS, specification of the CNS midline is dependent upon the basic helix-loop-helix Per-Arnt-Sim transcription factor single-minded (sim), which serves as the master regulator of midline differentiation (327, 328). Singleminded-2 (SIM2) is one of two vertebrate orthologs of the *Drosophila sim* (dsim) protein, but it differs in functioning as a transcriptional repressor (329-332). SIM2 was initially identified by positional cloning around the DS (DS) critical region of chromosome 21 and is believed to contribute to many of the physiological abnormalities associated with trisomy 21 (333). SIM2 functions as a heterodimer with ARNT, similar to *drosophila* counterpart dsim that dimerizes with the ARNT ortholog Tango to control expression of midline genes in the central nervous system (CNS) (334, 335). SIM2 is expressed in multiple tissues including the kidneys, lungs, brain, and breast, in both adult and developing tissues (329, 336-338). Sim2 plays an important role in development, as Sim2 null mice die shortly after birth due to multiple abnormalities, including cleft palate, improper diaphragm development, and rib defects (337, 338). The molecular mechanisms controlling these processes are complex and involve the concerted actions of many factors, and suggesting a master regulatory role for SIM2 in the many developmental processes that are severely disrupted in Sim2 null mice. Indeed, SIM2s, a splice variant of SIM2, was recently identified as a regulator of MMP3 gene expression, which plays a critical role in the development of the palate, mammary gland, and neuromuscular

junctions (15, 339-342). As the phenotype of MMP3 null mice is significantly different from and less severe than that of Sim2 null mice, it is clear than many more important developmental targets of SIM2 remain to be elucidated.

1.16 The Down syndrome (DS) tumor profile

Individuals with DS have a markedly different tumor spectrum than the general population. Specifically, leukemias are greatly increased while solid tumors are decreased in DS patients (343-350). Most striking is the profound protection women with DS enjoy from breast cancer, with as much as 25-fold protection compared to the non-DS population (344, 347-350). Recently, this solid tumor protection was proposed to be due to at least in part to gene dosage-mediated increases in ETS2 levels (351). However, this cannot explain the protection that women with DS enjoy, as there is overwhelming evidence that ETS2 acts as an oncogene in breast tissue by promoting tamoxifen resistance and suppressing the tumor suppressor BRCA1 (352-355). Therefore, other mechanisms must be invoked to fully explain the tumor spectrum of DS patients.

Due to its position in the DSCR of chromosome 21, and its roles in regulating responses to xenobiotics and hypoxia, SIM2 is a strong candidate for contributing to trisomy 21-related solid tumor suppression. Other laboratories have reported that SIM2s is oncogenic in the pancreas, prostate, and colon (356-359), a conclusion based largely on the observation that antisense oligos targeted to the 3' untranslated region of the SIM2s mRNA resulted in apoptosis. However, as loss of tumor suppressors such as VHL can

lead to senescence (360), this conclusion requires mechanistic support, especially in light of the frequency of SIM2s loss in breast tumors (336).

1.17 The mechanism of SIM2-mediated tumor suppression

To attempt to shed light on the true nature of SIM2s as relates to cancer, we used a retroviral shRNA system to silence SIM2s in the relatively non-invasive breast cancer cell line MCF-7, which expresses high amounts of SIM2s relative to more invasive cell lines (336). Based on previous studies from MDA-MB-435 cells, we hypothesized that loss of SIM2s would confer enhanced invasiveness and tumorigeneic properties. As expected, silencing of SIM2s lead to enhanced invasiveness, and also promoted EMT, xenograft tumor growth, and metastasis. Investigation into the mechanism underlying these observations revealed that the oncogenic E-cadherin repressor slug and the invasion-associated metalloprotease MMP2 are direct targets of SIM2s-mediated transcriptional repression. Furthermore, SIM2s binds the slug promoter directly and represses transcription, making it the first known repressor of slug expression. Sim2-/- mammary glands also displayed hallmarks of EMT such as E-cadherin loss and increased nuclear accumulation of β-catenin, suggesting that Sim2s' roles in regulating slug is conserved amongst mammals. Silencing of SIM2 also severely disrupted acinar morphogenesis in untransformed MCF-10A cells, but was not sufficient to induce EMT.

As slug plays an important role in stem cell biology and SIM2*i* cells were much more tumorigenic than their control "scrambled" (SCR) counterparts, we asked whether SIM2 loss affected self-renewal capacity or expression of stem cell markers. When

grown under low attachment conditions in normal growth media, SIM2*i* cells had a decided advantage in self-renewal as measured by mammosphere formation, but this effect was masked by supplementation with growth factors. Using commonly used markers for tumor-initiating cells in MCF-7 populations, we found that SIM2*i* cells had a significantly larger number of putative tumor-initiating CD29+ CD24lo cells, consistent with their enhanced tumorgenecity. In both stem cells and cancer cells, slug has been reported to enhance cell survival in the face of DNA damage, and therefore we asked whether depletion of SIM2s enhanced chemoresistance. MCF-7 cells infected with the SIM2-specific virus (SIM2*i*) were resistant to doxorubicin, but not ionizing radiation when compared to SCR cells. Additionally, we found that the reported slug target PUMA was not induced in response to DNA damage in SIM2*i* cells, consistent with their high levels of slug expression. Interestingly, SIM2s deficient MCF-7 cells also failed to induce the cyclin-dependent kinase inhibitor p21/ WAF1/CIP1 under conditions where it was robustly induced in SCR cells, suggesting a role for SIM2 in DNA damage signaling. Further examination of the DNA damage response in SIM2*i* cells revealed that they were p53 positive, and had extremely elevated constitutive p53 levels, with no mutations in p53. While apparently insufficient to drive expression of p21 or PUMA, other p53 targets such as MDM2 and NOXA were induced similarly in both cell types in response to DNA damaging agents. ChIP analysis of the p21 promoter confirmed that SIM2 binds the p21 promoter near the p53 response element in response to doxorubicin and ionizing radiation (R. Metz, unpublished results), raising the question of whether SIM2 and p53 interact either directly or in a complex. Indeed, we observed a DNA-damage dependent interaction between SIM2 and p53, which occurred with 4 hours of DNA damage. We

also found that SIM2 is itself stablized by DNA damage, while its RNA expression remains unchanged. Our studies suggest strongly that SIM2s is a tumor suppressor, although it is possible that SIM2 has tissue-specific activities that make tumor-promoting in other tissues. Based on our data presented here and published work on slug, EMT, and basal-like carcinomas of the breast, we hypothesize that SIM2 loss contributes to the basal phenotype and may be a useful diagnostic marker for these tumors.

CHAPTER II

MATERIALS AND METHODS

2.1 Cell line maintenance and drug treatment

MCF7 cells were maintained in DMEM supplemented with 10% fetal bovine serum and 1% penicillin and streptomycin. MCF10A cells were maintained in DMEM/F-12 supplemented with 5% fetal bovine serum, 1% penicillin and streptomycin as well as 20 ng/ml epidermal growth factor, 0.5 μg/ml hydrocortisone, 100 ng/ml cholera toxin and 10 μg/ml insulin. All cells were grown in 5% CO_2 at 37^{o}C.

2.2 Plasmids

A 3,280 bp region of the human *SLUG* gene promoter region was amplified from human genomic DNA (Roche) using Accuprime Taq DNA polymerase (Invitrogen) and the primers F 5'-GCC TAT GCC ACA CTC TGG TT-3' and R 5'-GGC GCC TCT GAA GTC ACC-3' and cloned into the pGL3-basic luciferase reporter vector (Promega). The human SIM2s expression vector has been described previously (336). The human SIM2-specific shRNA constructs were generated by ligating a dsDNA insert designed by Ambion into their pSilencer U6-retro 5.1 shRNA vector. The dsDNA insert sequences were based upon Ambion pre-designed siRNA sequences #3116 (SIM2*i* #1), 114477 (SIM2*i* #2), and 114478 (SIM2*i* #3). The insert was created by annealing the oligos 5'-GAT CCG GTC GTT CTT TCT TCG AAT TTC AAG AGA ATT CGA AGA AAG AAC GAC CTC TTT TTT GGA AA-3' (top) and 5'-AGC TTT TCC AAA AAA GAG GTC GTT CTT TCT TCG AAT TCT CTT GAA ATT CGA AGA AAG AAC GAC CG-

3' (bottom) for 3116; 5'-GAT CCG CAG TGA CCT TCT GTA CAC TTC AAG AGA GTG TAC AGA AGG TCA CTG CTT TTT TGG AAA-3' (top) and AGC TTT TCC AAA AAA GCA GTG ACC TTC TGT ACA CTC TCT TGA AGT GTA CAG AAG GTC ACT GCG-3' (bottom) for 114477; and 5'-GAT CCG CGG GCA ACA GTA TTT ATG ATT CAA GAG ATC ATA AAT ACT GTT GCC CGT GTT TTT TGG AAA-3' (top) and 5'-AGC TTT TCC AAA AAA CAC GGG CAA CAG TAT TTA TGA TCT CTT GAA TCA TAA ATA CTG TTG CCC GCG-3' (bottom) for 114478 to yield overhangs compatible with the vector. The scrambled control vector was provided by Ambion.

2.3 RNA isolation and real time RT-PCR

RNA was isolated using a Qiaquick RNeasy Mini kit with Qiashredder columns (Qiagen) and DNase digested (Roche). Two μg of RNA was reverse transcribed with Superscript II Reverse Transcriptase (Invitrogen) with an oligo $d(T)_{12-18}$ primer. Relative quantitative PCR was performed using Sybr Green master mix and cDNA-specific primers. TBP was used as the housekeeping gene. Data were collected using ABI 7500 system software, and analyzed by the $\Delta\Delta C_T$ method. Primers used for real time RT-PCR are shown in the table 3.

Table 3. Real-time RT-PCR primers.

Gene	Forward Primer	Reverse Primer
ATM	CCG ACG GGC CGA ATG T	AGC CGC AGA GCA CGG TAT
ATR	TTG CCA ACG TTT TCG ACT TTC	TCC TAA AGT TCG AAT GAG AGC AGA A
β2M	CGC TCC GTG GCC TTA GC	AAT CTT TGG AGT ACG CTG GAT AGC
BCL2	CAT GTG TGT GGA GAG CGT CAA	GCC GGT TCA GGT ACT CAG TCA
BID	CTT TTT CTC TTT CCA TGA CAT CAA GA	GGG CAT CGC AGT AGC TTC TG
BIM	CGG TCT CCT GGT GCC ATT AT	AGC TCG GTG TCT TCT GAA ACG
BRCA1	AGC GGT AGC CCC TTG GTT	GCG CAG TCG CAG TTT TAA TTT
BRCA2	CGC GGT TTT TGT CAG CTT ACT	ACG ATA TTC CTC CAA TGC TTG GT
E-cadherin	CAC AGA CGC GGA CGA TGA T	GAT CTT GGC TGA GGA TGG TGT AA
ERα	TCT GCC AAG GAG ACT CGC TAC T	CGT TAT GTC CTT GAA TAC TTC TCT TGA
GATA3	CTG GCT CGC AGA ATT GCA	AAC TGG GTA TGG CAG AAT AAA ACG
Keratin 18	GAG GCT GAG ATC GCC ACC TA	CCA AGG CAT CAC CAA GAT TAA AG
MDM2	GGG ACG CCA TCG AAT CC	TGA ATC CTG ATC CAA CCA ATC A
MDM4	CAG CAG GAG CAG CAT ATG GTA T	AGA AGC TCT GAC GTC CCA GTA GTT
MMP2	CAA GGA GTA CAA CAG CTG CAC TGA TA	GGT GCA GCT CTC TCA TAT TTG TTG C
MMP3	TTC CTG ATG TTG GTC ACT TCA GA	TCC TGT ATG TAA GGT GGG TTT TCC
MMP14	GCC TGC GTC CAT CAA CAC T	ACA CCC AAT GCT TGT CTC CTT T
N-cadherin	CAG CAA CGA CGG GTT AGT CA	TGC AGC AAC AGT AAG GAC AAA CA
NOXA	CTG CAG GAC TGT TCG TGT TCA	GGA ACC TCA GCC TCC AAC TG
p21	CCT AAT CCG CCC ACA GGA A	AAG ATG TAG AGC GGG CCT TTG
p27	GCT AAC TCT GAG GAC ACG CAT TT	CGC ATT GCT CCG CTA ACC
p53	TCT TTG AAC CCT TGC TTG CA	CCG GGA CAA AGC AAA TGG
PR	CCG GGC ACT GAG TGT TGA AT	GTT TCA CCA TCC CTG CCA AT
PS2	GTG CCT CGG CTC ACA ACA C	CGA TCT CTT TTA ATT TTT AGG CCA AT
PUMA	GGG CCC AGA CTG TGA ATC CT	CGT CGC TCT CTC TAA ACC TAT GC
SIM2	AGA CAA AGC TGA GAA CAA ACC	CCG CAT TCC AGT TTG TCC AT
SLUG	GGC TGG CCA AAC ATA AGC A	CCT TGT CAC AGT ATT TAC AGC TGA AA
SNAIL	GCG TGT GGC TTC GGA TGT	CTG CAA ATA CTG CAA CAA GGA ATA C
TIMP2	CCC CTC CTC GGC AGT GT	CCC CCT CGG CCT TTC C
TBP	TGC ACA GGA GCC AAG AGT GAA	CAC ATC ACA GCT CCC CAC CA
Vimentin	TTC TCT GCC TCT TCC AAA CTT TTC	GGG TAT CAA CCA GAG GGA GTG A

All primers were designed based on the human NCBI reference mRNA sequence using primer express software from ABI and purchased from IDT.

2.4 Chromatin immunoprecipitation

ChIP assays were carried out as described by the manufacturer (Upstate Cell Signaling) with a few modifications. Briefly, cells were fixed with 1% formaldehyde for 10 minutes. Crosslinking was stopped by addition of 125 mM glycine. Cells were washed in the presence of protease inhibitors (Complete tablets, Roche), pelleted at 2000 rpm for 4 minutes at 4^{o}C and resuspended in SDS lysis buffer with protease inhibitors (Complete tablets, Roche). Aliquots of 200 µl ($1x10^{6}$ cells) were sonicated for 10 pulses of 10 seconds each to shear chromatin to between 200 and 1500 bp. The supernatant was collected and diluted in ChIP dilution buffer to an appropriate amount. After pre-clearing twice with salmon sperm DNA/protein A agarose-50% slurry in TE/Na azide/0.1% BSA, the supernatant was incubated overnight with antibody at 4^{o}C. Antibodies used were normal rabbit IgG (5 µg, Upstate), anti-Sim2 (Rb pAb, 5 µg, Chemicon), and anti-slug (Rb pAb, 5 µg, Santa Cruz). The salmon sperm DNA/protein A agarose-50% slurry was then used to collect the antibody complexes for 1 hour at 4^{o}C. Agarose was pelleted at 1000 x *g* at 4^{o}C for 1 minute and washed sequentially with low salt wash buffer, high salt wash buffer, lithium chloride wash buffer and TE buffer. The protein complex was eluted with 1% SDS, 0.1 M $NaHCO_3$, and the crosslinking was reversed in 200 mM NaCl at 65^{o}C for 4 hours. Ethanol was added to precipitate the DNA, which was then resuspended in TE and digested with proteinase K for 1-2 hours at 45^{o}C. DNA was purified using the Qiaquick PCR purification kit. PCR was performed with primers flanking the CME in the SLUG promoter region (5′- TGT GTC CAC GTG GCT CTA AG -3′ and 5′- CGC GTG CTA GCG AGT AAC A -3′), and sites 500-1000 bp upstream (5′-ATG CCC GCT CTG ACA ATT T-3′ and 5′-GGT GTG TAA AAA GCA GTG

CAA-3′), and downstream (5′-CCA GGT TTC CAG TTT GTG TG-3′ and 5′-TGT GTA TGG TCT TCA ATC TA-3′) of the CME primer set. Primers flanking the first two E-box elements in the E-cadherin promoter were: 5′- AAA AGC CCT TTC TGA TCC CA -3′ and 5′- TGG AGT CTG AAC TGA CTT CCG -3′.

2.5 Western blot

Protein was isolated using RIPA buffer (25 mM Tris-HCl pH 7.6, 150 mM NaCl, 1% NP-40, 1% sodium deoxycholate, 0.1% SDS) with protease inhibitors and MG-132 added or with Nonidet-P40 (NP-40) buffer (20 mM Tris HCl pH 8, 137 mM NaCl, 10% glycerol, 1% nonidet P-40, 2 mM EDTA) with protease and phosphatase inhibitors. Protein was loaded and run on an 8% or 10% acrylamide gel at 110 V until the dye front reached the bottom of the gel. Protein was transferred to a PVDF membrane (Bio-Rad) at 100 mA for 2 hours or at 60 mA overnight in a cold room. Membranes were blocked in 5% milk and probed with the primary antibody for 2 hours at RT or overnight at 4^{o}C. Membranes were washed in PBS, 0.1% Tween-20 and probed with the appropriate secondary antibody, anti-rabbit (Bio-Rad) or anti-mouse (Santa Cruz), at 1:5000 for 45 minutes at room temperature. Blots were again washed in PBS, 0.1% Tween-20 and developed with the ECL Plus Western Blotting Detection System (Amersham). All washing, blocking, and antibody incubation steps were peformed with gentle rocking. Antibodies used for western blotting and immunostaining are summarized in table 4.

Table 4. Antibodies and conditions.

Antibody	Manufacturer	Host	IF/IHC Conditions	WB Conditions
β-actin	SIGMA	M	N/A	1:8000
Active β-Catenin Clone 8E7	Upstate	M	M.O.M. kit recommedations	N/A
Aquaporin 5	Alpha Diagnostics	Rb	1:150	N/A
BrdU	Molecular Probes		1:50	N/A
CD31	Santa Cruz	G	1:100	N/A
E-Cadherin	BD Transduction	M	1:1000	1:2500
ERα	Santa Cruz	Rb	1:500	1:1000
γ-H2AX	Calbiochem	Rb	1:1000	N/A
Keratin 14	Covance	Rb	1:1000	1:2000
Keratin 18	Neomarkers	M	1:500	1:1500
Ki-67	Santa Cruz	G	1:100	N/A
Laminin V	Chemicon	M	1:1000	N/A
MDM2	Chemicon	M	N/A	1:1000
MMP2	Affinity Bioreagents	Rb	1:250	1:2000
MMP3	Affinity Bioreagents	Rb	1:250	1:2000
N-Cadherin	BD Transduction	M	1:1000	1:2500
NOXA	Abcam	M	N/A	1:1000
p21	DAKO	M	1:1000	1:2000
p53	R&D Systems	G	1:1000	1:2500
p53	NeoMarkers	M	1:250	1:1000
PUMA	Santa Cruz	G	1:250	1:1000
Phospho- β-Catenin	Cell Signaling	Rb	1:250	N/A
α-Smooth Muscle Actin	SIGMA	M	1:1000	1:2000
SIM2	Chemicon	Rb	1:250	1:700
Sim2s	Santa Cruz	G	1:100	N/A
Slug	Santa Cruz	Rb	1:500	1:1000
VEGF	DAKO	M	Manufacturer's recommendations	
Vimentin Clone V9	Sigma	M	1:500	1:1000

N/A indicates that the antibody is suitable for the application but was not used or opimized.

2.6 Zymography

To determine MMP2 activity, conditioned medium from cells was concentrated ~20-fold using Centricon 10 spin concentrators (Amicon). Equal amounts of protein were mixed with Laemmli sample buffer without reducing agents, incubated for 15 minutes at 37°C, and separated on 8% polyacrylamide slab gels containing 1 mg/ml gelatin. Following electrophoresis, gels were placed in 2.5% Triton X-100 for 30 minutes then incubated at 37°C in 50 mM Tris-HCl, pH 7.4, containing 5 mM $CaCl_2$ for 18 hrs. MMP2 activity was visualized by Coomassie blue staining.

2.7 Stable transduction

HEK-293T amphotrophic Phoenix cells were transfected with 15 μg pSilencer U6-retro 5.1 retroviral vector (Ambion, Austin, TX) with SIM2-specific insert or a non-specific "scrambled" insert, or a non-retroviral plasmid (pcDNA3) for mock infection. After 24 hours, cells were placed at 32^{o}C. Viral media was harvested 48 and 72 hours after transfection and used to infect cells after passage through a 0.45 μM filter. Infected cells were centrifuged at room temperature immediately after application of viral media, and housed at 32^{o}C during infection. 24 hours after the second application of viral media, cells were rested for 24 hours in their respective normal growth media before initiation of puromycin selection. Selection was considered complete when all mock-infected cells had died.

2.8 Transient transfection

MCF-7 cells were used for all transient transfections. One hundred ng (0.1 μg) of plasmid containing transcription factor was mixed with 0.2 μg of plasmid containing promoter construct. Three μL of Genejuice (Novagen) was used per microgram of DNA. DNA and Genejuice were mixed in Opti-MEM media (Invitrogen). Protein was harvested 2 days after transfection, using Reporter Lysis Buffer (Promega). Luciferase activity and total protein were measured as described previously (336). Luciferase activities were normalized to total protein values and are represented as the means ± SE for three wells per condition.

2.9 Cell proliferation/death assay

Cells were seeded at 25,000 cells/well (MCF-7) or 10,000 cells/well (MCF-10A) in triplicate in 6-well plates containing selection medium. Cells were harvested and counted with a Coulter counter days 2-7 after plating. For drug-induced cell death assays, SCR and SIM2-depleted MCF-7 cells were seeded at 500,000 cells per well in 6-well plates. The next day cells were treated with 1 μM doxorubicin or 10Gy of ionizing radiation. Cells were counted, using a Coulter counter, in triplicate (3 wells) at the time of treatment and 24 hours intervals thereafter for 3 days.

2.10 Migration and invasion assays

Migration and invasion were measured using control and matrigel-coated invasion chambers (Falcon BD, Franklin Lakes, New Jersey). 12,500 cells were seeded in serum-free DMEM in the upper chamber with serum-containing medium in the lower chamber as a chemoattractant. After 20 hours at 37°C, cells were scraped from the upper chamber with a cotton swab, and the underside of the membranes were fixed in 100% MeOH, stained with DAPI, and counted. Percent invasion was calculated as per the manufacturer's instructions.

2.11 Immunofluorescence

Cells were seeded on cover slips in 6-well plates. The following day the cells were fixed in 3.8% paraformaldehyde and permeabilized with 0.1% Triton X-100 for 15 minutes at 4^{o}C. The cells were blocked in 5% BSA for 45 minutes and then probed with primary antibody for 2 hours at room temperature. After washing in PBS, the secondary antibody was applied in blocking buffer for 45 minutes at room temperature. The secondary antibody was then washed off in PBS and 5ug/mL DAPI was applied for 5 minutes in the dark at room temperature. After thorough washing in PBS, Cells were mounted in Prolong Gold fluorescence mounting media without DAPI (Molecular Probes) and allowed to cure overnight before viewing. DAPI and fluorescent Alexa Fluor-conjugated secondary antibodies and phalloidin were purchased from Molecular Probes and applied according to the manufacturer's instructions.

2.12 Immunohistochemistry

Mammary gland and xenograft tumor sections on Superfrost plus microscope slides were baked at 62^{o}C for 30 minutes in an upright position then rehydrated by sequential washes in xylene and a series of graded ethanol washes. Antigen retrieval was performed for 10 minutes at 98°C in 0.01 mol/L sodium citrate buffer, pH 6.0, in a microwave oven. When appropriate, sections were incubated in 3% hydrogen peroxide for 6 minutes to block endogenous peroxidase activity. After a 45 minute block in 10% serum, the sections were incubated with the primary antibody overnight at 4^{o}C or for two hours at room temperature. Secondary detection was performed with a fluorescent secondary antibody or the appropriate biotinylated secondary antibody, Vectastain ABC elite kit, and DAB (Vector Labs, Burlingame, CA).

2.13 Co-immunoprecipitation

Protein samples from MCF-7 cells were harvested in non-denaturing protein lysis buffer supplemented with protease and phosphostase inhibtors. 100 were pre-cleared twice with salmon sperm DNA/protein A agarose-50% slurry in TE/Na azide/0.1%BSA, the supernatant was incubated overnight with antibody at 4^{o}C. Antibodies used were anti-Sim2 (1:100, Chemicon), normal rabbit IgG (1:1000, Upstate), and anti-NFκB p65 (1:100, Abcam). The salmon sperm DNA/protein A agarose-50% slurry was then used to collect the antibody complexes for 1 hour at 4^{o}C. Agarose was pelleted at 1000 x *g* at 4^{o}C for 1 minute and washed consecutively with low salt immune complex wash buffer, high salt immune complex wash buffer, lithium chloride immune complex wash buffer and TE buffer. The pellet was resuspended in 50 µl of 1X SDS-PAGE loading buffer,

boiled for 5 minutes and 10 µl of sample was run by SDS-PAGE. Western blotting was performed as described above, with anti-Sim2 and rabbit anti-NFκB p65 (1:1000, Abcam) primary antibodies.

2.14 Flow cytometry

MCF-7 cells bearing either a control (SCR) or SIM2-specific (SIM2*i*) shRNA expression construct were analysed by flow cytometry according to the protocol recommended by BD. Briefly, cells were washed, trypsinized, counted on a Coulter counter, and resuspended in PBS, 1% FBS at 2.5 million cells per ml. 250,000 cell aliquots of this suspension were incubated with 20 µl of experimental antibodies or isotype controls for 30 minutes at RT in the dark as recommended by BD. Cells were again washed, resuspended in PBS 1% FBS and analyzed on a FACSCalibur (Becton Dickinson Immunocytometry Systems) flow cytometer, equipped with a 15 mW air-cooled argon laser, using CellQuest (Becton Dickinson) acquisition software. List mode data were acquired on a minimum of 10,000 events falling within light scatter gates set to include cells while excluding dead cells and clumps of cells. Data analysis was performed in FlowJo (Treestar, Inc.) using forward and side light scatter to gate the cells. Antibodies and isotype controls used in flow cytometry experiments were purchased from Becton Dickinson and used according to the manufacturer's protocol.

CHAPTER III

LOSS OF SIM2s INDUCES EMT IN MCF-7 CELLS*

3.1 shRNA directed to SIM2s promotes EMT

Previously, we have shown that SIM2s expression is lost in human breast tumors and correlates inversely with breast cancer cell invasiveness (336). Furthermore, reintroduction of SIM2s into highly invasive cancer cells resulted in decreased proliferation, migration and invasion. To determine if loss of SIM2s is sufficient to cause progression, MCF-7 cells were transduced with either a non-specific "scrambled" control (SCR) shRNA retroviral construct, or one of three SIM2-specific shRNA constructs targeting different regions of the SIM2 mRNA (SIM2i_{114478}, and SIM2i_{3116} and SIM2i_{114477}, Fig. 7A). Significant reduction in SIM2s protein was observed in the SIM2i_{114478}, and SIM2i_{3116} cell lines (Fig. 7B), but not in SIM2i_{114477} (data not shown). In three independent infections, MCF-7 SIM2i_{3116} and SIM2i_{114478} cells showed significantly enhanced invasive ability (Fig. 6C) and underwent a morphological change from the cobblestone epithelial shape typical of MCF-7 cells to a spindly mesenchymal cell-like morphology (Fig. 7D), suggesting that loss of SIM2s expression had induced EMT.

---

*Part of the data reported in this chapter is reprinted with permission from "Loss of singleminded-2s in the mouse mammary gland induces an epithelial-mesenchymal transition associated with up-regulation of slug and matrix metalloprotease 2" by Laffin et al., 2008. *Molecular and Cellular Biology*, 2008 Mar;28(6):1936-46. Copyright 2008 American Society for Microbiology

To confirm that the morphological changes observed with the loss of SIM2s was indeed an EMT, we utilized the SIM2*i*$_{3116}$ MCF-7 cell line, which will be referred to from here on as SIM2*i*, to assay the expression of additional epithelial and mesenchymal cell markers. Western blots (Fig. 7E), differential interference contrast microscopy (Fig. 8A) and immunofluorescence analysis (Fig. 8B) confirmed that SIM2*i* cells lost expression of keratin 18 and E-cadherin and increased expression of N-cadherin and vimentin. Although SIM2*i* MCF-7 cells express mesenchymal markers and do not express E-cadherin, increased nuclear accumulation of ß-catenin was not detectable by antibodies against the active, non-phosphorylated (S37, T41) form (data not shown). There was, however, a marked increase in nuclear accumulation of the phospho-S33, S37, T41 form of ß-catenin (Fig. 8B), a phenomenon recently shown to be associated with poor prognosis in aggressive breast carcinomas (361). Changes in SIM2*i* protein levels were accompanied by dramatic decreases in keratin 18 and E-cadherin message and increased N-cadherin and vimentin mRNA, as measured by real-time RT-PCR (Fig. 8C). Together, these data indicate that loss of SIM2s in MCF-7 cells results in a morphological, functional and biochemical switch from an epithelial to a more mesenchymal-like phenotype.

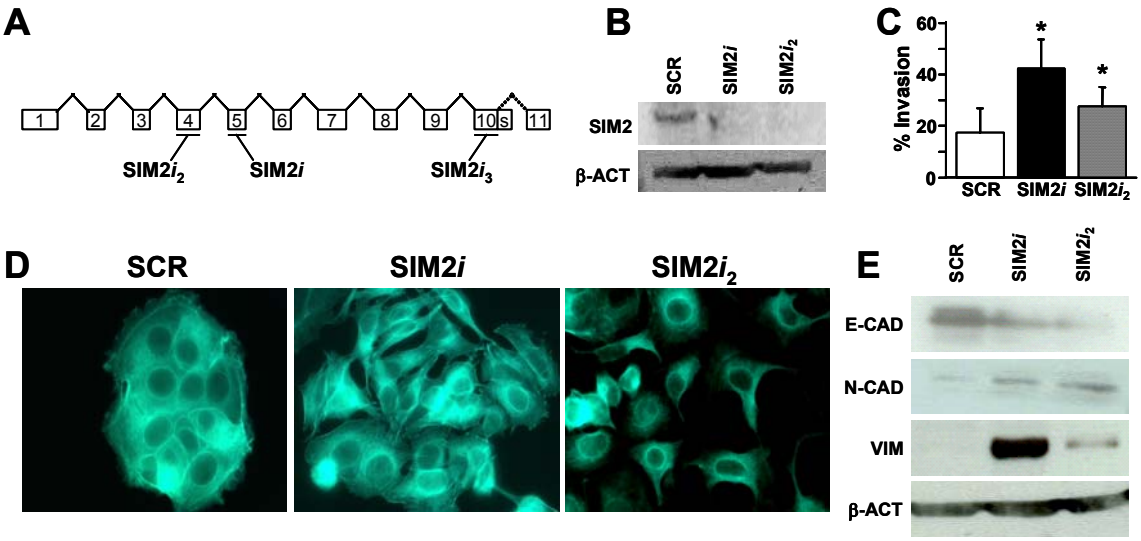

Figure 7. Silencing of SIM2s causes EMT in MCF-7 cells. (A) Structure of the SIM2s mRNA transcript showing region targeted by shRNA constructs. Exons are indicated by numbered boxes. (B) Infection of MCF-7 cells with shRNA constructs SIM2*i*3116 (SIM2*i*) or SIM2*i*114478 (SIM2*i*2) resulted in decreased SIM2s protein levels in comparison to a non-specific control shRNA construct (SCR). SIM2*i*3 was ineffective (data not shown). (C) Down regulation of SIM2s significantly increased MCF-7 cell invasive ability. Data are represented as the mean ± SEM, * indicates $p<0.05$. (D) Phaloidin staining demonstrates that decreased SIM2s expression correlated with loss of epithelial morphology and acquisition of a more spindly appearance. Bar = 100μm. (E) Western analyses of SCR Keratin, E-cadherin, N-cadherin, and Vimentin indicated that MCF-7 cells targeted for SIM2s down regulation lose epithelial markers and gain mesenchymal ones.

3.2 SIM2*i* MCF-7 cells form rapidly growing ERα$^-$ tumors in nude mice

To assess the tumorigenic effects of SIM2s loss, we compared tumor forming ability of SIM2*i* cells to control cells using a nude mouse xenograft assay. SIM2*i* cells rapidly developed into tumors that were three times larger than controls by day 10 (Fig. 9A). SIM2*i* cell derived tumors maintained this size advantage throughout the experiment and were 6-fold larger than SCR-derived tumors with an average weight 7-fold higher than control tumors at the conclusion of the study seventeen days after injection (Fig. 9B). SIM2*i* tumors appeared to be more vascularized than control tumors (Fig. 9C), an observation that was confirmed by increased CD31 and VEGF immunoreactivity of SIM2*i*-derived tumor sections (Fig. 9D). Quantification of BrdU-positive cells from

xenograft tumor sections showed a 35-fold increase in SIM2*i* cell proliferation (Fig. 9D; SCR = 1.1% ± 0.543%, SIM2*i* = 35.1% ± 2.24%), suggesting a link between increased vascularity, cell proliferation and tumor growth in SIM2*i*-derived tumors. Similar to our in vitro studies (Fig. 8), SIM2i-derived tumors displayed signs of EMT with decreased E-cadherin and increased vimentin staining (Fig. 9D).

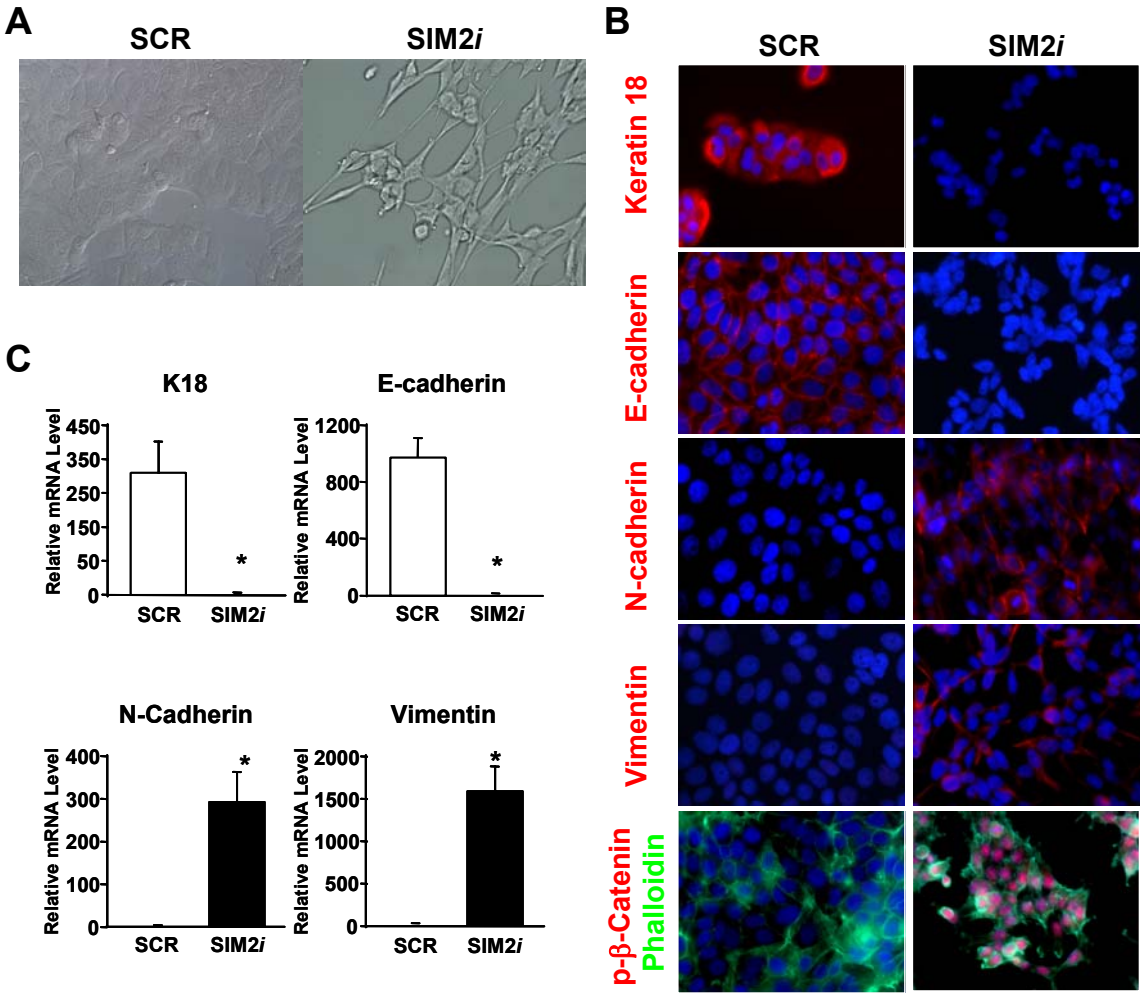

Figure 8. Conformation of EMT in SIM2*i* MCF-7 cells. (A) Differential interference contrast images showing detailed morphology of SCR and SIM2*i* MCF-7 cells. (B)Immunofluorescent staining of control (SCR, top panels) and SIM2*i* (bottom panels) MCF-7 cells corroborated the Western blot data showing that loss of SIM2s expression results in a switch from an epithelial to a more mesenchymal phenotype. In addition, increased nuclear staining of phosphorylated ß-catenin, a phenomenon recently associated with poor breast cancer prognosis, can be seen in SIM2*i* cells. (C) Real time RT-PCR analyses of SCR and SIM2*i* MCF-7 cells for expression of Keratin 18, E-cadherin, N-cadherin and Vimentin mRNA. Data were obtained from three wells per group, analyzed by the ΔCT method and are expressed as the average fold difference ± S.E.M. * p>0.05.

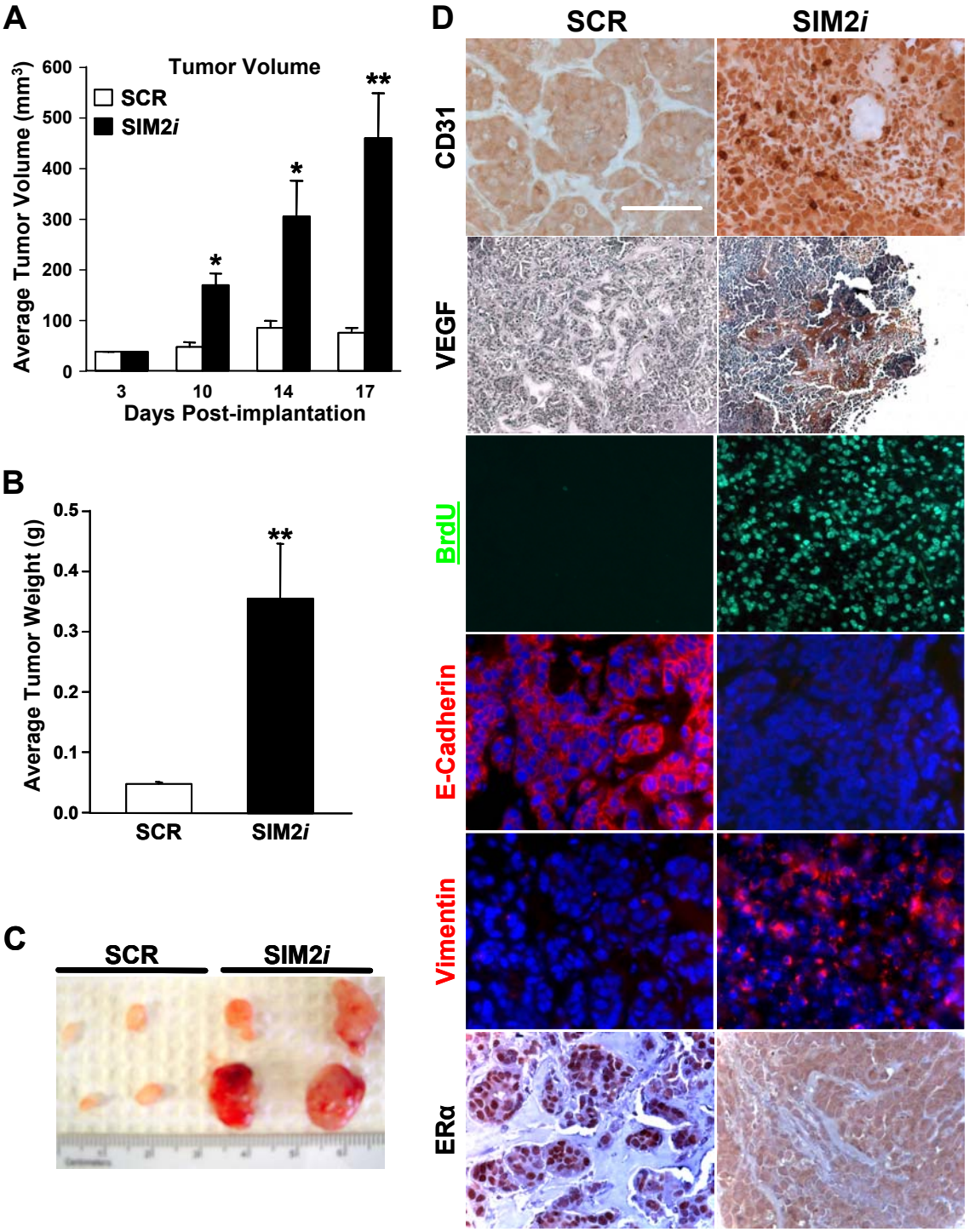

Figure 9. Loss of SIM2s enhances *in vivo* tumorigenicity. SCR and SIM2i MCF-7 cells were mixed with Matrigel and injected into the flanks of nude mice to determine the effects of SIM2s loss on tumor growth (A) SIM2*i* MCF-7 tumors were significantly larger than control tumors by ten days post-injection (B) The average weight of SIM2*i* derived tumors was significantly higher than control tumors. (C) Representative tumors from SCR and SIM2*i* MCF-7 cells. Note the apparent increased vascularization in SIM2*i*-derived tumors, supported by CD31 and VEGF protein staining (D). BrdU staining indicated that SIM2i tumor cells divide at a significantly higher rate than SCR control tumors, which maintained their EMT phenotype *in vivo* (D). The lack of an exogenous estrogen requirement, corresponded with loss of ER□expression. Bar = 100μm. Data are represented as mean ± SEM, * indicates $p<0.05$, ** indicates $p<0.005$.

Normally, tumor development in the MCF-7 xenograft model requires exogenous estrogen to sustain growth. Therefore, we were surprised to see tumors develop so rapidly in the absence of estrogen. The accelerated rate of SIM2*i* tumor growth coupled with the apparent estrogen-independent nature of this growth prompted us to look at ERα expression. Indeed, ERα was undetectable in SIM2*i*-derived tumors by immunohistochemistry (Fig. 9D), or in SIM2*i* MCF-7 cells by either real-time RT-PCR (Fig. 10A) or western blot (Fig. 10B). Furthermore, SIM2*i* cells no longer responded to estrogen treatment as measured by induction of the estrogen-responsive genes PR and PS2 (Fig. 10C and 9D). The striking increase in SIM2*i* MCF-7 cell tumorigenesis confirms that loss of SIM2 has functional consequences *in vivo* and provides further evidence that SIM2s may represent an important hurdle to breast cancer progression.

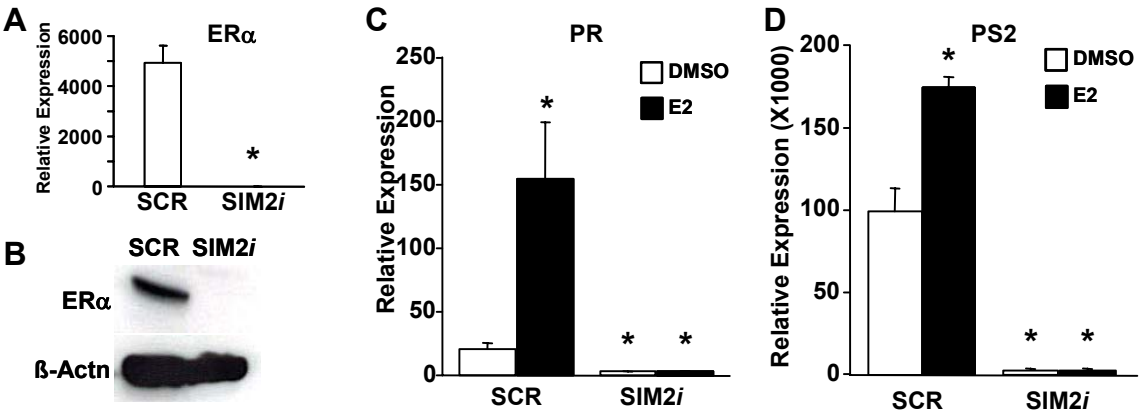

Figure 10. Loss of ER□expression and estrogen responsiveness in SIM2*i* MCF-7 cells. (A) Quantitative real time PCR analysis of control (SCR) and SIM2i MCF-7 cells for ER□RNA. Data were obtained from three wells per group, analyzed by the ΔCT method and are expressed as the average fold difference ± S.E.M. * p>0.05. (B) Western analysis of SCR and SIM2*i* MCF-7 cells corroborated the mRNA data and confirmed that loss of SIM2s expression results in loss of □R□. (C-D) Quantitative real time PCR analysis of vehicle (DMSO) and estradiol (E2) treated SCR and SIM2*i* MCF-7 cells indicated that estrogen-responsiveness is lost in SIM2*i* cells. Both progesterone receptor (C) and PS2 (D) mRNA induction following estradiol treatment was lost in SIM2*i* cells. Data are presented as the average fold difference ± S.E.M. * p>0.05.

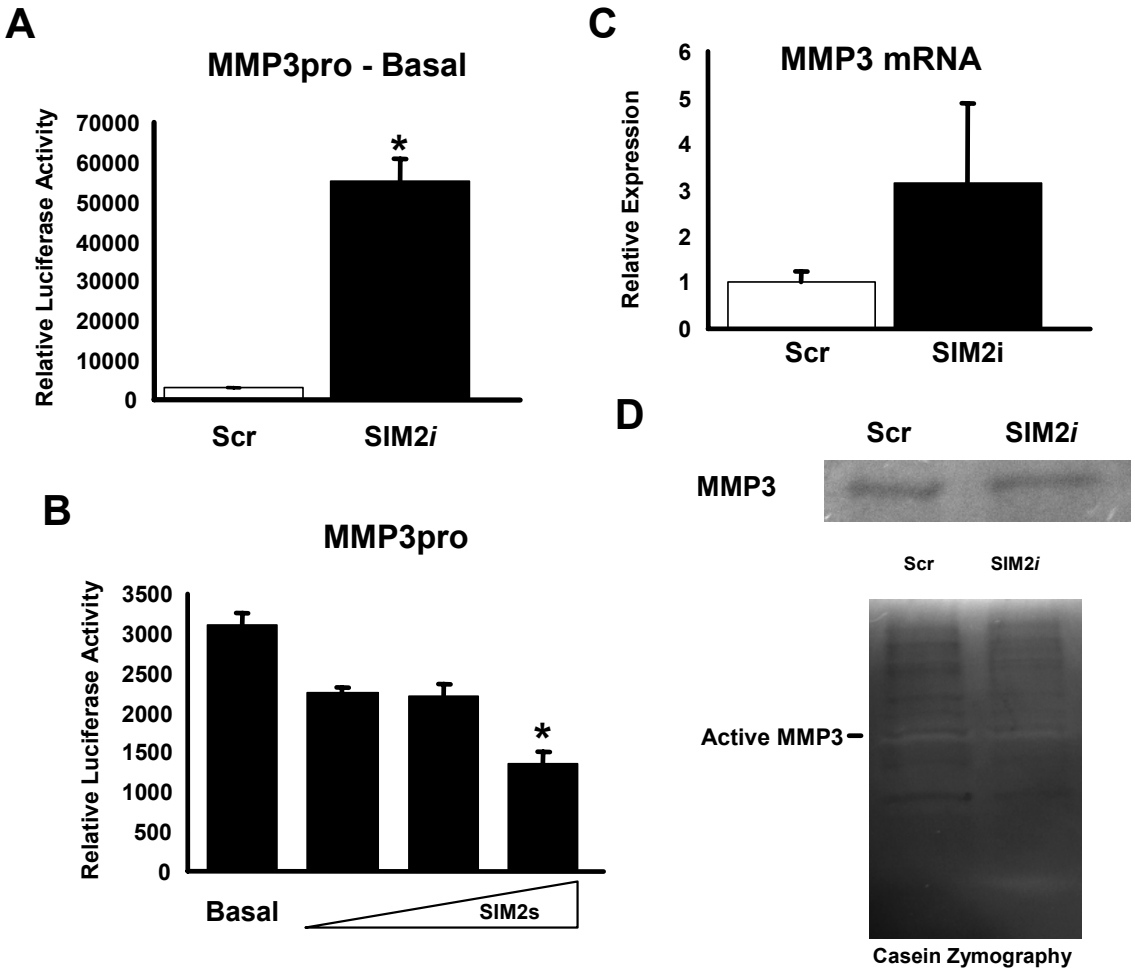

Figure 11. MMP3 expression and activity in SCR and SIM2*i* MCF-7 cells. (A) Basal MMP3 promoter activty is increased in SIM2*i* MCF-7 cells. (B) SIM2s represses expression from an MMP3 promoter construct in a dose-dependent fashion. (C) MMP3 mRNA expression is elevated in SIM2*i* MCF-7 cells. (D) Loss of SIM2 has no measurable effect on MMP3 protein secretion (top panel) or activation (bottom panel) in conditioned media from MCF-7 cells.

3.3 MMP3 and Rac1b are not induced in MCF-7 cells upon loss of SIM2s and MMP inhibition does not affect the EMT phenotype

In previous studies utilizing MDA-MB-435 cells, we reported that MMP3 is a direct target of SIM2s-mediated transcriptional repression (362). MMP3 has also been

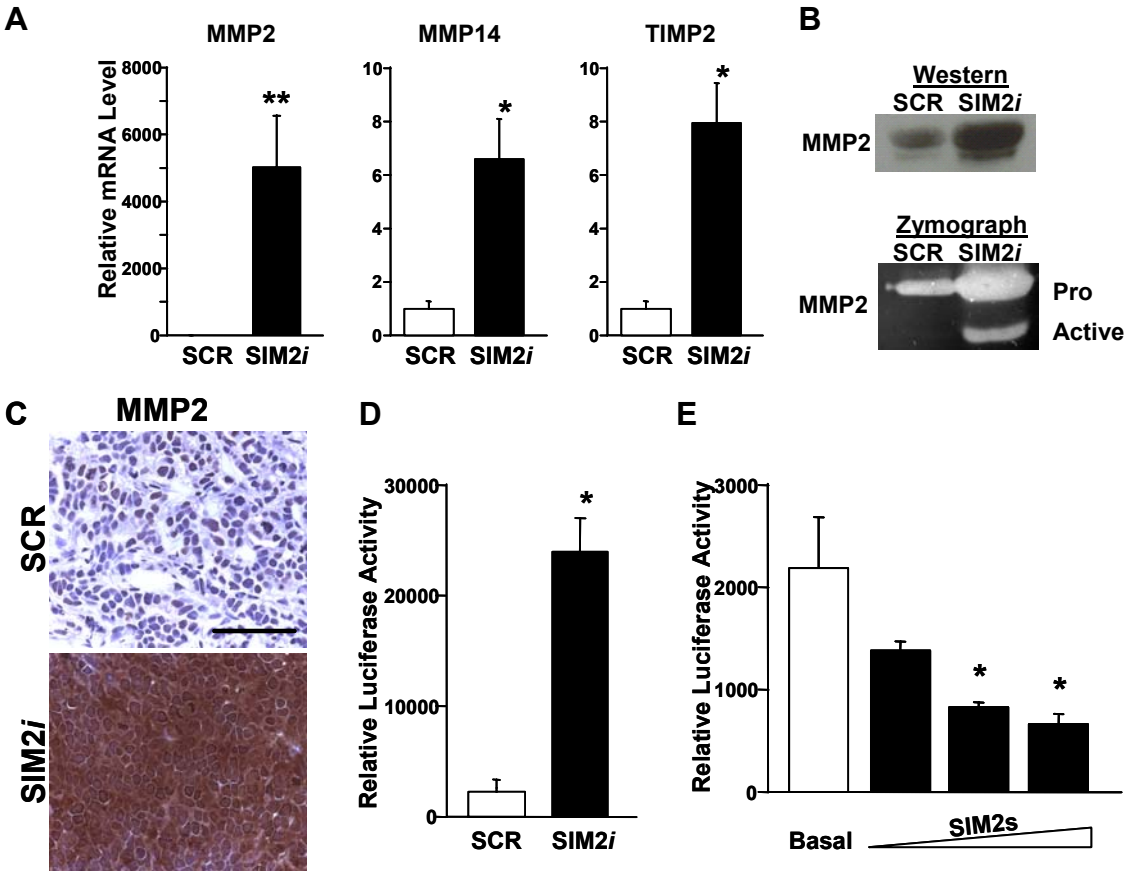

Figure 12. SIM2s inhibits MMP2 expression and activation. (A) Expression of MMP2,MMP14 and TIMP2 was increased in SIM2*i* MCF-7 cells in comparison to control cells. (B) Increased MMP2 mRNA corresponded to increased MMP2 protein (top) and activity (bottom) in SIM2*i* MCF-7 (C) Immunostaining of SCR and SIM2*i*-derived tumor sections indicated that MMP2 expression was significantly elevated in SIM2*i*-derived tumors. (D) Basal expression of an MMP2 promoter controlled reporter was significantly elevated in SIM2*i* cells suggesting that SIM2s can directly repress MMP2 expression, consistent with dose-dependant effects of SIM2s on repression of an MMP2-controled reporter (E). Data are represented as mean ± SEM, * indicates $p<0.05$, ** indicates $p<0.005$, Bar = 100μm.

reported to be sufficient to initiate EMT via generation of reactive oxygen species and a splice variant of Rac1, Rac1b (363). Therefore, we hypothesized that up-regulation of MMP3 may contribute to the aggressive, invasive phenotype observed in SIM2s-depleted cells. We observed an increase in MMP3 promoter activity in the SIM2*i* cells, and SIM2s retained its ability to repress the MMP3 promoter in a dose-dependent fashion in MCF-7 cells (Fig. 11A and 10B), consistent with previous results. However, in contrast to our

findings in MDA-MB-435 cells, MMP3 mRNA expression was not significantly altered (Fig. 11C), and MMP3 protein expression and activity were unchanged (Fig. 11D), suggesting that this apparently inconsistent result is due to intrinsic differences in basal MMP3 expression between MDA-MB-435 and MCF-7 cells.

3.4 SIM2s represses MMP2 expression and activity

As previous work had suggested that SIM2s may regulate several MMPs, we measured expression of several MMPs and related factors in SCR and SIM2*i* cells by real time RT-PCR to determine if another MMP could be playing a similar role to MMP3 in EMT promotion. We found MMP2 to be up regulated >4,500-fold in SIM2*i* cells, while others including MMP9 were unchanged (Fig. 12A and not shown). MMP14 and TIMP2, which are required for MMP2 activation, were also up regulated approximately 6- and 7-fold, respectively, in SIM2*i* cells (Fig. 12A). The MMP2 mRNA increase observed in SIM2*i* cells was corroborated at the protein and activity levels (Fig. 12B). In addition, MMP2 levels were markedly elevated in xenograft tumor sections derived from SIM2*i* cells in comparison to those derived from control cells (Fig. 12C), confirming that loss of SIM2s lead to increased MMP2 expression.

Increased MMP2 expression was attributable to de-repression of the MMP2 promoter, as expression of an MMP2-controlled luciferase reporter was significantly higher in SIM2*i* cells (Fig. 12D). Co-transfection of the MMP2 reporter and increasing amounts of SIM2s expression vector into MCF-7 cells resulted in dose-dependent inhibition of luciferase activity (Fig. 12E). These results suggested that MMP2 could be playing a role in EMT regulation similar to MMP3, however, we could not modulate expression of any EMT-related factors in MCF-7 with MMP inhibitors or free radical scavengers, and Rac1b expression was lower after the onset of EMT (data not shown). This implies that MMP2 does not regulate EMT in MCF-7 cells, and that protease-mediated mechanisms are not involved in the EMT observed after SIM2 depletion. Recently, other studies have also shown that MMP activity is not required for EMT (136). These findings suggest that regulation of MMPs by SIM2s is important for its tumor suppressor function but is not the mechanism by which SIM2s regulates EMT-like processes.

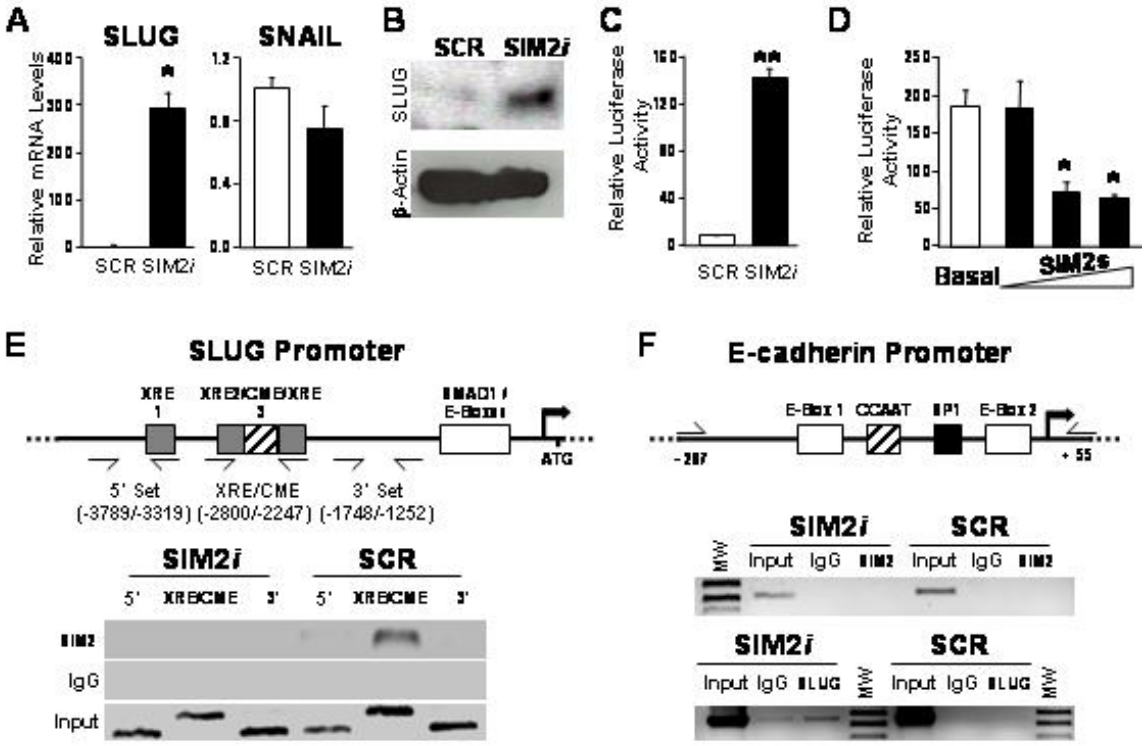

Figure 13. SIM2s binds and represses expression from the SLUG promoter. (A) SLUG, but not SNAIL, mRNA levels are significantly reduced following loss of SIM2s expression in MCF-7 cells. (B) Increased SLUG mRNA observed in SIM2*i* cells corresponded to significantly elevated SLUG protein levels, as measured by Western blot. (C) Expression of a SLUG promoter-controlled reporter was siginificantly increased in SIM2*i* MCF-7 cells. Data are represented as mean ±SEM, * indicates $p<0.05$. (D) SIM2s-mediated repression of SLUG is dose-dependent as increasing amounts of SIM2s expression vector repressed expression of the SLUG reporter. Data are represented as mean ±SEM, * indicates $p<0.05$, ** indicates $p<0.005$. (E) Several putative regulatory regions are present in the first 3280 bp of the SLUG promoter (top). ChIP analysis using an antibody to SIM2 was used to ascertain SIM2s binding to the SLUG promoter in SCR and SIM2*i* MCF-7 cells. Precipitated chromatin was assayed for the presence of SLUG promoter DNA surrounding a region containing a CME and multiple XRE consensus sequences using primers indicated by arrows in the promoter schematic. SIM2s protein was detectable in this region of the SLUG promoter in SCR cells ony. Binding of SIM2 was not observed in regions 500-1000 bp upstream or downstream of the CME region. XRE; xenobiotic response element, CME; central midline response element, LEF-TCF; lymphoid enhancer factor / T-cell factor response element. (F) SLUG and SIM2s binding to the E-cadherin promoter was analyzed in SCR and SIM2*i* MCF-7 cells by ChIP. A schematic representation of the human E-cadherin promoter from -287 to +55 with respect to the transcriptional start point shows putative E-box, CCAAT enhancer binding protein and SP1 regulatory regions as well as the relative positions of primers used to assay binding. SLUG binding to the E-cadherin promoter was detectable in SIM2*i* cells, but not in SCR cells. In contrast, SIM2s binding to the e-cadherin promoter could not be detected in either cell line. Data are represented as mean ±SEM, * indicates $p<0.05$, ** indicates $p<0.005$.

3.5 SIM2s participates in maintenance of E-cadherin expression via repression of slug

We next explored the possibility that SIM2s may regulate other factors involved in EMT. Members of the SNAIL family of transcription factors have been implicated in regulation of both normal and pathological EMT events (242, 364-366). During cancer progression, increased SNAIL binding to E-box regulatory DNA elements causes transcriptional repression of E-cad, which contributes to transformation, angiogenesis and EMT (242, 364-366). To determine if members of the SNAIL family are involved in the EMT induced by SIM2s loss, SCR and SIM2*i* cells were analyzed for snail and slug mRNA levels by real time RT-PCR. SNAIL mRNA levels were not significantly affected by SIM2 loss in MCF-7 cells (Fig. 13A). In contrast, slug expression was up regulated more than 250-fold in SIM2*i* cells (Fig. 13A), which corresponded to an increase in slug protein levels as determined by Western analysis (Fig. 13B).

Since SIM2s functions as a transcriptional repressor (18, 20, 25), we hypothesized that SIM2s directly inhibits slug expression at the promoter level. A luciferase reporter under control of the human SLUG promoter was transfected into SCR and SIM2*i* MCF7 cells and analyzed for activity. In SIM2*i* MCF-7 cells, basal reporter expression was increased 10-fold over control cells (Fig. 13C). In addition, we observed concentration-dependent repression of SLUG promoter-controlled gene expression with increasing amounts of SIM2s in MCF-7 cells (Fig. 13D). The human SLUG promoter contains multiple putative regulatory elements including E-boxes, xenobiotic response elements (XREs), and central midline element (CME) core sequences (Fig. 13E). Using an

antibody to SIM2 in ChIP analyses, we found that SIM2s binds a region of the SLUG promoter containing the CME and two XRE core sequences in SCR, but not SIM2*i* MCF-7 cells (Fig. 13E). Analysis with primer sets 500 bp upstream and 500 bp downstream of the CME demonstrate that the binding is specific to the CME region (Fig 12E). SIM2s was unable to bind a region of the E-cadherin promoter containing E-boxes that are targeted by SNAIL protein family members; however, increased binding of SLUG to this region was apparent in SIM2*i* MCF-7 cells (Fig. 13F). As the ChIP primers used in our study flank the putative CME and two XREs, it seems likely that SIM2s-mediated repression of SLUG involves binding of SIM2s to one or more of these elements. Taken together, these data suggest that loss of SIM2s leads to de-repression of SLUG expression and increased slug binding to the E-cadherin promoter where it potentially plays a role in repressing E-cadherin transcription.

3.6 Sim2$^{-/-}$ mammary glands display hallmarks of EMT

Our initial analyses of Sim2$^{-/-}$ mammary outgrowths, coupled with *in vitro* MCF-7 cell studies, strongly suggest that Sim2s restricts tumor progression associated with EMT-like events. To confirm this *in vivo*, Sim2$^{-/-}$ mammary sections were analyzed for various epithelial and mesenchymal markers. Uniform polarity (measured by Aquaporin-5 staining) and robust E-cadherin staining was observed throughout wild-type mammary epithelium, but was totally absent in Sim2$^{-/-}$ glands (Fig. 14A). Not surprisingly, the increased invasive ability of Sim2$^{-/-}$ epithelial cells was associated with increased Mmp2 protein levels (Fig. 14A). These observations strongly suggest that an EMT similar to that observed in SIM2*i* MCF-7 cells had occurred in Sim2$^{-/-}$ glands. This was further

supported by increased nuclear accumulation of ß-catenin in Sim2$^{-/-}$ ductal epithelium (Fig. 14A). Consistent with our model that SIM2s-mediated repression of SLUG suppresses EMT, we found increased slug staining in Sim2$^{-/-}$ glands (Fig. 14A). Taken together, these data show that loss of Sim2s during mouse mammary gland ductal development results in slug up regulation, loss of epithelial cell characteristics, increased Mmp2 expression and invasion into the surrounding stroma, reminiscent of an EMT.

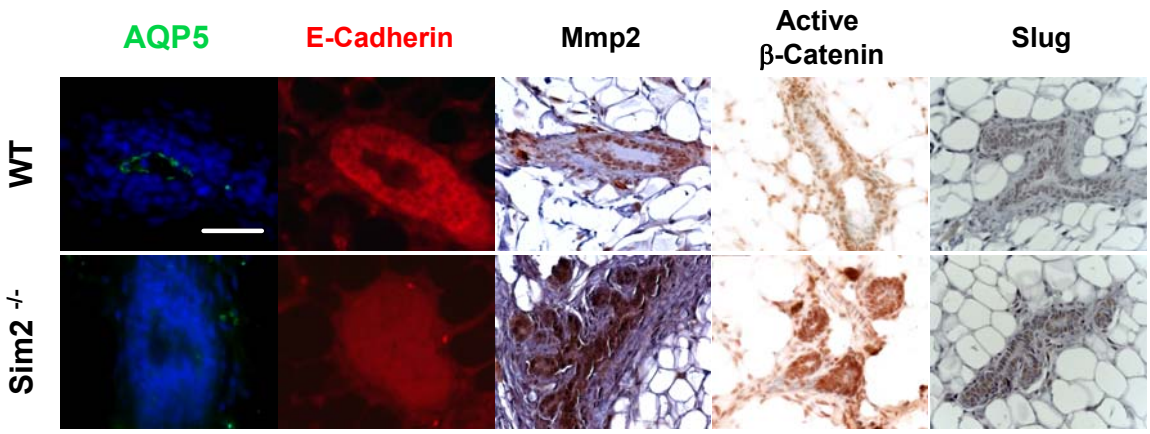

Figure 14. Loss of Sim2s in the mouse mammary gland results in a phenotype consistent with EMT. Analysis of mouse mammary outgrowths from WT and Sim2/- mice revealed that loss of Sim2s expression is associated with events including disrupted polarity as measured by aquaporin5 expression, loss of Ecadherin, up regulation of Mmp2 and increased nuclear accumulation of ß- catenin Consisten with our hypothesis that Sim2s mediated down regulation of Slug represses EMT, we found thatslug protein levels were significantly elevated in Sim2-/- mammary glands.

3.7 Silencing of SIM2 in normal breast-derived cells results in increased motility, invasiveness, and abnormal 3D acinar morphogenesis

EMT is rarely observed in breast tumors, typically in the most advanced metastatic cancers. Therefore, we asked whether silencing SIM2 in non-tumorigenic MCF-10A cells was sufficient to cause cellular transformation and / or EMT. SIM2

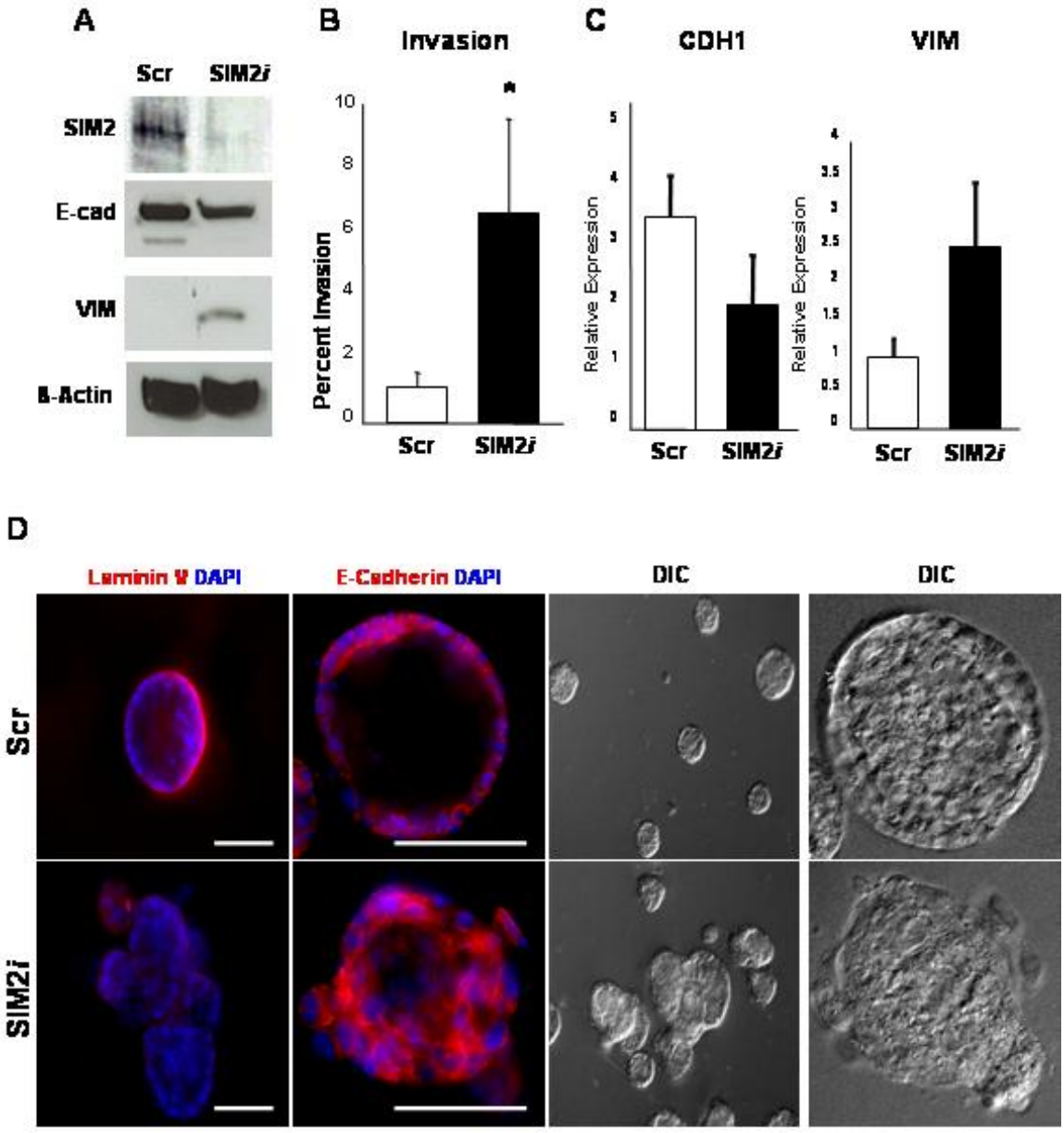

Figure 15. Silencing of SIM2 in MCF-10A Cells Disrupts Acinar Morphogenesis. (A) Western blot analysis of SIM2, E-cadherin, and Vimentin in Scr and SIM2*i* MCF-10A cells, demonstrating efficacy of knockdown and modest Vimentin expression. (B) Boyden invasion chamber assay comparing Scr and SIM2*i* MCF-10A cells. (C) Real-time RT-PCR did not reveal significant differences in expression of E-cadherin and Vimentin. (D) Immunofluorescence and DIC images of Scr and SIM2*i* MCF-10A acini grown on a matrigel basement showing loss of polarity and basement membrane intergrity, malformed lumens, and multilobular appearance upon loss of SIM2. Data presented as mean ± SEM * indicates $p<0.05$.

depletion had no effect on *in vitro* proliferation rate, consistent with results from MCF-7 cells (Fig. 15A and not shown). However, SIM2 loss did increase invasiveness and cause up-regulation of mesenchymal markers in cells grown as monolayers (Fig. 15A and 15B). Gene expression changes were modest, and not statistically significant (Fig. 15C). Thus, as expected, silencing of SIM2 was not sufficient to cause EMT in MCF-10A cells. This likely reflects that in the tumor-derived MCF-7 cells, other barriers to EMT have been lost, or that MCF-7 cells could overcome the cell cycle arrest often seen during EMT (30, 243, 367, 368). MCF-10A cells can be grown in a matrigel basement as three-dimensional spheroids, which more closely recreate the natural microenvironment of epithelial cells than does monolayer culture (369, 370). As in the mouse or human mammary gland, cells in these spheroids growth arrest and form a hollow lumen through an apoptotic mechanism, and in some cases can be induced to differentiate and produce milk (30, 371-374). Due to the highly disrupted structure we had observed in Sim2-/- mammary glands, we expected that depletion of SIM2 would disrupt acinar structure. By day 15, the control SCR MCF-10A cells had formed regular spheres with a single layer of polarized cells and a hollow lumen (Fig. 15D). In contrast, SIM2*i* MCF-10A cells were irregular and in some cases multi-lobular, and had small, misshapen, or absent lumens (Fig. 15D). Individual cells could be observed delaminating from the acinar structures and invading into the matrigel basement (Fig. 15D), suggestive of an EMT like event. However, E-cadherin expression was maintained in the SIM2*i* acini and no mesenchymal markers assayed were seen to be upregulated (Fig. 15D). As in Sim2 -/- mammary glands, the cells surrounding the lumens of SIM2*i* acini were poorly polarized and disorganized (Fig. 15D). Although highly abnormal, the SIM2*i* acini did undergo growth

arrest and remained growth factor dependent (not shown), suggesting that loss of SIM2 expression caused at most a partial transformation.

CHAPTER IV

EFFECT OF DEPLETION OF SIM2s ON SELF RENEWAL AND DNA DAMAGE RESPONSES IN MCF-7 CELLS

4.1 Loss of SIM2s increases mammosphere formation in MCF-7 cells

Multiple reports have established that a subpopulation of cells within tumors and cell lines is the reservoir of the vast majority of self-renewal and tumorigenic capacities possessed by the population as a whole (3, 375-379), and have termed these cells cancer stem cells or tumor-initiating cells. The SLUG oncogene, which we have previously shown to be a direct target of SIM2s in breast cancer cells (Fig. 13), has been shown to play a role in DNA damage responses and the biology of normal and transformed stem cells (114, 124, 277-280, 380). Therefore, we assessed *in vitro* self-renewal activity and DNA damage signaling in SCR and SIM2*i* MCF-7 cells. When plated under ultra-low attachment conditions in standard growth media, SIM2*i* MCF-7 cells had a 6-fold greater rate of mammosphere formation (Fig. 15), suggesting that depletion of SIM2s resulted in enhanced self-renewal capacity. However, when plated in serum free media supplemented with EGF and bFGF, there was no significant advantage for either cell line (not shown). This may indicate that loss of SIM2 did not increase self-renewal capacity per se, but conferred resistantance to the pro-differentiation effects of serum. Alternatively, the mammosphere forming population in the SCR MCF-7 line may be more growth factor-dependent than their counterparts in the SIM2*i* cells, which is masked by excess growth factors in the media.

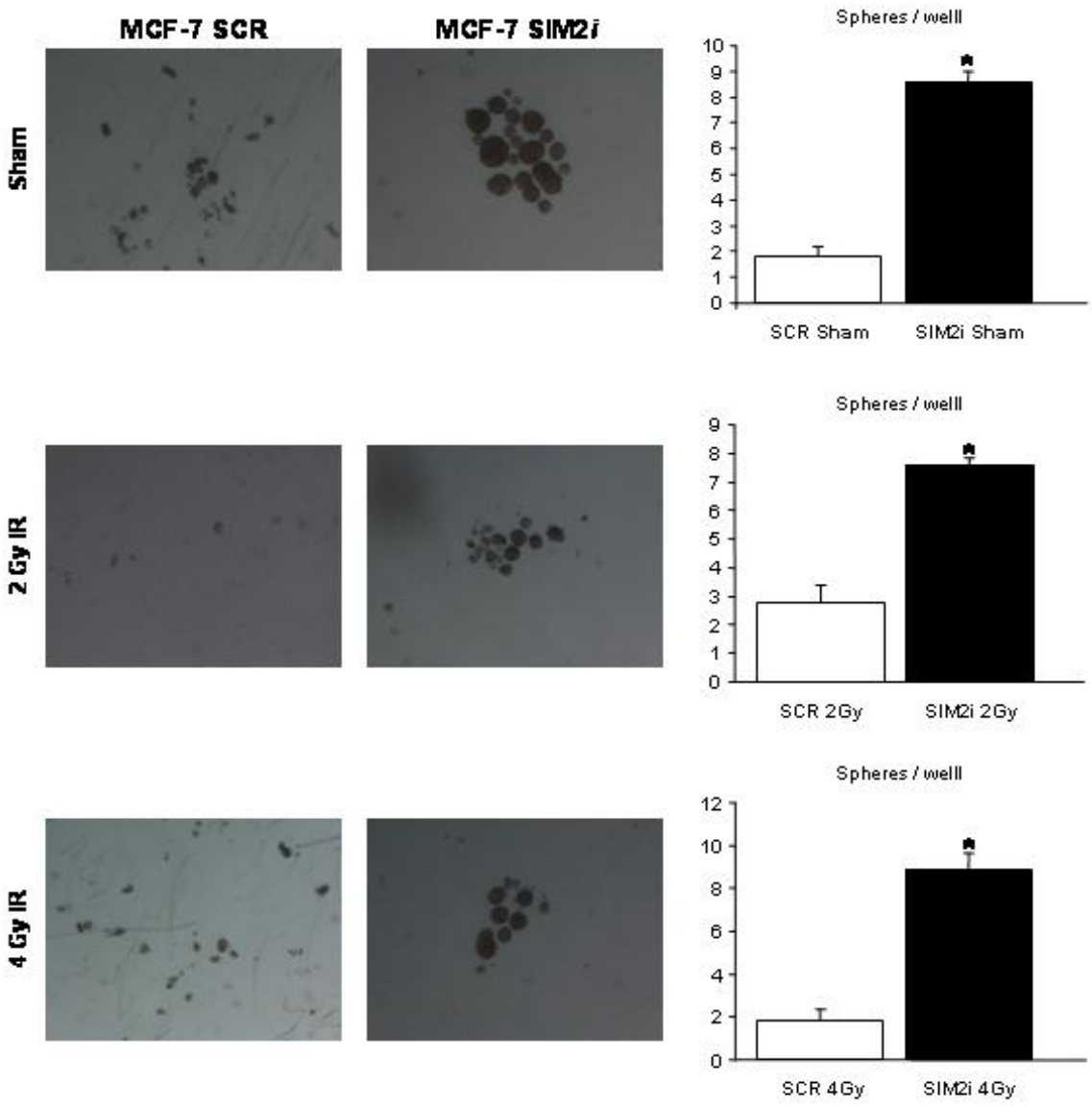

Figure 16.Silencing of SIM2 increases mammosphere forming capacity in MCF-7 cells. SIM2*i* cells display consistently higher mammosphere generation than SCR controls, with increasing doses of ionizing radiation having little to no effect on self renewal in either population. Sphere counts are presented as mean ± SEM, with a minimum of 12 wells counted per treatment group for each cell line, 14 days after plating. Spheres over 50µM were considered bona fide mammospheres and spheres below this size were not included in counts. * indicates $p<0.05$, ** indicates $p<0.005$.

Several reports suggest that expression of CD24, in combination with either CD29 or CD44, can be used in FACS experiments to sort out stem cell-like tumor initiating cells in MCF-7 cells (270, 381, 382), which are generally CD24lo and CD29 or CD44 positive.

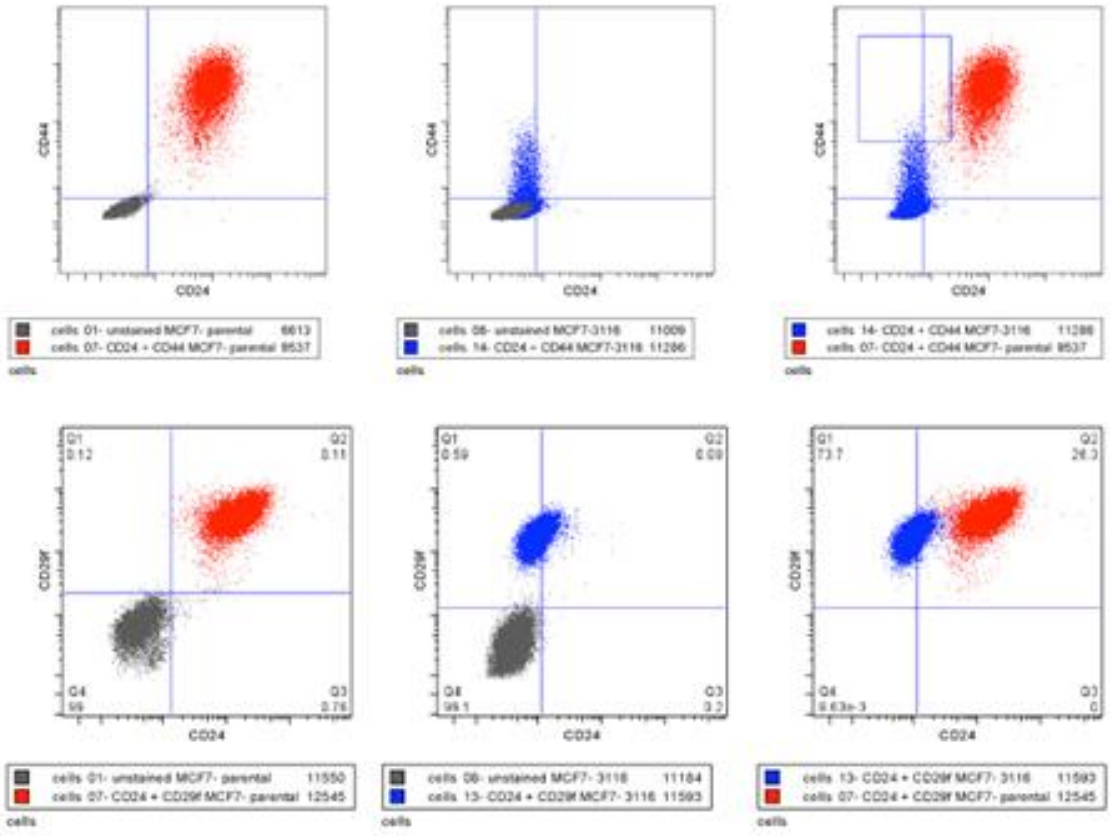

Figure 17. Assessment of putative tumor-initiating cell markers in SCR and SIM2*i* MCF-7 cells. The control MCF-7 line is represented by the red plot points and the SIM2*i* cells by the blue points. The majority of the SCR cells were CD24+/ CD44 double positive, with the putative tumor-initiating CD24lo CD44+ subpopulation comprising approximately 5% of the population (top row). SIM2*i* cells had dramatically reduced expression of both markers, with CD44 being essentially absent, consistent with EMT. SIM2*i* cells that did express CD24 did so at very low levels, consistent with increased numbers of stem-cell like cells, but the lack CD44 expression makes these results difficult to interpret. CD24 and CD29 have also been proposed as a useful tumor-initiating cell marker set. Similar to results obtained with CD24 and CD44, the majority of the control cells were double positive (bottom row). The SIM2*i* cells were largely CD24 negative as before, however, they maintained expression of CD29. The CD29+ CD24lo population in the SIM2*i* population was roughly 11% of the cells, as opposed to 5% for the SCR line, consistent with the increased mammosphere and tumor forming capacity displayed by the SIM2*i* cells.

Comparison of these markers in SCR and SIM2*i* MCF-7 revealed that nearly all SCR MCF-7 cells were CD24+ CD44+, and the putative tumor-initiating cell enriched CD24low CD44+ population comprised approximately 5% of the total population, consistent with previous results from other laboratories (Fig. 16). SIM2*i* cells had largely ceased to express CD44, consistent with an EMT (Fig. 16). CD24 expression was also

greatly reduced, but a significant population of CD24low cells could still be observed (Fig. 16). These results were difficult to interpret due to the complete loss of CD44 in the SIM2*i* cells, so we performed a similar experiment using antibodies to CD24 and CD29. As shown in Fig 16, the SCR cells were largely double positive for the markers assayed, but contained a CD24low CD29+ subpopulation which accounted for approximately 5% of the cells. The majority of SIM2*i* MCF-7 cells were also CD29+, but only a small fraction were CD24+, and these expressed low amounts of CD24 (Fig. 16). There appeared to greater numbers of CD24low CD29+ cells in the SIM2*i* cells, suggesting that they contained more tumor-initiating cells, which is consistent with their greater tumorgenicity (Fig. 16 and 8). It has been observed that treatments with ionizing radiation can enrich for stem-like cells, which are more resistant to cellular stress and DNA damage (278, 381). In order to determine if the expanded CD24low CD29+ population in the SIM2*i* MCF-7 cells could be stem-cell like, we analyzed sham exposed and 10Gy - exposed cells for expression of CD24 and CD29. As expected, treatment with ionizing radiation enriched for CD24low CD29+ cells, suggesting that expansion of this cell type in the SIM2*i* MCF-7 cells may explain their greater tumorgenicity and *in vitro* self-renewal (Fig. 17).

4.2 Loss of SIM2s increases DNA damage resistance and alters DNA damage responses

Expression of slug and stem cell-like behavior are associated with drug resistance, and therefore we expected that SIM2*i* MCF-7 cells would be more resistant to DNA

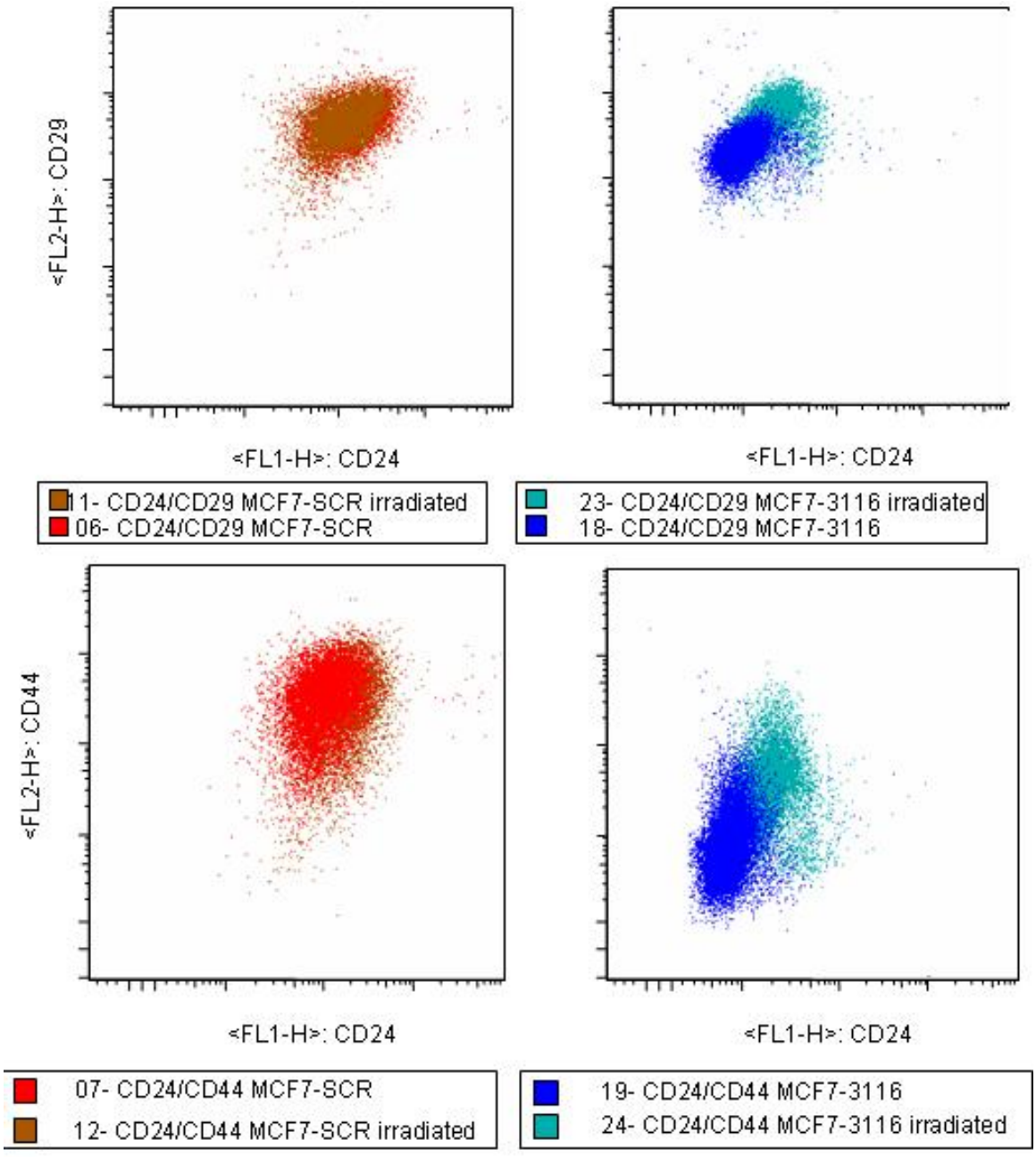

Figure 18. Effect of ionizing radiation on tumor-initiating cell marker expression in SCR and SIM2*i* MCF-7 cells. Treatment with 10Gy of IR significantly increased the proportion of CD29+ CD24lo and CD44+ CD24lo cells in SIM2*i* cells and to a lesser degree in the SCR MCF-7 cell line, suggesting that these cells are the self-renewing portion of the population.

damaging agents than their SCR counterparts. As expected, SIM2*i* MCF-7 cells were resistant to the anthrcycline radiomimetic doxorubicin (Fig. 18A). However, the SIM2*i* MCF-7 cells were at least as sensitive to ionizing radiation as the SCR cells (Fig. 18A), raising the possibility that the resistance to doxorubicin was due to stem cell associated drug pumps (383).

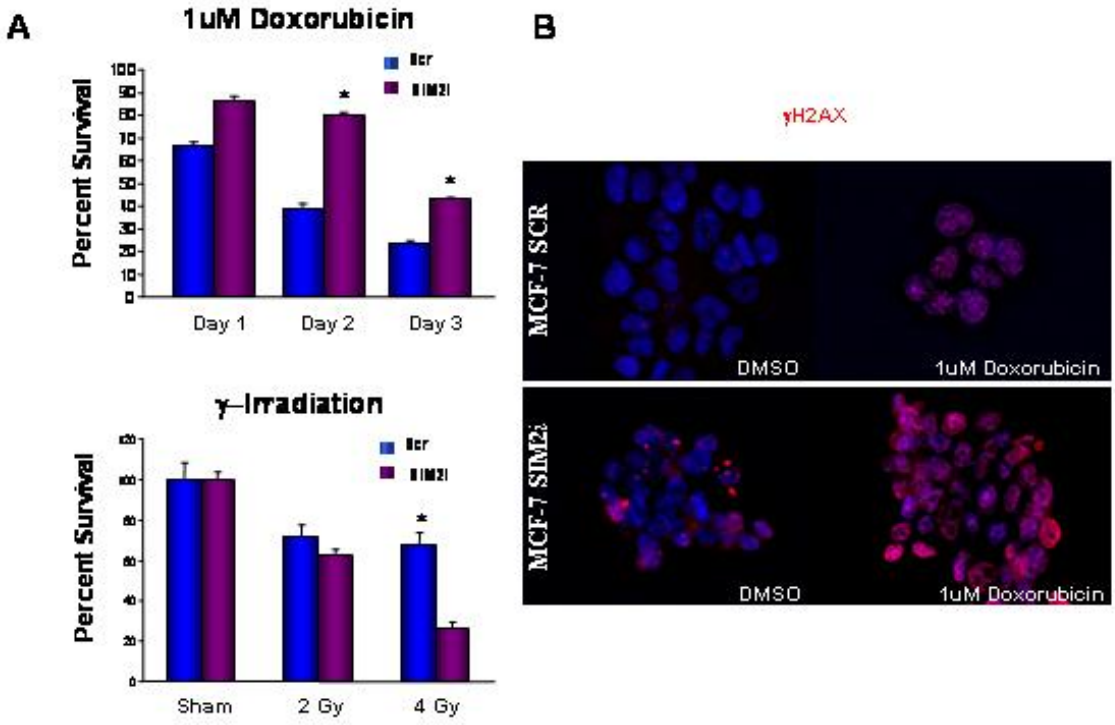

Figure 19. SIM2*i* MCF-7 are resistant to Doxorubicin via a mechanism that does not involve drug reflux. (A) SIM2*i* MCF-7 display siginificant resistance to doxorubicin, despite being sensitized to higher doses of ionizing radiation. (B) The resistance of SIM2*i* MCF-7 is unlikely to be due to drug efflux, as staining of phopho-γH2AX double strand break foci reveals that the SIM2*i* cells sustain at least as much DNA damage as the SCR cells after doxorubicin treatment.

In order to test this, we performed immunofluorescent staining of gH2AX foci, which localized to sites of DNA damage under repair. Both SCR and SIM2*i* MCF-7 cells had numerous gH2AX foci after doxorubicin treatment, and there was no observable

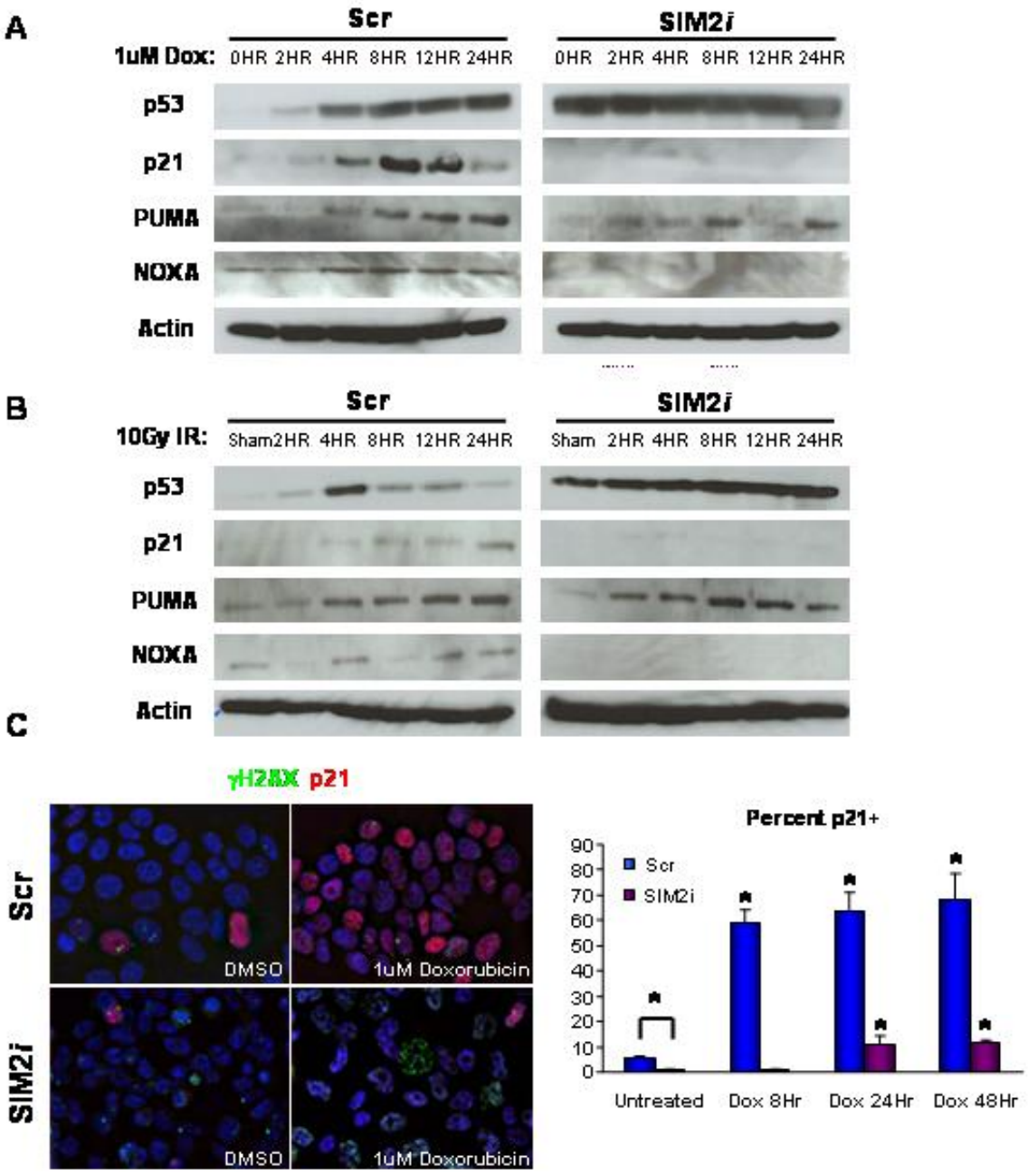

Figure 20. Aberrant p53 signaling in the absence of SIM2. (A) Basal p53 levels are elevated in SIM2*i* MCF-7 cells, but is not inducible by DNA damage, whereas p53 is strongly induced by doxorubicin in SCR cells. Studies on p53 target kinetics revealed that while PUMA is induced normally by both SCR and SIM2*i* cells, p21 and NOXA are inducible only in SCR cells, a pattern that held true in cells treated with ionizing radiation (B). Lack of p21 induction was confirmed by immunofluorescence analysis (C), and co-staining with γH2AX demonstrates that even in cells that sustain massive DNA damage p21 induction does not occur. Quantification of p21 positive cells was performed by counting at least 5 random fields containing 10 or more cells for each group. Data is presented as mean ± S.E.M. * $p>0.05$

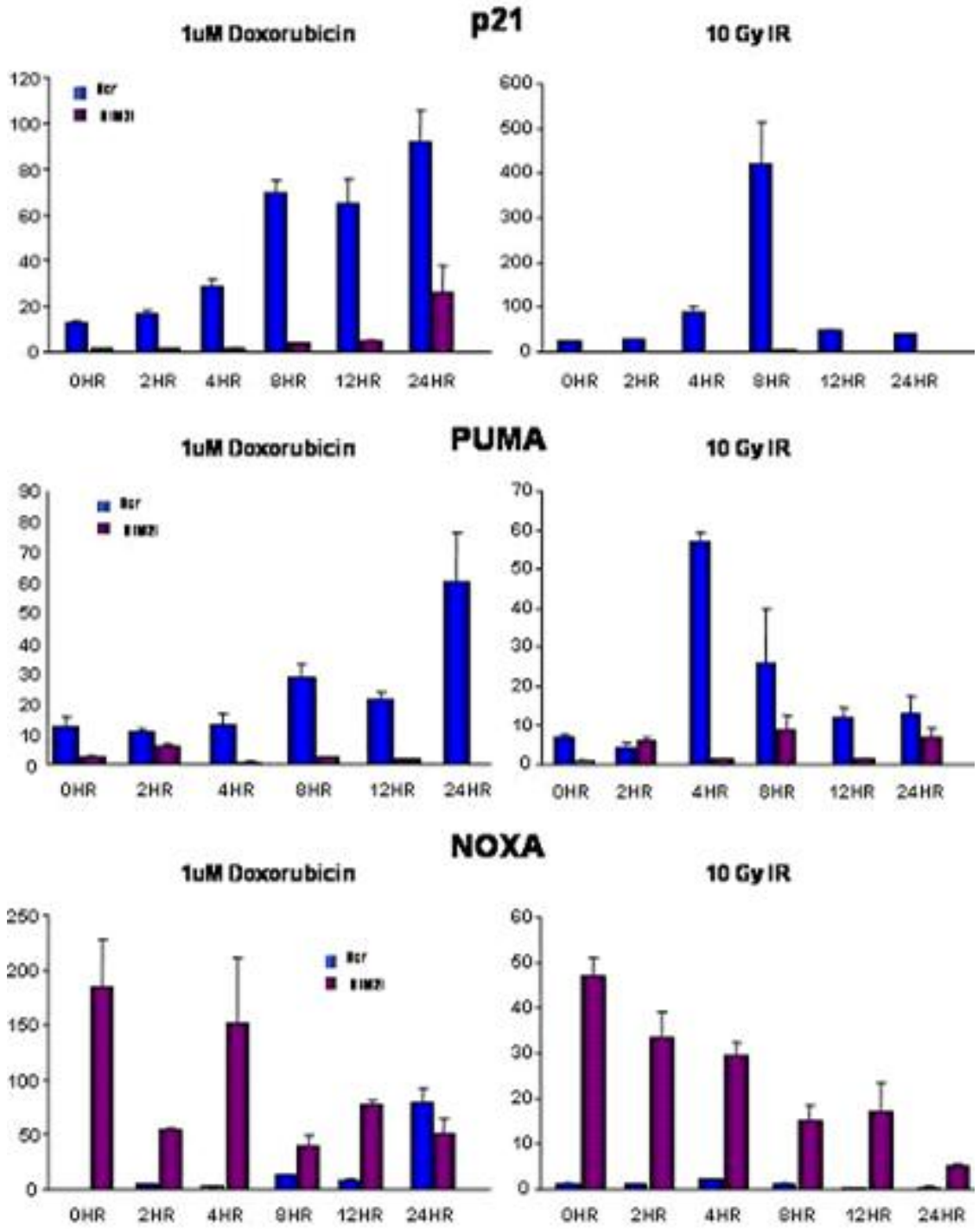

Figure 21. Expression of cell death, DNA damage response, and cell cycle genes in the presence and absence of SIM2. SCR and SIM2*i* MCF-7 were treated with doxorubicin or 10Gy of ionizing radiation and harvested at the indicated time points post treatment. Consistent with Western blot data, p21 is not induced by DNA damage in the absence of SIM2. Data obtained from three wells per group, analyzed by the ΔΔCT method and are expressed as the average fold difference ± SEM * indicates $p<0.05$.

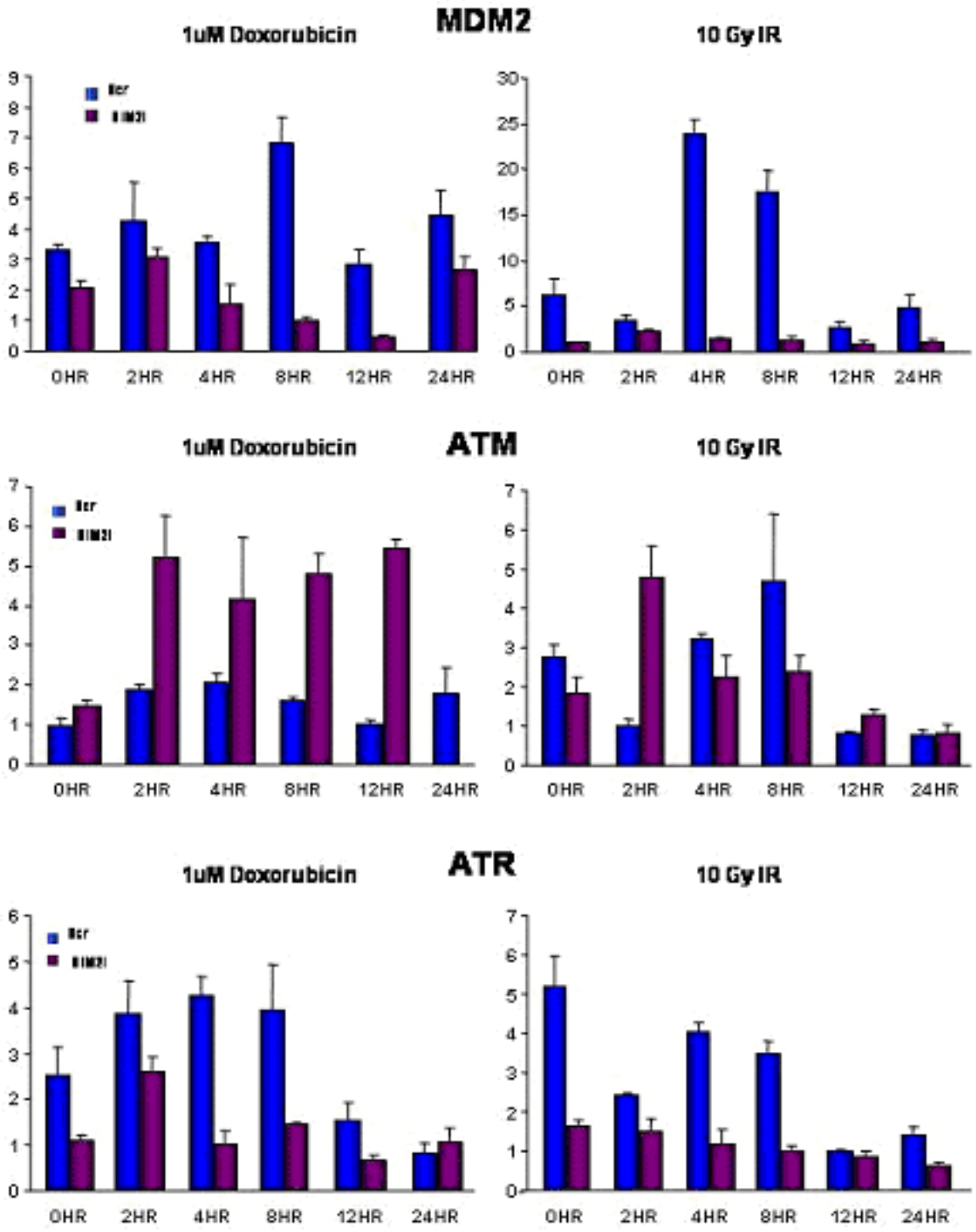

Figure 21, Continued.

difference the number of foci or repair kinetics (Fig. 18B and not shown), indicating that the SIM2*i* MCF-7 cells resistance to doxorubicin was unlikely to be due to enhanced drug efflux. MCF-7 cells have a functional p53 response that closely resembles that found in tumors with wild-type p53 (384).

To ensure that the differences in survival were not due to alterations in p53 status, we performed western blot analysis of p53 and sequenced the p53 mRNA in SCR and SIM2*i* MCF-7 cells. Sequence analysis revealed no mutations in the mRNA. However, we observed that p53 levels in the SIM2*i* MCF-7 cells were dramatically higher than in the SCR cells, in the absence of any stress treatment (Fig. 19A and 19B). This caused us to ask how p53 target gene expression was affected in SCR and SIM2*i* MCF-7 cells. The majority of p53 target proteins such as NOXA and MDM2 were induced normally by ionizing radiation and doxorubicin, with most genes induced more rapidly by ionizing radiation (Fig. 19A and 19B). However, p21 and the pro-apoptotic protein NOXA were not induced by either treatment in the absence of SIM2 (Fig. 19A and 19B). Immunofluoerescence analysis confirmed that even in cells that had sustained massive DNA damage as measured by formation of H2AX repair foci, p21 was uninducible in SIM2*i* MCF-7 cells (Fig. 19C). Analysis of p53 target gene mRNA expression suggested that the defect in induction of p21 was at the level of transcription, while the effect on NOXA was unclear (Fig. 20).Other p53 targets such as MDM2 were induced normally in the absence of SIM2 (Fig. 20), suggesting that SIM2 may be a promoter-specific p53 co-regulator. ChIP experiments confirmed that SIM2s binds to the p21 promoter after doxorubicin treatment (R. Metz, unpublished observations), raising the possibility that

transcriptional complexes containing SIM2 and p53 regulate p21 expression. To begin to address this, we asked if SIM2 is inducible by DNA damage and performed co-immunoprecipitation experiments with p53 and SIM2. We found that SIM2 is not induced by DNA damage at the RNA level (not shown).

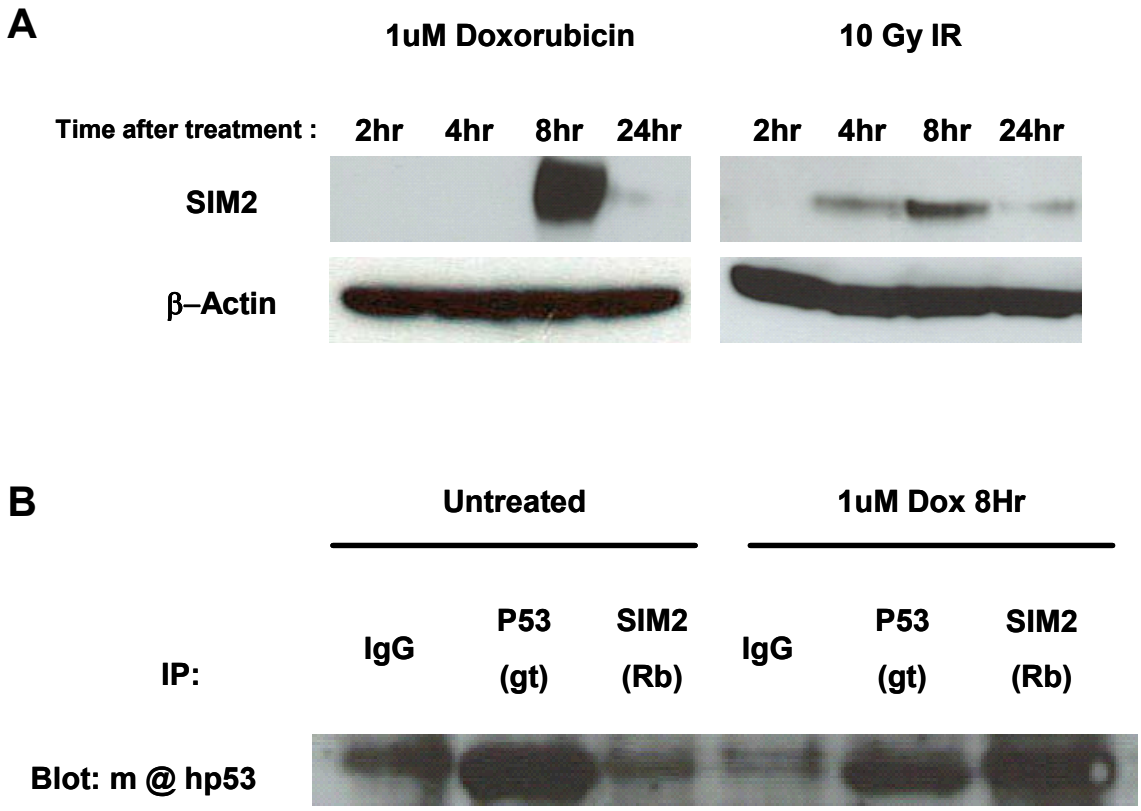

Figure 22. DNA damage triggers stabilization of SIM2 and interaction with p53 complexes. (A) Western blot analysis of SIM2 expression at the indicated times after treatment with either Doxorubicin or ionizing radiation. (B) Co-immunoprecipitation of SIM2 and p53. Antibodies used for IP are indicated above lanes. IP samples were blotted with anti-p53 antibody.

Intriguingly, SIM2 protein levels were robustly increased by both ionizing radiation and by doxorubicin (Fig. 22A), and as SIM2 is regulated by ubiquitin ligases (385, 386), this data suggests a stabilization mechanism similar to those known to mediate p53 and HIF1α responses (387-391). Additionally, we found that SIM2 and p53 appear to interact after treatment with DNA damaging agents (Fig. 22B), leading to hypothesize that SIM2 is a promoter-specific co-regulator of p53 target genes during DNA damage response signaling. These studies demonstrate that the molecular basis of tumor suppression by SIM2s is highly complex and multi-facetted, involving at least 3 distinct pathways: MMPs, EMT, and DNA damage response.

CHAPTER V

CONCLUSIONS

5.1 SIM2 is a transcriptional barrier to EMT

EMT has been studied in the context of development for several decades. However, only recently has the relevance of EMT to carcinogenesis and metastasis become widely accepted. Despite the rarity of full-blown EMT in human tumors, hundreds of published articles have identified dozens of transcription factors that initiate or promote EMT. Many of these factors such as twist, slug, and snail have been shown to be oncogenic *in vivo*, despite a lack of association in tumors with the clear EMTs they elicit in some contexts *in vitro*. The majority of studies on EMT involve ectopic expression techniques that raise the expression levels of these factors to hundreds or thousands of times beyond physiologic levels, which taken together with data from tumor samples suggests that a relatively high threshold of pro-EMT signalling must be reached before a clear phenotypic change results. This implies the existence of multiple factors that coordinately oppose EMT, though these factors have received little attention compared to pro-EMT pathways and transcription factors. In this study, we demonstrated that loss of SIM2 promotes EMT-like changes *in vivo* and *in vitro* (Fig. 8 and Fig.13). SIM2 is to our knowledge the first factor shown to repress the SLUG oncogene, and with the exception of work showing that estrogen signaling suppresses Snail expression via MTA3 (246), the first to elucidate a factor that opposes EMT at the level of transcription. SIM2 has been shown previously to stifle xenobiotic and hypoxia-driven gene expression (329, 330), suggesting that SIM2 stands astride and stifles several paths to EMT. Loss of

SIM2 was insufficient to stimulate EMT in non-transformed MCF-10A cells (Fig. 15), implying that multiple redundant factors block EMT in mature tissues and that these factors tend to be lost during transformation, whether the tumor cells display EMT-like features or not. SIM2-/- mammary glands displayed some features of EMT such as loss of E-cadherin, overexpression of slug, and nuclear accumulation of β-catenin (Fig.13). This apparent discrepancy between the untransformed cells in the gland and the MCF-10A cells which did not undergo EMT may be explained by the difference in effectiveness between a gene knockout and shRNA-mediated silencing. If SIM2 were to be fully deleted in MCF-10A cells, it is possible that the anti-EMT barrier would be lowered sufficiently to allow for EMT to occur.

EMT is central to developmental processes in the early embryo and structural assembly of tissues such as the heart, palate, muscle, and bone (392, 393), although uncontrolled EMT can lead to defects due to mesenchymal hyperplasia (297). Development of many tissues such as the kidneys also requires MET, which suggests a critical role for proteins that restrict EMT. Defects in palate fusion, diaphragm development, and bone formation in Sim2-/- mice imply that SIM2-mediated cessation of EMT is crucial for development of multiple tissues (337). Considering that EMT-like changes tend to occur in advanced tumors and EMT-promoting factors are tumor-promoting without regard to EMT, strategies aimed at re-establishing expression of SIM2 or other barriers to EMT identified in the future have great therapeutic potential.

5.2 SIM2 has important tumor suppressor function independent of slug regulation

Previously, MMP3 was identified as a direct target of SIM2-mediated repression (336). In this study, we showed that SIM2 represses MMP2 at the expression and activation levels. Both MMP2 and MMP3 are associated with poor outcomes multiple tumor types, with one of the consistent associations being MMP2 and poor outcome in breast tumors (394-400). MMP2 is associated with metastasis, angiogenesis, tumor grade, size, and relapse free survival (401-403), consistent with the rapid metastasis and large vascular tumors formed by SIM2*i* MCF-7 cells in our study (Fig. 9). While the mechanism by which SIM2s represses MMP2 is unclear, we hypothesize it involves direct binding and repression of the MMP2 promoter. How SIM2 loss resulted in MMP2 activation is likely to be more complicated and indirect. NF-κB has been reported to promote MMP2 activation via induction of MMP14, which processes the MMP2 proenzyme (404, 405). Additionally, preliminary results suggest that SIM2 can antagonize NF-κB in some cases (T. Gustafson and R. Metz, unpublished observations), and MMP14 expression is elevated in SIM2*i* MCF-7 cells (Fig. 12), suggesting that this pathway may explain the effect of SIM2 on MMP2 activation. These results strongly suggest that SIM2 has multiple oncogenic targets and provide a rationale for therapeutic strategies based on re-establishing SIM2 expression in tumors without EMT-like features.

5.3 p53 responses are modulated by SIM2

We show in this study that SIM2 modulates p53 signaling directly through target genes such as p21, and likely indirectly through regulation of slug (Fig. 13). As p53 is central to DNA damage responses and suppression of tumorigenesis in virtually every, if

not all tissues, this implies that SIM2 is crucial for tumor suppression in a variety of tissues. By co-regulating genes such as p21 and PUMA, and through suppressing slug, SIM2 may function to fine tune the output of p53 activation, which can lead either to cell cycle arrest or apoptosis. Given the tumor suppressive potency of p53 and the frequency with which it is deleted or mutated in human cancers, it seems possible that those tumors with no overt defects in p53 itself may have found other ways to neutralize p53 pathway output, that is, all tumors are to one degree or another aberrant in p53 signaling. SIM2, as a promoter-specific modulator of p53 function, may represent a path for evasion of p53. It is noteworthy that the p53 targets whose transcription is apparently promoted by SIM2 are generally tumor suppressive (p21, PUMA), while some of those unaffected are oncogenic (MDM2). SIM2 loss may even in some cases act as a gain-of function p53 mutation, and allow hijacking of p53 signaling to benefit the tumor, which can differentially effect treatment response (406). As SIM2*i* cells displayed altered responses to ionizing radiation and the radiomimetic doxorubicin (Fig. 16), SIM2 may therefore have value not only as a prognostic indicator, but assist in selection of appropriate therapies.

5.4 Implications of SIM2 loss in breast cancer

Given the known oncongenic potency of the SIM2 target genes SLUG and MMP2, we hypothesize that SIM2 loss associates with poor prognosis in breast cancer. Slug and MMP2 promote angiogenesis, metastasis, and recurrence, suggesting that loss of SIM2 would also be associated with these processes. SIM2s-mediated antagonism of HIF1α is another factor that could influence the effect of SIM2 loss in breast tumors. In

addition to promoting EMT, angiogenesis and metastasis, hypoxia interfaces with p53 signaling in the presence and absence of DNA damage, resulting in unique gene expression patterns in each case (407). It is possible that SIM2 loss could act as a hypoxia mimetic, or simply compound the hypoxia that is found in even the smallest tumors (301). SIM2 is also likely to function in the interface between hypoxia and p53, and play a role in the cell's decision to survive and initiate angiogenesis or undergo apoptosis.

We also demonstrated that loss of SIM2 increased self-renewal and putative stem-cell-like tumor initiating cell populations in MCF-7 cells (Fig. 15). These cells are thought to be the root of tumor recurrence, and to play roles in angiogenesis(1). This implies that SIM2 promotes differentiation, and that reestablishment of SIM2 expression would synergize with many treatments in use and under investigation. This is supported by the ability of Singleminded proteins to promote differentiation of isotocin cells, CNS midline cells, and possibly TRH and somatostatin-secreting neurons (408-410). The potential role of SIM2 in suppression of stem cell identity will require *in vivo* validation, and studies underway to generate a conditional SIM2 allele that will clarify this issue.

5.5 SIM2 and basal-like breast carcinoma

Basal-like carcinomas are associated with poor prognosis, EMT, recurrence, drug resistance, aggressive clinical course, and are hypothesized to contain greater numbers of tumor-initiating cells (108, 110, 117, 121). Recently, it was reported that the basal phenotype is regulated by slug and hypoxia (114), suggesting that loss of SIM2 might also form part of the molecular definition of basal-like tumors via permission of slug

expression and HIF1α activity. Consistent with this theory, SIM2 is not expressed in basal / myoepithelial cells in the mouse mammary gland, indicating its expression may suppress basal identity, or that basal-like carcinomas arise from cells that do not express SIM2. SIM2 loss is not likely to be sufficient to permit manifestation of the basal phenotype, as SIM2 is lost or reduced in up to 70% of tumors while basal-like carcinomas comprise less than 15% of invasive ductal carcinomas (113, 336). Whether SIM2 loss promotes the basal phenotype or basal carcinomas arise from cells without SIM2, SIM2 is a potential diagnostic marker to distinguish basal-like carcinomas.

5.6 SIM2 and Down syndrome

Individuals with DS have a spectrum of health disorders that is significantly different from the general population. In addition to differential risk for development of many cancers, DS patients have increased incidence of palatal abnormalities and atrioventricular (AV) septum defects, all of which involve EMT or genes that control EMT (136, 137, 151, 411). DS patients have greatly increased risk for development of leukemias, but we are unable to detect SIM2 in white blood cells and believe SIM2 does not play a role in DS-related leukemias. We hypothesize that regulation of EMT and tissue remodeling factors by SIM2 contributes both to the physical abnormalities and unique solid tumor protection experienced by DS patients.

5.7 Proposed model of SIM2 function in epithelia

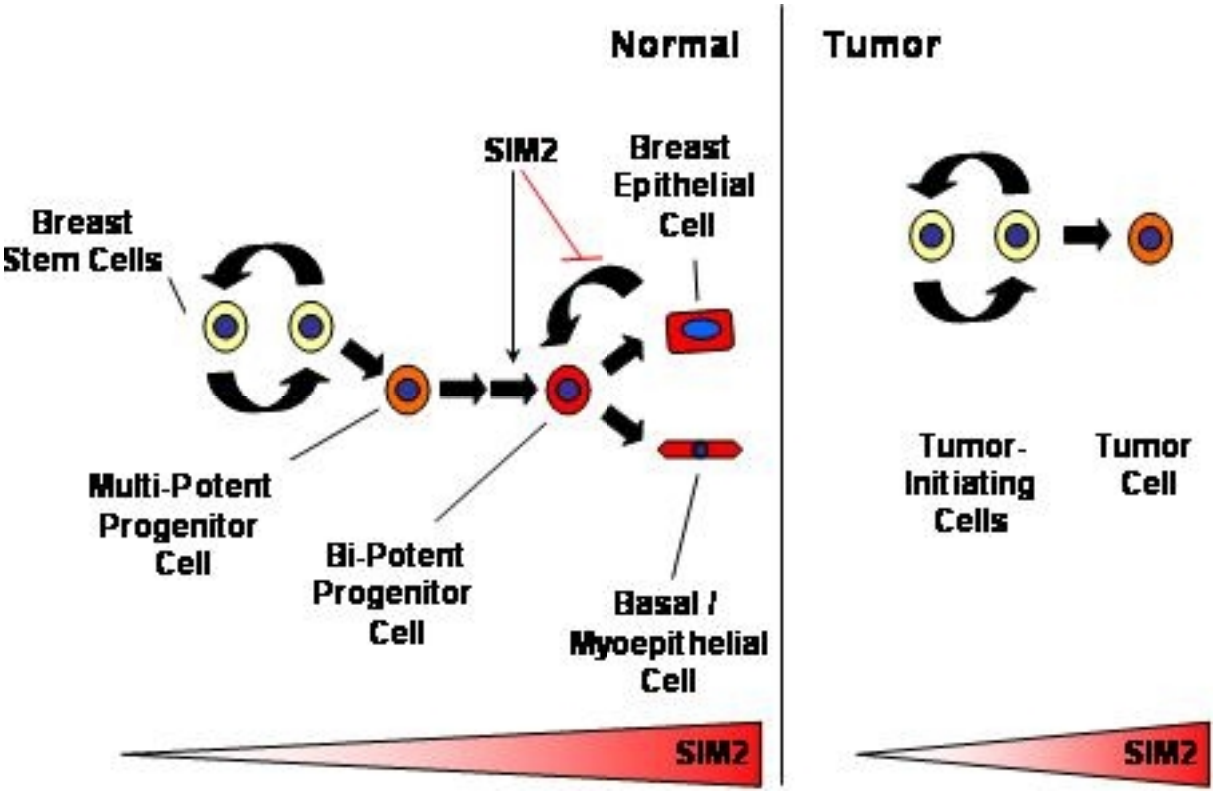

Figure 23. The role of SIM2 in breast epithelium. In normal cells, SIM2 contributes to maintenance of differentation by suppressing slug, thereby preserving expression of epithelial genes such as E-cadherin and keratin 18. SIM2 may also actively promote differentiation by this mechanism, though it is not known at which point during differentiation of mammary stem cells SIM2 expression commences. In tumor cells, SIM2 exerts similar pro-differentiation effects and its loss leads to progression. Via regulation of MMPs and slug, SIM2 inhibits invasion and metastasis

Our results in mouse mammary epithelium and breast cancer cells suggest the function of SIM2 in mature tissue is to preserve epithelial identity within individual cells and in the tissue as a whole (Fig. 23), and does so along 3 main paths: Suppression of slug and possibly other EMT-promoting factors, maintenance of tissue integrity by suppression of MMPs, and by ensuring an appropriate response to DNA damage. We hypothesize that SIM2 expression is low under normal conditions, perhaps via E3 ubiquitin ligase-mediated degradation. Upon a challenge such as hypoxia or DNA

damage, SIM2 is rapidly stabilized, perhaps under the control of DNA-damage activated kinases such as CHK1. SIM2 would then suppress genes that might perturb the epithelium such as slug, while promoting cell cycle arrest via p21, thereby maintaining the tissue. As progenitor cells rely upon slug for protection from radiation-induced death (124, 278), SIM2 may be an important difference between the DNA damage responses of stem cells and differentiated cells. This also suggests that lack of SIM2 might be a useful stem cell marker, as based upon its apparently pro-differentiation effects SIM2 seems highly unlikely to be expressed in stem cells, and it is restricted to the epithelial compartment where stem cells are thought to reside. While it remains to be elucidated whether SIM2 is a cause or effect of differentiation, this study strongly suggests that SIM2 has a key role in safeguarding the structural and genomic integrity of epithelial tissues.

REFERENCES

1. Shen R, Ye Y, Chen L, Yan Q, Barsky SH, Gao JX. Precancerous stem cells can serve as tumor vasculogenic progenitors. PLoS ONE 2008;3:e1652.
2. Neth P, Ries C, Karow M, Egea V, Ilmer M, Jochum M. The Wnt signal transduction pathway in stem cells and cancer cells: influence on cellular invasion. Stem Cell Rev 2007;3:18-29.
3. Yu F, Yao H, Zhu P, et al. let-7 regulates self renewal and tumorigenicity of breast cancer cells. Cell 2007;131:1109-23.
4. Li F, Tiede B, Massague J, Kang Y. Beyond tumorigenesis: cancer stem cells in metastasis. Cell Res 2007;17:3-14.
5. Bao S, Wu Q, McLendon RE, et al. Glioma stem cells promote radioresistance by preferential activation of the DNA damage response. Nature 2006;444:756-60.
6. Balinsky BI. On the prenatal growth of the mammary gland rudiment in the mouse. J Anat 1950;84:227-35.
7. Robinson GW. Cooperation of signalling pathways in embryonic mammary gland development. Nat Rev Genet 2007;8:963-72.
8. Oftedal OT. The origin of lactation as a water source for parchment-shelled eggs. J Mammary Gland Biol Neoplasia 2002;7:253-66.
9. Oftedal OT. The mammary gland and its origin during synapsid evolution. J Mammary Gland Biol Neoplasia 2002;7:225-52.
10. Veltmaat JM, Van Veelen W, Thiery JP, Bellusci S. Identification of the mammary line in mouse by Wnt10b expression. Dev Dyn 2004;229:349-56.

11. Drews U. Regression of mouse mammary gland anlagen in recombinants of Tfm and wild-type tissues: testosterone acts via the mesenchyme. Cell 1977;10:401-4.

12. Kratochwil K. Development and loss of androgen responsiveness in the embryonic rudiment of the mouse mammary gland. Dev Biol 1977;61:358-65.

13. Kratochwil K, Schwartz P. Tissue interaction in androgen response of embryonic mammary rudiment of mouse: identification of target tissue for testosterone. Proc Natl Acad Sci USA 1976;73:4041-4.

14. Hens JR, Dann P, Zhang JP, Harris S, Robinson GW, Wysolmerski J. BMP4 and PTHrP interact to stimulate ductal outgrowth during embryonic mammary development and to inhibit hair follicle induction. Development 2007;134:1221-30.

15. Wiseman BS, Sternlicht MD, Lund LR, et al. Site-specific inductive and inhibitory activities of MMP-2 and MMP-3 orchestrate mammary gland branching morphogenesis. J Cell Biol 2003;162:1123-33.

16. Sympson CJ, Bissell MJ, Werb Z. Mammary gland tumor formation in transgenic mice overexpressing stromelysin-1. Semin Cancer Biol 1995;6:159-63.

17. Sympson CJ, Talhouk RS, Alexander CM, et al. Targeted expression of stromelysin-1 in mammary gland provides evidence for a role of proteinases in branching morphogenesis and the requirement for an intact basement membrane for tissue-specific gene expression. J Cell Biol 1994;125:681-93.

18. Warburton D, Bellusci S, De Langhe S, et al. Molecular mechanisms of early lung specification and branching morphogenesis. Pediatr Res 2005;57:26R-37R.

19. Costantini F. Renal branching morphogenesis: concepts, questions, and recent advances. Differentiation 2006;74:402-21.

20. Nelson CM, Vanduijn MM, Inman JL, Fletcher DA, Bissell MJ. Tissue geometry determines sites of mammary branching morphogenesis in organotypic cultures. Science 2006;314:298-300.

21. Bocchinfuso WP, Lindzey JK, Hewitt SC, et al. Induction of mammary gland development in estrogen receptor-alpha knockout mice. Endocrinology 2000;141:2982-94.

22. Mallepell S, Krust A, Chambon P, Brisken C. Paracrine signaling through the epithelial estrogen receptor alpha is required for proliferation and morphogenesis in the mammary gland. Proc Natl Acad Sci USA 2006;103:2196-201.

23. McBryan J, Howlin J, Napoletano S, Martin F. Amphiregulin: role in mammary gland development and breast cancer. J Mammary Gland Biol Neoplasia 2008;13:159-69.

24. Ciarloni L, Mallepell S, Brisken C. Amphiregulin is an essential mediator of estrogen receptor alpha function in mammary gland development. Proc Natl Acad Sci USA 2007;104:5455-60.

25. Huh JI, Qiu TH, Chandramouli GV, et al. 2-methoxyestradiol induces mammary gland differentiation through amphiregulin-epithelial growth factor receptor-mediated signaling: molecular distinctions from the mammary gland of pregnant mice. Endocrinology 2007;148:1266-77.

26. Luetteke NC, Qiu TH, Fenton SE, et al. Targeted inactivation of the EGF and amphiregulin genes reveals distinct roles for EGF receptor ligands in mouse mammary gland development. Development 1999;126:2739-50.

27. Sternlicht MD, Sunnarborg SW, Kouros-Mehr H, Yu Y, Lee DC, Werb Z. Mammary ductal morphogenesis requires paracrine activation of stromal EGFR via ADAM17-dependent shedding of epithelial amphiregulin. Development 2005;132:3923-33.

28. Snedeker SM, Brown CF, DiAugustine RP. Expression and functional properties of transforming growth factor alpha and epidermal growth factor during mouse mammary gland ductal morphogenesis. Proc Natl Acad Sci USA 1991;88:276-80.

29. Humphreys RC, Krajewska M, Krnacik S, et al. Apoptosis in the terminal endbud of the murine mammary gland: a mechanism of ductal morphogenesis. Development 1996;122:4013-22.

30. Mailleux AA, Overholtzer M, Schmelzle T, Bouillet P, Strasser A, Brugge JS. BIM regulates apoptosis during mammary ductal morphogenesis, and its absence reveals alternative cell death mechanisms. Dev Cell 2007;12:221-34.

31. Brisken C, Park S, Vass T, Lydon JP, O'Malley BW, Weinberg RA. A paracrine role for the epithelial progesterone receptor in mammary gland development. Proc Natl Acad Sci USA 1998;95:5076-81.

32. Ormandy CJ, Camus A, Barra J, et al. Null mutation of the prolactin receptor gene produces multiple reproductive defects in the mouse. Genes Dev 1997;11:167-78.

33. Anderson SM, Rudolph MC, McManaman JL, Neville MC. Key stages in mammary gland development. Secretory activation in the mammary gland: it's not just about milk protein synthesis! Breast Cancer Res 2007;9:204.

34. Rosen JM, Wyszomierski SL, Hadsell D. Regulation of milk protein gene expression. Annu Rev Nutr 1999;19:407-36.

35. Kazansky AV, Raught B, Lindsey SM, Wang YF, Rosen JM. Regulation of mammary gland factor/Stat5a during mammary gland development. Mol Endocrinol 1995;9:1598-609.

36. Liu X, Robinson GW, Hennighausen L. Activation of Stat5a and Stat5b by tyrosine phosphorylation is tightly linked to mammary gland differentiation. Mol Endocrinol 1996;10:1496-506.

37. Liu X, Robinson GW, Wagner KU, Garrett L, Wynshaw-Boris A, Hennighausen L. Stat5a is mandatory for adult mammary gland development and lactogenesis. Genes Dev 1997;11:179-86.

38. Choi KM, Barash I, Rhoads RE. Insulin and prolactin synergistically stimulate beta-casein messenger ribonucleic acid translation by cytoplasmic polyadenylation. Mol Endocrinol 2004;18:1670-86.

39. Moshel Y, Rhoads RE, Barash I. Role of amino acids in translational mechanisms governing milk protein synthesis in murine and ruminant mammary epithelial cells. J Cell Biochem 2006;98:685-700.

40. Lund LR, Romer J, Thomasset N, et al. Two distinct phases of apoptosis in mammary gland involution: proteinase-independent and -dependent pathways. Development 1996;122:181-93.

41. Green KA, Streuli CH. Apoptosis regulation in the mammary gland. Cell Mol Life Sci 2004;61:1867-83.

42. Monks J, Smith-Steinhart C, Kruk ER, Fadok VA, Henson PM. Epithelial cells remove apoptotic epithelial cells during post-lactation involution of the mouse mammary gland. Biol Reprod 2008;78:586-94.

43. McDaniel SM, Rumer KK, Biroc SL, et al. Remodeling of the mammary microenvironment after lactation promotes breast tumor cell metastasis. Am J Pathol 2006;168:608-20.

44. Schedin P, Mitrenga T, McDaniel S, Kaeck M. Mammary ECM composition and function are altered by reproductive state. Mol Carcinog 2004;41:207-20.

45. Gilman A, Philips FS. The Biological Actions and Therapeutic Applications of the B-Chloroethyl Amines and Sulfides. Science 1946;103:409-36.

46. Goodman LS, Wintrobe MM, Dameshek W, Goodman MJ, Gilman A, McLennan MT. Landmark article Sept. 21, 1946: Nitrogen mustard therapy. Use of methyl-bis(beta-chloroethyl)amine hydrochloride and tris(beta-chloroethyl)amine hydrochloride for Hodgkin's disease, lymphosarcoma, leukemia and certain allied and miscellaneous disorders. By Louis S. Goodman, Maxwell M. Wintrobe, William Dameshek, Morton J. Goodman, Alfred Gilman and Margaret T. McLennan. JAMA 1984;251:2255-61.

47. Timothy FE. The Reach to Recovery program in America and Europe. Cancer 1980;46:1059-60.

48. Bonadonna G, Brusamolino E, Valagussa P, et al. Combination chemotherapy as an adjuvant treatment in operable breast cancer. N Engl J Med 1976;294:405-10.

49. Jaffe N, Link MP, Cohen D, et al. High-dose methotrexate in osteogenic sarcoma. Natl Cancer Inst Monogr 1981:201-6.

50. Deininger MW, Druker BJ. Specific targeted therapy of chronic myelogenous leukemia with imatinib. Pharmacol Rev 2003;55:401-23.

51. Piccart-Gebhart MJ, Procter M, Leyland-Jones B, et al. Trastuzumab after adjuvant chemotherapy in HER2-positive breast cancer. N Engl J Med 2005;353:1659-72.

52. Tumours of the breast and female genital organs, World Health Organization classification of tumours. 2003.

53. Adeniran A, Al-Ahmadie H, Mahoney MC, Robinson-Smith TM. Granular cell tumor of the breast: a series of 17 cases and review of the literature. Breast J 2004;10:528-31.

54. Akbulut M, Gunhan-Bilgen I, Zekioglu O, Duygulu G, Oktay A, Ozdemir N. Fine needle aspiration cytology of inflammatory myofibroblastic tumour (inflammatory pseudotumour) of the breast: a case report and review of the literature. Cytopathology 2007;18:384-7.

55. Akbulut M, Zekioglu O, Kapkac M, Erhan Y, Ozdemir N. Fine needle aspiration cytology of glycogen-rich clear cell carcinoma of the breast: review of 37 cases with histologic correlation. Acta Cytol 2008;52:65-71.

56. Bergman S, Hoda SA, Geisinger KR, Creager AJ, Trupiano JK. E-cadherin-negative primary small cell carcinoma of the breast. Report of a case and review of the literature. Am J Clin Pathol 2004;121:117-21.

57. Brodie C, Provenzano E. Vascular proliferations of the breast. Histopathology 2008;52:30-44.

58. Celis JE, Gromova I, Gromov P, et al. Molecular pathology of breast apocrine carcinomas: a protein expression signature specific for benign apocrine metaplasia. FEBS Lett 2006;580:2935-44.

59. Charafe-Jauffret E, Tarpin C, Bardou VJ, et al. Immunophenotypic analysis of inflammatory breast cancers: identification of an 'inflammatory signature'. J Pathol 2004;202:265-73.

60. Chu PG, Weiss LM. Immunohistochemical characterization of signet-ring cell carcinomas of the stomach, breast, and colon. Am J Clin Pathol 2004;121:884-92.

61. Coyne JD, Irion L. Mammary mucinous cystadenocarcinoma. Histopathology 2006;49:659-60.

62. Damiani S, Eusebi V, Losi L, D'Adda T, Rosai J. Oncocytic carcinoma (malignant oncocytoma) of the breast. Am J Surg Pathol 1998;22:221-30.

63. Diallo R, Tognon C, Knezevich SR, Sorensen P, Poremba C. Secretory carcinoma of the breast: a genetically defined carcinoma entity. Verh Dtsch Ges Pathol 2003;87:193-203.

64. Glazebrook KN, Magut MJ, Reynolds C. Angiosarcoma of the breast. AJR Am J Roentgenol 2008;190:533-8.

65. Hacking EA, Tiltman AJ, Dent DM. Angiosarcoma of the breast. Clin Oncol 1984;10:177-80.

66. Hameed M. Pathology and genetics of adipocytic tumors. Cytogenet Genome Res 2007;118:138-47.

67. Hanby AM, Hughes TA. In situ and invasive lobular neoplasia of the breast. Histopathology 2008;52:58-66.

68. Hennessy BT, Gilcrease MZ, Kim E, Gonzalez-Angulo AM. Breast carcinoma with neuroendocrine differentiation and myocardial metastases. Clin Breast Cancer 2007;7:892-4.

69. Heron DE, Komarnicky LT, Hyslop T, Schwartz GF, Mansfield CM. Bilateral breast carcinoma: risk factors and outcomes for patients with synchronous and metachronous disease. Cancer 2000;88:2739-50.

70. Hisaoka M, Takamatsu Y, Hirano Y, Maeda H, Hamada T. Sebaceous carcinoma of the breast: case report and review of the literature. Virchows Arch 2006;449:484-8.

71. Jacquemier J, Padovani L, Rabayrol L, et al. Typical medullary breast carcinomas have a basal/myoepithelial phenotype. J Pathol 2005;207:260-8.

72. Kaufman MW, Marti JR, Gallager HS, Hoehn JL. Carcinoma of the breast with pseudosarcomatous metaplasia. Cancer 1984;53:1908-17.

73. Korsching E, Jeffrey S, Meinerz W, Decker T, Boecker W, Buerger H. Basal carcinomas of the breast revisited - an old entity with new interpretations. J Clin Pathol 2008;61(5):553-60

74. Kurisu Y, Tsuji M, Akashi K, et al. Composite type of breast carcinoma with endocrine differentiation: a cytological and immunohistochemical study. Pathol Int 2004;54:105-10.

75. Kyriazis AP, Kyriazis AA. Primary rhabdomyosarcoma of the female breast: report of a case and review of the literature. Arch Pathol Lab Med 1998;122:747-9.

76. Lee AH. Recent developments in the histological diagnosis of spindle cell carcinoma, fibromatosis and phyllodes tumour of the breast. Histopathology 2008;52:45-57.

77. Luini A, Aguilar M, Gatti G, et al. Metaplastic carcinoma of the breast, an unusual disease with worse prognosis: the experience of the European Institute of Oncology and review of the literature. Breast Cancer Res Treat 2007;101:349-53.

78. Magro G, Gangemi P, Greco P. Deciduoid-like myofibroblastoma of the breast: a potential pitfall of malignancy. Histopathology 2008;52:652-4.

79. Malavaud B, Pessonnier A, Martel P, Roche H, Marques B. [Angiosarcoma of the breast]. J Gynecol Obstet Biol Reprod (Paris) 1989;18:173-6.

80. Mardi K, Sharma J. A rare case of secretory breast carcinoma in an elderly woman: correlation of aspiration cytology and histology. Indian J Pathol Microbiol 2007;50:865-7.

81. Milde S, Gaedcke J, v Wasielewski R, et al. [Diagnosis and immunohistochemistry of medullary breast cancer]. Pathologe 2006;27:358-62.

82. Miremadi A, Pinder SE, Lee AH, et al. Neuroendocrine differentiation and prognosis in breast adenocarcinoma. Histopathology 2002;40:215-22.

83. Moritani S, Ichihara S, Hasegawa M, et al. Serous papillary adenocarcinoma of the female genital organs and invasive micropapillary carcinoma of the breast.

Are WT1, CA125, and GCDFP-15 useful in differential diagnosis? Hum Pathol 2008 ;39(5):666-71.

84. Mukkamala A, Blight C, Azher Q, Danish R. Breast carcinoma with osteoclastic giant cells. Breast J 1999;5:149-50.

85. Mulligan AM, O'Malley FP. Papillary lesions of the breast: a review. Adv Anat Pathol 2007;14:108-19.

86. Munitiz V, Rios A, Canovas J, et al. Primitive leiomyosarcoma of the breast: case report and review of the literature. Breast 2004;13:72-6.

87. Ng WK, Chiu CS, Han KC, Chow JC. Mammary pseudoangiomatous stromal hyperplasia. A reappraisal of the fine needle aspiration cytology findings. Acta Cytol 2003;47:373-80.

88. Page DL, Dixon JM, Anderson TJ, Lee D, Stewart HJ. Invasive cribriform carcinoma of the breast. Histopathology 1983;7:525-36.

89. Palacios J, Sarrio D, Garcia-Macias MC, Bryant B, Sobel ME, Merino MJ. Frequent E-cadherin gene inactivation by loss of heterozygosity in pleomorphic lobular carcinoma of the breast. Mod Pathol 2003;16:674-8.

90. Peintinger F, Leibl S, Reitsamer R, Moinfar F. Primary acinic cell carcinoma of the breast: a case report with long-term follow-up and review of the literature. Histopathology 2004;45:645-8.

91. Porter GJ, Evans AJ, Lee AH, Hamilton LJ, James JJ. Unusual benign breast lesions. Clin Radiol 2006;61:562-9.

92. Rao P, Lyons B. Pure mucinous carcinoma of the breast with extensive psammomatous calcification. Histopathology 2008;52:650-2.

93. Rapidis AD, Givalos N, Gakiopoulou H, et al. Mucoepidermoid carcinoma of the salivary glands. Review of the literature and clinicopathological analysis of 18 patients. Oral Oncol 2007;43:130-6.

94. Resetkova E, Sahin A, Ayala AG, Sneige N. Breast carcinoma with choriocarcinomatous features. Ann Diagn Pathol 2004;8:74-9.

95. Ridolfi RL, Rosen PP, Port A, Kinne D, Mike V. Medullary carcinoma of the breast: a clinicopathologic study with 10 year follow-up. Cancer 1977;40:1365-85.

96. Rosen PP, Ernsberger D. Low-grade adenosquamous carcinoma. A variant of metaplastic mammary carcinoma. Am J Surg Pathol 1987;11:351-8.

97. Sentani K, Tashiro T, Oue N, Yasui W. Synchronous squamous cell carcinoma of the breast and invasive lobular carcinoma. APMIS 2007;115:1422-5.

98. Sullivan T, Raad RA, Goldberg S, et al. Tubular carcinoma of the breast: a retrospective analysis and review of the literature. Breast Cancer Res Treat 2005;93:199-205.

99. Tjalma WA, Verslegers IO, De Loecker PA, Van Marck EA. Low and high grade mucoepidermoid carcinomas of the breast. Eur J Gynaecol Oncol 2002;23:423-5.

100. Torrao MM, da Costa JM, Ferreira E, da Silva MV, Paiva I, Lopes C. Adenoid cystic carcinoma of the breast. Breast J 2007;13:206.

101. Triantafillidou K, Dimitrakopoulos J, Iordanidis F, Koufogiannis D. Mucoepidermoid carcinoma of minor salivary glands: a clinical study of 16 cases and review of the literature. Oral Dis 2006;12:364-70.

102. Tunon de Lara C, Roussillon E, Rivel J, Maugey-Laulom B, Alfonso AL, Horovitz J. [Liposarcoma of the breast. A case report]. J Gynecol Obstet Biol Reprod (Paris) 1998;27:201-4.

103. Vorobiof G, Hariparsad G, Freinkel W, Said H, Vorobiof DA. Primary osteosarcoma of the breast: a case report. Breast J 2003;9:231-3.

104. Perou CM, Sorlie T, Eisen MB, et al. Molecular portraits of human breast tumours. Nature 2000;406:747-52.

105. Sorlie T, Perou CM, Tibshirani R, et al. Gene expression patterns of breast carcinomas distinguish tumor subclasses with clinical implications. Proc Natl Acad Sci USA 2001;98:10869-74.

106. Finetti P, Cervera N, Charafe-Jauffret E, et al. Sixteen-kinase gene expression identifies luminal breast cancers with poor prognosis. Cancer Res 2008;68:767-76.

107. Fadare O, Tavassoli FA. Clinical and pathologic aspects of basal-like breast cancers. Nat Clin Pract Oncol 2008;5:149-59.

108. Arnes JB, Collett K, Akslen LA. Independent prognostic value of the basal-like phenotype of breast cancer and associations with EGFR and candidate stem cell marker BMI-1. Histopathology 2008;52:370-80.

109. Rodriguez-Pinilla SM, Sarrio D, Honrado E, et al. Prognostic significance of basal-like phenotype and fascin expression in node-negative invasive breast carcinomas. Clin Cancer Res 2006;12:1533-9.

110. Ihemelandu CU, Naab TJ, Mezghebe HM, et al. Basal cell-like (triple-negative) breast cancer, a predictor of distant metastasis in African American women. Am J Surg 2008;195:153-8.

111. Hamperl H. The myothelia (myoepithelial cells). Normal state; regressive changes; hyperplasia; tumors. Curr Top Pathol 1970;53:161-220.

112. Murad TM. A proposed histochemical and electron microscopic classification of human breast cancer according to cell of origin. Cancer 1971;27:288-99.

113. Da Silva L, Clarke C, Lakhani SR. Demystifying basal-like breast carcinomas. J Clin Pathol 2007;60:1328-32.

114. Storci G, Sansone P, Trere D, et al. The basal-like breast carcinoma phenotype is regulated by SLUG gene expression. J Pathol 2008;214:25-37.

115. Gauthier ML, Berman HK, Miller C, et al. Abrogated response to cellular stress identifies DCIS associated with subsequent tumor events and defines basal-like breast tumors. Cancer Cell 2007;12:479-91.

116. Korsching E, Packeisen J, Liedtke C, et al. The origin of vimentin expression in invasive breast cancer: epithelial-mesenchymal transition, myoepithelial histogenesis or histogenesis from progenitor cells with bilinear differentiation potential? J Pathol 2005;206:451-7.

117. Sarrio D, Rodriguez-Pinilla SM, Hardisson D, Cano A, Moreno-Bueno G, Palacios J. Epithelial-mesenchymal transition in breast cancer relates to the basal-like phenotype. Cancer Res 2008;68:989-97.

118. Vincent-Salomon A, Lucchesi C, Gruel N, et al. Integrated Genomic and transcriptomic analysis of ductal carcinoma in situ of the breast. Clin Cancer Res 2008;14:1956-65.

119. Bryan BB, Schnitt SJ, Collins LC. Ductal carcinoma in situ with basal-like phenotype: a possible precursor to invasive basal-like breast cancer. Mod Pathol 2006;19:617-21.

120. Dabbs DJ, Chivukula M, Carter G, Bhargava R. Basal phenotype of ductal carcinoma in situ: recognition and immunohistologic profile. Mod Pathol 2006;19:1506-11.

121. Bertheau P, Turpin E, Rickman DS, et al. Exquisite sensitivity of TP53 mutant and basal breast cancers to a dose-dense epirubicin-cyclophosphamide regimen. PLoS Med 2007;4:e90.

122. Carey LA, Dees EC, Sawyer L, et al. The triple negative paradox: primary tumor chemosensitivity of breast cancer subtypes. Clin Cancer Res 2007;13:2329-34.

123. Stingl J, Eirew P, Ricketson I, et al. Purification and unique properties of mammary epithelial stem cells. Nature 2006;439:993-7.

124. Inoue A, Seidel MG, Wu W, et al. Slug, a highly conserved zinc finger transcriptional repressor, protects hematopoietic progenitor cells from radiation-induced apoptosis in vivo. Cancer Cell 2002;2:279-88.

125. Tarin D, Thompson EW, Newgreen DF. The fallacy of epithelial mesenchymal transition in neoplasia. Cancer Res 2005;65:5996-6000; discussion -1.

126. Hardy RG, Vicente-Duenas C, Gonzalez-Herrero I, et al. Snail family transcription factors are implicated in thyroid carcinogenesis. Am J Pathol 2007;171:1037-46.

127. Castro Alves C, Rosivatz E, Schott C, et al. Slug is overexpressed in gastric carcinomas and may act synergistically with SIP1 and Snail in the down-regulation of E-cadherin. J Pathol 2007;211:507-15.

128. Bolos V, Peinado H, Perez-Moreno MA, Fraga MF, Esteller M, Cano A. The transcription factor Slug represses E-cadherin expression and induces epithelial to mesenchymal transitions: a comparison with Snail and E47 repressors. J Cell Sci 2003;116:499-511.

129. Hajra KM, Chen DY, Fearon ER. The SLUG zinc-finger protein represses E-cadherin in breast cancer. Cancer Res 2002;62:1613-8.

130. Park SM, Gaur AB, Lengyel E, Peter ME. The miR-200 family determines the epithelial phenotype of cancer cells by targeting the E-cadherin repressors ZEB1 and ZEB2. Genes Dev 2008;22:894-907.

131. Mandal M, Myers JN, Lippman SM, et al. Epithelial to mesenchymal transition in head and neck squamous carcinoma: association of Src activation with E-cadherin down-regulation, vimentin expression, and aggressive tumor features. Cancer 2008;112(9):2088-100.

132. Trimboli AJ, Fukino K, de Bruin A, et al. Direct evidence for epithelial-mesenchymal transitions in breast cancer. Cancer Res 2008;68:937-45.

133. McCarthy A, Savage K, Gabriel A, Naceur C, Reis-Filho JS, Ashworth A. A mouse model of basal-like breast carcinoma with metaplastic elements. J Pathol 2007;211:389-98.

134. Liu X, Holstege H, van der Gulden H, et al. Somatic loss of BRCA1 and p53 in mice induces mammary tumors with features of human BRCA1-mutated basal-like breast cancer. Proc Natl Acad Sci USA 2007;104:12111-6.

135. Trelstad RL, Hay ED, Revel JD. Cell contact during early morphogenesis in the chick embryo. Dev Biol 1967;16:78-106.

136. Nath AK, Brown RM, Michaud M, Sierra-Honigmann MR, Snyder M, Madri JA. Leptin affects endocardial cushion formation by modulating EMT and migration via Akt signaling cascades. J Cell Biol 2008.

137. Nawshad A, Medici D, Liu CC, Hay ED. TGFbeta3 inhibits E-cadherin gene expression in palate medial-edge epithelial cells through a Smad2-Smad4-LEF1 transcription complex. J Cell Sci 2007;120:1646-53.

138. Ohta S, Suzuki K, Tachibana K, Tanaka H, Yamada G. Cessation of gastrulation is mediated by suppression of epithelial-mesenchymal transition at the ventral ectodermal ridge. Development 2007;134:4315-24.

139. Taneyhill LA, Coles EG, Bronner-Fraser M. Snail2 directly represses cadherin6B during epithelial-to-mesenchymal transitions of the neural crest. Development 2007;134:1481-90.

140. Shook D, Keller R. Mechanisms, mechanics and function of epithelial-mesenchymal transitions in early development. Mech Dev 2003;120:1351-83.

141. Komatsu Y, Scott G, Nagy A, Kaartinen V, Mishina Y. BMP type I receptor ALK2 is essential for proper patterning at late gastrulation during mouse embryogenesis. Dev Dyn 2007;236:512-7.

142. Liem KF, Jr., Tremml G, Roelink H, Jessell TM. Dorsal differentiation of neural plate cells induced by BMP-mediated signals from epidermal ectoderm. Cell 1995;82:969-79.

143. Ohta K, Lupo G, Kuriyama S, et al. Tsukushi functions as an organizer inducer by inhibition of BMP activity in cooperation with chordin. Dev Cell 2004;7:347-58.

144. Boyer AS, Erickson CP, Runyan RB. Epithelial-mesenchymal transformation in the embryonic heart is mediated through distinct pertussis toxin-sensitive and TGFbeta signal transduction mechanisms. Dev Dyn 1999;214:81-91.

145. Krishnan S, Deora AB, Annes JP, Osoria J, Rifkin DB, Hajjar KA. Annexin II-mediated plasmin generation activates TGF-beta3 during epithelial-mesenchymal transformation in the developing avian heart. Dev Biol 2004;265:140-54.

146. Liebner S, Cattelino A, Gallini R, et al. Beta-catenin is required for endothelial-mesenchymal transformation during heart cushion development in the mouse. J Cell Biol 2004;166:359-67.

147. Ma L, Lu MF, Schwartz RJ, Martin JF. Bmp2 is essential for cardiac cushion epithelial-mesenchymal transition and myocardial patterning. Development 2005;132:5601-11.

148. Romano LA, Runyan RB. Slug is an essential target of TGFbeta2 signaling in the developing chicken heart. Dev Biol 2000;223:91-102.

149. Timmerman LA, Grego-Bessa J, Raya A, et al. Notch promotes epithelial-mesenchymal transition during cardiac development and oncogenic transformation. Genes Dev 2004;18:99-115.

150. Kang P, Svoboda KK. Epithelial-mesenchymal transformation during craniofacial development. J Dent Res 2005;84:678-90.

151. Martinez-Alvarez C, Blanco MJ, Perez R, et al. Snail family members and cell survival in physiological and pathological cleft palates. Dev Biol 2004;265:207-18.

152. Nawshad A, Hay ED. TGFbeta3 signaling activates transcription of the LEF1 gene to induce epithelial mesenchymal transformation during mouse palate development. J Cell Biol 2003;163:1291-301.

153. Pungchanchaikul P, Gelbier M, Ferretti P, Bloch-Zupan A. Gene expression during palate fusion in vivo and in vitro. J Dent Res 2005;84:526-31.

154. Zohn IE, Li Y, Skolnik EY, Anderson KV, Han J, Niswander L. p38 and a p38-interacting protein are critical for downregulation of E-cadherin during mouse gastrulation. Cell 2006;125:957-69.

155. Gregory PA, Bert AG, Paterson EL, et al. The miR-200 family and miR-205 regulate epithelial to mesenchymal transition by targeting ZEB1 and SIP1. Nat Cell Biol 2008 ;10(5):593-601.

156. Korpal M, Lee ES, Hu G, Kang Y. The miR-200 family inhibits epithelial-mesenchymal transition and cancer cell migration by direct targeting of E-cadherin transcriptional repressors ZEB1 and ZEB2. J Biol Chem 2008 ;283(22):14910-4.

157. Choi J, Park SY, Joo CK. Transforming growth factor-beta1 represses E-cadherin production via slug expression in lens epithelial cells. Invest Ophthalmol Vis Sci 2007;48:2708-18.

158. Martinez-Estrada OM, Culleres A, Soriano FX, et al. The transcription factors Slug and Snail act as repressors of Claudin-1 expression in epithelial cells. Biochem J 2006;394:449-57.

159. Maeda M, Johnson KR, Wheelock MJ. Cadherin switching: essential for behavioral but not morphological changes during an epithelium-to-mesenchyme transition. J Cell Sci 2005;118:873-87.

160. Tomita K, van Bokhoven A, van Leenders GJ, et al. Cadherin switching in human prostate cancer progression. Cancer Res 2000;60:3650-4.

161. Yang J, Mani SA, Donaher JL, et al. Twist, a master regulator of morphogenesis, plays an essential role in tumor metastasis. Cell 2004;117:927-39.

162. Yang MH, Wu MZ, Chiou SH, et al. Direct regulation of TWIST by HIF-1alpha promotes metastasis. Nat Cell Biol 2008;10:295-305.

163. Duguay D, Foty RA, Steinberg MS. Cadherin-mediated cell adhesion and tissue segregation: qualitative and quantitative determinants. Dev Biol 2003;253:309-23.

164. Lee JM, Dedhar S, Kalluri R, Thompson EW. The epithelial-mesenchymal transition: new insights in signaling, development, and disease. J Cell Biol 2006;172:973-81.

165. Niu RF, Zhang L, Xi GM, et al. Up-regulation of Twist induces angiogenesis and correlates with metastasis in hepatocellular carcinoma. J Exp Clin Cancer Res 2007;26:385-94.

166. Come C, Magnino F, Bibeau F, et al. Snail and slug play distinct roles during breast carcinoma progression. Clin Cancer Res 2006;12:5395-402.

167. Comijn J, Berx G, Vermassen P, et al. The two-handed E box binding zinc finger protein SIP1 downregulates E-cadherin and induces invasion. Mol Cell 2001;7:1267-78.

168. Shih JY, Tsai MF, Chang TH, et al. Transcription repressor slug promotes carcinoma invasion and predicts outcome of patients with lung adenocarcinoma. Clin Cancer Res 2005;11:8070-8.

169. Shioiri M, Shida T, Koda K, et al. Slug expression is an independent prognostic parameter for poor survival in colorectal carcinoma patients. Br J Cancer 2006;94:1816-22.

170. Sivertsen S, Hadar R, Elloul S, et al. Expression of Snail, Slug and Sip1 in malignant mesothelioma effusions is associated with matrix metalloproteinase, but not with cadherin expression. Lung Cancer 2006;54:309-17.

171. Guarino M, Rubino B, Ballabio G. The role of epithelial-mesenchymal transition in cancer pathology. Pathology 2007;39:305-18.

172. Chaffer CL, Brennan JP, Slavin JL, Blick T, Thompson EW, Williams ED. Mesenchymal-to-epithelial transition facilitates bladder cancer metastasis: role of fibroblast growth factor receptor-2. Cancer Res 2006;66:11271-8.

173. Hugo H, Ackland ML, Blick T, et al. Epithelial--mesenchymal and mesenchymal--epithelial transitions in carcinoma progression. J Cell Physiol 2007;213:374-83.

174. Vincan E, Barker N. The upstream components of the Wnt signalling pathway in the dynamic EMT and MET associated with colorectal cancer progression. Clin Exp Metastasis 2008; Epub ahead of print. PMID: 18350253.

175. Zeng ZS, Weiser MR, Kuntz E, et al. c-Met gene amplification is associated with advanced stage colorectal cancer and liver metastases. Cancer Lett 2008; 265(2):258-69.

176. Yook JI, Li XY, Ota I, et al. A Wnt-Axin2-GSK3beta cascade regulates Snail1 activity in breast cancer cells. Nat Cell Biol 2006;8:1398-406.

177. Garriock RJ, Krieg PA. Wnt11-R signaling regulates a calcium sensitive EMT event essential for dorsal fin development of Xenopus. Dev Biol 2007;304:127-40.

178. Xian W, Schwertfeger KL, Rosen JM. Distinct roles of fibroblast growth factor receptor 1 and 2 in regulating cell survival and epithelial-mesenchymal transition. Mol Endocrinol 2007;21:987-1000.

179. Xian W, Schwertfeger KL, Vargo-Gogola T, Rosen JM. Pleiotropic effects of FGFR1 on cell proliferation, survival, and migration in a 3D mammary epithelial cell model. J Cell Biol 2005;171:663-73.

180. Lee JG, Kay EP. FGF-2-mediated signal transduction during endothelial mesenchymal transformation in corneal endothelial cells. Exp Eye Res 2006;83:1309-16.

181. Strutz F, Zeisberg M, Ziyadeh FN, et al. Role of basic fibroblast growth factor-2 in epithelial-mesenchymal transformation. Kidney Int 2002;61:1714-28.

182. Thuault S, Valcourt U, Petersen M, Manfioletti G, Heldin CH, Moustakas A. Transforming growth factor-beta employs HMGA2 to elicit epithelial-mesenchymal transition. J Cell Biol 2006;174:175-83.

183. Monzen K, Ito Y, Naito AT, et al. A crucial role of a high mobility group protein HMGA2 in cardiogenesis. Nat Cell Biol 2008;10(5):567-74.

184. Morita T, Mayanagi T, Sobue K. Dual roles of myocardin-related transcription factors in epithelial mesenchymal transition via slug induction and actin remodeling. J Cell Biol 2007;179:1027-42.

185. Shirakihara T, Saitoh M, Miyazono K. Differential regulation of epithelial and mesenchymal markers by deltaEF1 proteins in epithelial mesenchymal transition induced by TGF-beta. Mol Biol Cell 2007;18:3533-44.

186. Mani SA, Yang J, Brooks M, et al. Mesenchyme Forkhead 1 (FOXC2) plays a key role in metastasis and is associated with aggressive basal-like breast cancers. Proc Natl Acad Sci USA 2007;104:10069-74.

187. Alexander NR, Tran NL, Rekapally H, Summers CE, Glackin C, Heimark RL. N-cadherin gene expression in prostate carcinoma is modulated by integrin-dependent nuclear translocation of Twist1. Cancer Res 2006;66:3365-9.

188. Fujii S, Ochiai A. Enhancer of zeste homolog 2 downregulates E-cadherin by mediating histone H3 methylation in gastric cancer cells. Cancer Sci 2008;99:738-46.

189. Gray AM, Mason AJ. Requirement for activin A and transforming growth factor--beta 1 pro-regions in homodimer assembly. Science 1990;247:1328-30.

190. Yeo C, Whitman M. Nodal signals to Smads through Cripto-dependent and Cripto-independent mechanisms. Mol Cell 2001;7:949-57.

191. Harrington AE, Morris-Triggs SA, Ruotolo BT, Robinson CV, Ohnuma S, Hyvonen M. Structural basis for the inhibition of activin signalling by follistatin. EMBO J 2006;25:1035-45.

192. Annes JP, Munger JS, Rifkin DB. Making sense of latent TGFbeta activation. J Cell Sci 2003;116:217-24.

193. Ge G, Greenspan DS. BMP1 controls TGFbeta1 activation via cleavage of latent TGFbeta-binding protein. J Cell Biol 2006;175:111-20.

194. Dallas SL, Rosser JL, Mundy GR, Bonewald LF. Proteolysis of latent transforming growth factor-beta (TGF-beta)-binding protein-1 by osteoclasts. A cellular mechanism for release of TGF-beta from bone matrix. J Biol Chem 2002;277:21352-60.

195. Mu D, Cambier S, Fjellbirkeland L, et al. The integrin alpha(v)beta8 mediates epithelial homeostasis through MT1-MMP-dependent activation of TGF-beta1. J Cell Biol 2002;157:493-507.

196. Feng XH, Derynck R. Specificity and versatility in tgf-beta signaling through Smads. Annu Rev Cell Dev Biol 2005;21:659-93.

197. Shi Y, Massague J. Mechanisms of TGF-beta signaling from cell membrane to the nucleus. Cell 2003;113:685-700.

198. Allendorph GP, Vale WW, Choe S. Structure of the ternary signaling complex of a TGF-beta superfamily member. Proc Natl Acad Sci USA 2006;103:7643-8.

199. Feng XH, Lin X, Derynck R. Smad2, Smad3 and Smad4 cooperate with Sp1 to induce p15(Ink4B) transcription in response to TGF-beta. EMBO J 2000;19:5178-93.

200. Nagahara H, Ezhevsky SA, Vocero-Akbani AM, Kaldis P, Solomon MJ, Dowdy SF. Transforming growth factor beta targeted inactivation of cyclin E:cyclin-dependent kinase 2 (Cdk2) complexes by inhibition of Cdk2 activating kinase activity. Proc Natl Acad Sci USA 1999;96:14961-6.

201. Feng XH, Liang YY, Liang M, Zhai W, Lin X. Direct interaction of c-Myc with Smad2 and Smad3 to inhibit TGF-beta-mediated induction of the CDK inhibitor p15(Ink4B). Mol Cell 2002;9:133-43.

202. Gomis RR, Alarcon C, Nadal C, Van Poznak C, Massague J. C/EBPbeta at the core of the TGFbeta cytostatic response and its evasion in metastatic breast cancer cells. Cancer Cell 2006;10:203-14.

203. Yang J, Zhang W, Evans PM, Chen X, He X, Liu C. Adenomatous polyposis coli (APC) differentially regulates beta-catenin phosphorylation and ubiquitination in colon cancer cells. J Biol Chem 2006;281:17751-7.

204. Lee YN, Gao Y, Wang HY. Differential mediation of the Wnt canonical pathway by mammalian Dishevelleds-1, -2, and -3. Cell Signal 2008;20:443-52.

205. Yang L, Lin C, Liu ZR. P68 RNA helicase mediates PDGF-induced epithelial mesenchymal transition by displacing Axin from beta-catenin. Cell 2006;127:139-55.

206. Lu Z, Ghosh S, Wang Z, Hunter T. Downregulation of caveolin-1 function by EGF leads to the loss of E-cadherin, increased transcriptional activity of beta-catenin, and enhanced tumor cell invasion. Cancer Cell 2003;4:499-515.

207. Reichert M, Muller T, Hunziker W. The PDZ domains of zonula occludens-1 induce an epithelial to mesenchymal transition of Madin-Darby canine kidney I cells. Evidence for a role of beta-catenin/Tcf/Lef signaling. J Biol Chem 2000;275:9492-500.

208. Katoh M. Cross-talk of WNT and FGF signaling pathways at GSK3beta to regulate beta-catenin and SNAIL signaling cascades. Cancer Biol Ther 2006;5:1059-64.

209. Beiter K, Hiendlmeyer E, Brabletz T, et al. beta-Catenin regulates the expression of tenascin-C in human colorectal tumors. Oncogene 2005;24:8200-4.

210. Kim K, Lu Z, Hay ED. Direct evidence for a role of beta-catenin/LEF-1 signaling pathway in induction of EMT. Cell Biol Int 2002;26:463-76.

211. Dissanayake SK, Wade M, Johnson CE, et al. The Wnt5A/protein kinase C pathway mediates motility in melanoma cells via the inhibition of metastasis suppressors and initiation of an epithelial to mesenchymal transition. J Biol Chem 2007;282:17259-71.

212. Mikheev AM, Mikheeva SA, Maxwell JP, et al. Dickkopf-1 mediated tumor suppression in human breast carcinoma cells. Breast Cancer Res Treat 2007; Epub ahead of print. PMID: 18157634.

213. Palmer HG, Gonzalez-Sancho JM, Espada J, et al. Vitamin D(3) promotes the differentiation of colon carcinoma cells by the induction of E-cadherin and the inhibition of beta-catenin signaling. J Cell Biol 2001;154:369-87.

214. Pendas-Franco N, Garcia JM, Pena C, et al. DICKKOPF-4 is induced by TCF/beta-catenin and upregulated in human colon cancer, promotes tumour cell invasion and angiogenesis and is repressed by 1alpha,25-dihydroxyvitamin D(3). Oncogene 2008; Epub ahead of print. PMID: 18408752.

215. Katoh M. Networking of WNT, FGF, Notch, BMP, and Hedgehog signaling pathways during carcinogenesis. Stem Cell Rev 2007;3:30-8.

216. Nakamura T, Tsuchiya K, Watanabe M. Crosstalk between Wnt and Notch signaling in intestinal epithelial cell fate decision. J Gastroenterol 2007;42:705-10.

217. Wang T, Holt CM, Xu C, et al. Notch3 activation modulates cell growth behaviour and cross-talk to Wnt/TCF signalling pathway. Cell Signal 2007;19:2458-67.

218. Zavadil J, Cermak L, Soto-Nieves N, Bottinger EP. Integration of TGF-beta/Smad and Jagged1/Notch signalling in epithelial-to-mesenchymal transition. EMBO J 2004;23:1155-65.

219. Ehebauer M, Hayward P, Martinez-Arias A. Notch signaling pathway. Sci STKE 2006;2006:cm7.

220. Brou C, Logeat F, Gupta N, et al. A novel proteolytic cleavage involved in Notch signaling: the role of the disintegrin-metalloprotease TACE. Mol Cell 2000;5:207-16.

221. Mumm JS, Schroeter EH, Saxena MT, et al. A ligand-induced extracellular cleavage regulates gamma-secretase-like proteolytic activation of Notch1. Mol Cell 2000;5:197-206.

222. Lieber T, Kidd S, Young MW. kuzbanian-mediated cleavage of Drosophila Notch. Genes Dev 2002;16:209-21.

223. Fortini ME. Gamma-secretase-mediated proteolysis in cell-surface-receptor signalling. Nat Rev Mol Cell Biol 2002;3:673-84.

224. Kao HY, Ordentlich P, Koyano-Nakagawa N, et al. A histone deacetylase corepressor complex regulates the Notch signal transduction pathway. Genes Dev 1998;12:2269-77.

225. Oswald F, Kostezka U, Astrahantseff K, et al. SHARP is a novel component of the Notch/RBP-Jkappa signalling pathway. EMBO J 2002;21:5417-26.

226. Fortini ME, Artavanis-Tsakonas S. The suppressor of hairless protein participates in notch receptor signaling. Cell 1994;79:273-82.

227. Tamura K, Taniguchi Y, Minoguchi S, et al. Physical interaction between a novel domain of the receptor Notch and the transcription factor RBP-J kappa/Su(H). Curr Biol 1995;5:1416-23.

228. Wu L, Aster JC, Blacklow SC, Lake R, Artavanis-Tsakonas S, Griffin JD. MAML1, a human homologue of Drosophila mastermind, is a transcriptional co-activator for NOTCH receptors. Nat Genet 2000;26:484-9.

229. Kitagawa M, Oyama T, Kawashima T, et al. A human protein with sequence similarity to Drosophila mastermind coordinates the nuclear form of notch and a

CSL protein to build a transcriptional activator complex on target promoters. Mol Cell Biol 2001;21:4337-46.

230. Fryer CJ, Lamar E, Turbachova I, Kintner C, Jones KA. Mastermind mediates chromatin-specific transcription and turnover of the Notch enhancer complex. Genes Dev 2002;16:1397-411.

231. Sahlgren C, Gustafsson MV, Jin S, Poellinger L, Lendahl U. Notch signaling mediates hypoxia-induced tumor cell migration and invasion. Proc Natl Acad Sci USA 2008.

232. Leong KG, Niessen K, Kulic I, et al. Jagged1-mediated Notch activation induces epithelial-to-mesenchymal transition through Slug-induced repression of E-cadherin. J Exp Med 2007;204:2935-48.

233. Sun L, Diamond ME, Ottaviano AJ, Joseph MJ, Ananthanarayan V, Munshi HG. Transforming growth factor-beta 1 promotes matrix metalloproteinase-9-mediated oral cancer invasion through snail expression. Mol Cancer Res 2008;6:10-20.

234. Cano A, Perez-Moreno MA, Rodrigo I, et al. The transcription factor snail controls epithelial-mesenchymal transitions by repressing E-cadherin expression. Nat Cell Biol 2000;2:76-83.

235. Batlle E, Sancho E, Franci C, et al. The transcription factor snail is a repressor of E-cadherin gene expression in epithelial tumour cells. Nat Cell Biol 2000;2:84-9.

236. Guaita S, Puig I, Franci C, et al. Snail induction of epithelial to mesenchymal transition in tumor cells is accompanied by MUC1 repression and ZEB1 expression. J Biol Chem 2002;277:39209-16.

237. Ohkubo T, Ozawa M. The transcription factor Snail downregulates the tight junction components independently of E-cadherin downregulation. J Cell Sci 2004;117:1675-85.

238. Dhasarathy A, Kajita M, Wade PA. The transcription factor snail mediates epithelial to mesenchymal transitions by repression of estrogen receptor-alpha. Mol Endocrinol 2007;21:2907-18.

239. Peinado H, Ballestar E, Esteller M, Cano A. Snail mediates E-cadherin repression by the recruitment of the Sin3A/histone deacetylase 1 (HDAC1)/HDAC2 complex. Mol Cell Biol 2004;24:306-19.

240. Nagel AC, Wech I, Schwinkendorf D, Preiss A. Involvement of co-repressors Groucho and CtBP in the regulation of single-minded in Drosophila. Hereditas 2007;144:195-205.

241. Nibu Y, Zhang H, Levine M. Interaction of short-range repressors with Drosophila CtBP in the embryo. Science 1998;280:101-4.

242. Vega S, Morales AV, Ocana OH, Valdes F, Fabregat I, Nieto MA. Snail blocks the cell cycle and confers resistance to cell death. Genes Dev 2004;18:1131-43.

243. Hu CT, Wu JR, Chang TY, Cheng CC, Wu WS. The transcriptional factor Snail simultaneously triggers cell cycle arrest and migration of human hepatoma HepG2. J Biomed Sci 2008;15:343-55.

244. Park JH, Sung IJ, Lee SW, Kim KW, Kim YS, Yoo MA. The zinc-finger transcription factor Snail downregulates proliferating cell nuclear antigen expression in colorectal carcinoma cells. Int J Oncol 2005;26:1541-7.

245. Escriva M, Peiro S, Herranz N, et al. Repression of PTEN phosphatase by Snail1 transcriptional factor during gamma radiation-induced apoptosis. Mol Cell Biol 2008;28:1528-40.

246. Fujita N, Jaye DL, Kajita M, Geigerman C, Moreno CS, Wade PA. MTA3, a Mi-2/NuRD complex subunit, regulates an invasive growth pathway in breast cancer. Cell 2003;113:207-19.

247. Toyama T, Zhang Z, Iwase H, et al. Low expression of the snail gene is a good prognostic factor in node-negative invasive ductal carcinomas. Jpn J Clin Oncol 2006;36:357-63.

248. Martin TA, Goyal A, Watkins G, Jiang WG. Expression of the transcription factors snail, slug, and twist and their clinical significance in human breast cancer. Ann Surg Oncol 2005;12:488-96.

249. Miyoshi A, Kitajima Y, Kido S, et al. Snail accelerates cancer invasion by upregulating MMP expression and is associated with poor prognosis of hepatocellular carcinoma. Br J Cancer 2005;92:252-8.

250. Lee TK, Poon RT, Yuen AP, et al. Twist overexpression correlates with hepatocellular carcinoma metastasis through induction of epithelial-mesenchymal transition. Clin Cancer Res 2006;12:5369-76.

251. Vesuna F, van Diest P, Chen JH, Raman V. Twist is a transcriptional repressor of E-cadherin gene expression in breast cancer. Biochem Biophys Res Commun 2008;367:235-41.

252. Connerney J, Andreeva V, Leshem Y, Muentener C, Mercado MA, Spicer DB. Twist1 dimer selection regulates cranial suture patterning and fusion. Dev Dyn 2006;235:1345-57.

253. Shelton EL, Yutzey KE. Twist1 function in endocardial cushion cell proliferation, migration, and differentiation during heart valve development. Dev Biol 2008;317:282-95.

254. Laursen KB, Mielke E, Iannaccone P, Fuchtbauer EM. Mechanism of transcriptional activation by the proto-oncogene Twist1. J Biol Chem 2007;282:34623-33.

255. Cheng GZ, Zhang W, Wang LH. Regulation of cancer cell survival, migration, and invasion by Twist: AKT2 comes to interplay. Cancer Res 2008;68:957-60.

256. Vesuna F, Winnard P, Jr., Glackin C, Raman V. Twist overexpression promotes chromosomal instability in the breast cancer cell line MCF-7. Cancer Genet Cytogenet 2006;167:189-91.

257. Kwok WK, Ling MT, Yuen HF, Wong YC, Wang X. Role of p14ARF in TWIST-mediated senescence in prostate epithelial cells. Carcinogenesis 2007;28:2467-75.

258. Cheng GZ, Chan J, Wang Q, Zhang W, Sun CD, Wang LH. Twist transcriptionally up-regulates AKT2 in breast cancer cells leading to increased migration, invasion, and resistance to paclitaxel. Cancer Res 2007;67:1979-87.

259. Pham CG, Bubici C, Zazzeroni F, et al. Upregulation of Twist-1 by NF-kappaB blocks cytotoxicity induced by chemotherapeutic drugs. Mol Cell Biol 2007;27:3920-35.

260. Horikawa T, Yang J, Kondo S, et al. Twist and epithelial-mesenchymal transition are induced by the EBV oncoprotein latent membrane protein 1 and are associated with metastatic nasopharyngeal carcinoma. Cancer Res 2007;67:1970-8.

261. Yang AD, Camp ER, Fan F, et al. Vascular endothelial growth factor receptor-1 activation mediates epithelial to mesenchymal transition in human pancreatic carcinoma cells. Cancer Res 2006;66:46-51.

262. Gort EH, van Haaften G, Verlaan I, et al. The TWIST1 oncogene is a direct target of hypoxia-inducible factor-2alpha. Oncogene 2008;27:1501-10.

263. Shibata K, Kajiyama H, Ino K, et al. Twist expression in patients with cervical cancer is associated with poor disease outcome. Ann Oncol 2008;19:81-5.

264. Kajiyama H, Hosono S, Terauchi M, et al. Twist expression predicts poor clinical outcome of patients with clear cell carcinoma of the ovary. Oncology 2006;71:394-401.

265. Yuen HF, Chan YP, Wong ML, et al. Upregulation of Twist in oesophageal squamous cell carcinoma is associated with neoplastic transformation and distant metastasis. J Clin Pathol 2007;60:510-4.

266. Song LB, Liao WT, Mai HQ, et al. The clinical significance of twist expression in nasopharyngeal carcinoma. Cancer Lett 2006;242:258-65.

267. Hosono S, Kajiyama H, Terauchi M, et al. Expression of Twist increases the risk for recurrence and for poor survival in epithelial ovarian carcinoma patients. Br J Cancer 2007;96:314-20.

268. Savagner P, Yamada KM, Thiery JP. The zinc-finger protein slug causes desmosome dissociation, an initial and necessary step for growth factor-induced epithelial-mesenchymal transition. J Cell Biol 1997;137:1403-19.

269. Esufali S, Charames GS, Pethe VV, Buongiorno P, Bapat B. Activation of tumor-specific splice variant Rac1b by dishevelled promotes canonical Wnt signaling and decreased adhesion of colorectal cancer cells. Cancer Res 2007;67:2469-79.

270. Wang XY, Yin Y, Yuan H, Sakamaki T, Okano H, Glazer RI. Musashi1 modulates mammary progenitor cell expansion through proliferin-mediated activation of the Wnt and Notch pathways. Mol Cell Biol 2008.

271. Hilton MJ, Tu X, Wu X, et al. Notch signaling maintains bone marrow mesenchymal progenitors by suppressing osteoblast differentiation. Nat Med 2008;14:306-14.

272. Zhang C, Chang J, Sonoyama W, Shi S, Wang CY. Inhibition of human dental pulp stem cell differentiation by Notch signaling. J Dent Res 2008;87:250-5.

273. Fleming HE, Janzen V, Lo Celso C, et al. Wnt signaling in the niche enforces hematopoietic stem cell quiescence and is necessary to preserve self-renewal in vivo. Cell Stem Cell 2008;2:274-83.

274. Congdon KL, Voermans C, Ferguson EC, et al. Activation of Wnt Signaling in Hematopoietic Regeneration. Stem Cells 2008 ;26(5):1202-10.

275. Scheller EL, Chang J, Wang CY. Wnt/beta-catenin inhibits dental pulp stem cell differentiation. J Dent Res 2008;87:126-30.

276. Vallier L, Alexander M, Pedersen RA. Activin/Nodal and FGF pathways cooperate to maintain pluripotency of human embryonic stem cells. J Cell Sci 2005;118:4495-509.

277. Catalano A, Rodilossi S, Rippo MR, Caprari P, Procopio A. Induction of stem cell factor/c-Kit/slug signal transduction in multidrug-resistant malignant mesothelioma cells. J Biol Chem 2004;279:46706-14.

278. Wu WS, Heinrichs S, Xu D, et al. Slug antagonizes p53-mediated apoptosis of hematopoietic progenitors by repressing puma. Cell 2005;123:641-53.

279. Perez-Losada J, Sanchez-Martin M, Perez-Caro M, Perez-Mancera PA, Sanchez-Garcia I. The radioresistance biological function of the SCF/kit signaling pathway is mediated by the zinc-finger transcription factor Slug. Oncogene 2003;22:4205-11.

280. Perez-Losada J, Sanchez-Martin M, Rodriguez-Garcia A, et al. Zinc-finger transcription factor Slug contributes to the function of the stem cell factor c-kit signaling pathway. Blood 2002;100:1274-86.

281. Perez-Caro M, Bermejo-Rodriguez C, Gonzalez-Herrero I, Sanchez-Beato M, Piris MA, Sanchez-Garcia I. Transcriptomal profiling of the cellular response to DNA damage mediated by Slug (Snai2). Br J Cancer 2008;98:480-8.

282. Tripathi MK, Misra S, Khedkar SV, et al. Regulation of BRCA2 gene expression by the SLUG repressor protein in human breast cells. J Biol Chem 2005;280:17163-71.

283. Kajita M, McClinic KN, Wade PA. Aberrant expression of the transcription factors snail and slug alters the response to genotoxic stress. Mol Cell Biol 2004;24:7559-66.

284. Tripathi MK, Misra S, Chaudhuri G. Negative regulation of the expressions of cytokeratins 8 and 19 by SLUG repressor protein in human breast cells. Biochem Biophys Res Commun 2005;329:508-15.

285. Vannini I, Bonafe M, Tesei A, et al. Short interfering RNA directed against the SLUG gene increases cell death induction in human melanoma cell lines exposed to cisplatin and fotemustine. Cell Oncol 2007;29:279-87.

286. Katoh M. Comparative genomics on SNAI1, SNAI2, and SNAI3 orthologs. Oncol Rep 2005;14:1083-6.

287. Ayyanathan K, Peng H, Hou Z, et al. The Ajuba LIM domain protein is a corepressor for SNAG domain mediated repression and participates in nucleocytoplasmic Shuttling. Cancer Res 2007;67:9097-106.

288. Hou Z, Peng H, Ayyanathan K, et al. The LIM protein AJUBA recruits protein arginine methyltransferase 5 (PRMT5) to mediate SNAIL-dependent transcriptional repression. Mol Cell Biol 2008.

289. Langer EM, Feng Y, Zhaoyuan H, Rauscher FJ, 3rd, Kroll KL, Longmore GD. Ajuba LIM proteins are snail/slug corepressors required for neural crest development in Xenopus. Dev Cell 2008;14:424-36.

290. Zhao P, Iezzi S, Carver E, et al. Slug is a novel downstream target of MyoD. Temporal profiling in muscle regeneration. J Biol Chem 2002;277:30091-101.

291. Sakai D, Tanaka Y, Endo Y, Osumi N, Okamoto H, Wakamatsu Y. Regulation of Slug transcription in embryonic ectoderm by beta-catenin-Lef/Tcf and BMP-Smad signaling. Dev Growth Differ 2005;47:471-82.

292. Ikuta T, Kawajiri K. Zinc finger transcription factor Slug is a novel target gene of aryl hydrocarbon receptor. Exp Cell Res 2006;312:3585-94.

293. Inukai T, Inoue A, Kurosawa H, et al. SLUG, a ces-1-related zinc finger transcription factor gene with antiapoptotic activity, is a downstream target of the E2A-HLF oncoprotein. Mol Cell 1999;4:343-52.

294. Wu SY, Ferkowicz M, McClay DR. Ingression of primary mesenchyme cells of the sea urchin embryo: a precisely timed epithelial mesenchymal transition. Birth Defects Res C Embryo Today 2007;81:241-52.

295. Brunet LJ, McMahon JA, McMahon AP, Harland RM. Noggin, cartilage morphogenesis, and joint formation in the mammalian skeleton. Science 1998;280:1455-7.

296. Tylzanowski P, Mebis L, Luyten FP. The Noggin null mouse phenotype is strain dependent and haploinsufficiency leads to skeletal defects. Dev Dyn 2006;235:1599-607.

297. Choi M, Stottmann RW, Yang YP, Meyers EN, Klingensmith J. The bone morphogenetic protein antagonist noggin regulates mammalian cardiac morphogenesis. Circ Res 2007;100:220-8.

298. Rappolee DA, Iyer A, Patel Y. Hepatocyte growth factor and its receptor are expressed in cardiac myocytes during early cardiogenesis. Circ Res 1996;78:1028-36.

299. Koch U, Radtke F. Notch and cancer: a double-edged sword. Cell Mol Life Sci 2007;64:2746-62.

300. Bussink J, Kaanders JH, van der Kogel AJ. Tumor hypoxia at the micro-regional level: clinical relevance and predictive value of exogenous and endogenous hypoxic cell markers. Radiother Oncol 2003;67:3-15.

301. Li XF, O'Donoghue JA. Hypoxia in microscopic tumors. Cancer Lett 2008; 264(2):172-80.

302. Li XF, Carlin S, Urano M, Russell J, Ling CC, O'Donoghue JA. Visualization of hypoxia in microscopic tumors by immunofluorescent microscopy. Cancer Res 2007;67:7646-53.

303. Choi KS, Bae MK, Jeong JW, Moon HE, Kim KW. Hypoxia-induced angiogenesis during carcinogenesis. J Biochem Mol Biol 2003;36:120-7.

304. Holmquist-Mengelbier L, Fredlund E, Lofstedt T, et al. Recruitment of HIF-1alpha and HIF-2alpha to common target genes is differentially regulated in neuroblastoma: HIF-2alpha promotes an aggressive phenotype. Cancer Cell 2006;10:413-23.

305. Lester RD, Jo M, Montel V, Takimoto S, Gonias SL. uPAR induces epithelial-mesenchymal transition in hypoxic breast cancer cells. J Cell Biol 2007;178:425-36.

306. Higgins DF, Kimura K, Bernhardt WM, et al. Hypoxia promotes fibrogenesis in vivo via HIF-1 stimulation of epithelial-to-mesenchymal transition. J Clin Invest 2007;117:3810-20.

307. Higgins DF, Kimura K, Iwano M, Haase VH. Hypoxia-inducible factor signaling in the development of tissue fibrosis. Cell Cycle 2008;7(9):1128-32.

308. Perkins ND. Integrating cell-signalling pathways with NF-kappaB and IKK function. Nat Rev Mol Cell Biol 2007;8:49-62.

309. Julien S, Puig I, Caretti E, et al. Activation of NF-kappaB by Akt upregulates Snail expression and induces epithelium mesenchyme transition. Oncogene 2007;26:7445-56.

310. Chua HL, Bhat-Nakshatri P, Clare SE, Morimiya A, Badve S, Nakshatri H. NF-kappaB represses E-cadherin expression and enhances epithelial to mesenchymal transition of mammary epithelial cells: potential involvement of ZEB-1 and ZEB-2. Oncogene 2007;26:711-24.

311. Cummins EP, Comerford KM, Scholz C, Bruning U, Taylor CT. Hypoxic regulation of NF-kappaB signaling. Methods Enzymol 2007;435:479-92.

312. Shin SR, Sanchez-Velar N, Sherr DH, Sonenshein GE. 7,12-dimethylbenz(a)anthracene treatment of a c-rel mouse mammary tumor cell line induces epithelial to mesenchymal transition via activation of nuclear factor-kappaB. Cancer Res 2006;66:2570-5.

313. Kuphal S, Poser I, Jobin C, Hellerbrand C, Bosserhoff AK. Loss of E-cadherin leads to upregulation of NFkappaB activity in malignant melanoma. Oncogene 2004;23:8509-19.

314. Wang X, Sonenshein GE. Induction of the RelB NF-kappaB subunit by the cytomegalovirus IE1 protein is mediated via Jun kinase and c-Jun/Fra-2 AP-1 complexes. J Virol 2005;79:95-105.

315. Cao Y, Karin M. NF-kappaB in mammary gland development and breast cancer. J Mammary Gland Biol Neoplasia 2003;8:215-23.

316. Wang X, Belguise K, Kersual N, et al. Oestrogen signalling inhibits invasive phenotype by repressing RelB and its target BCL2. Nat Cell Biol 2007;9:470-8.

317. Gordon MD, Dionne MS, Schneider DS, Nusse R. WntD is a feedback inhibitor of Dorsal/NF-kappaB in Drosophila development and immunity. Nature 2005;437:746-9.

318. Gustafson B, Smith U. Cytokines promote Wnt signaling and inflammation and impair the normal differentiation and lipid accumulation in 3T3-L1 preadipocytes. J Biol Chem 2006;281:9507-16.

319. Katoh M. AP1- and NF-kappaB-binding sites conserved among mammalian WNT10B orthologs elucidate the TNFalpha-WNT10B signaling loop implicated in carcinogenesis and adipogenesis. Int J Mol Med 2007;19:699-703.

320. Fernandez L, Rodriguez S, Huang H, et al. Tumor necrosis factor-alpha and endothelial cells modulate Notch signaling in the bone marrow microenvironment during inflammation. Exp Hematol 2008;36:545-58.

321. Rius J, Guma M, Schachtrup C, et al. NF-kappaB links innate immunity to the hypoxic response through transcriptional regulation of HIF-1alpha. Nature 2008; 453(7196):807-11.

322. Grandbarbe L, Michelucci A, Heurtaux T, Hemmer K, Morga E, Heuschling P. Notch signaling modulates the activation of microglial cells. Glia 2007;55:1519-30.

323. Neil JR, Schiemann WP. Altered TAB1:I kappaB kinase interaction promotes transforming growth factor beta-mediated nuclear factor-kappaB activation during breast cancer progression. Cancer Res 2008;68:1462-70.

324. Scortegagna M, Cataisson C, Martin RJ, et al. HIF-1alpha regulates epithelial inflammation by cell autonomous NFkappaB activation and paracrine stromal remodeling. Blood 2008;111:3343-54.

325. Nishi K, Oda T, Takabuchi S, et al. LPS induces hypoxia-inducible factor 1 activation in macrophage-differentiated cells in a reactive oxygen species-dependent manner. Antioxid Redox Signal 2008;10:983-95.

326. Li F, Sonveaux P, Rabbani ZN, et al. Regulation of HIF-1alpha stability through S-nitrosylation. Mol Cell 2007;26:63-74.

327. Kasai Y, Stahl S, Crews S. Specification of the Drosophila CNS midline cell lineage: direct control of single-minded transcription by dorsal/ventral patterning genes. Gene Expr 1998;7:171-89.

328. Nambu JR, Lewis JO, Wharton KA, Jr., Crews ST. The Drosophila single-minded gene encodes a helix-loop-helix protein that acts as a master regulator of CNS midline development. Cell 1991;67:1157-67.

329. Metz RP, Kwak HI, Gustafson T, Laffin B, Porter WW. Differential transcriptional regulation by mouse single-minded 2s. J Biol Chem 2006;281:10839-48.

330. Woods SL, Whitelaw ML. Differential activities of murine single minded 1 (SIM1) and SIM2 on a hypoxic response element. Cross-talk between basic helix-

loop-helix/per-Arnt-Sim homology transcription factors. J Biol Chem 2002;277:10236-43.

331. Moffett P, Pelletier J. Different transcriptional properties of mSim-1 and mSim-2. FEBS Lett 2000;466:80-6.

332. Moffett P, Reece M, Pelletier J. The murine Sim-2 gene product inhibits transcription by active repression and functional interference. Mol Cell Biol 1997;17:4933-47.

333. Dahmane N, Charron G, Lopes C, et al. Down syndrome-critical region contains a gene homologous to Drosophila sim expressed during rat and human central nervous system development. Proc Natl Acad Sci USA 1995;92:9191-5.

334. Probst MR, Fan CM, Tessier-Lavigne M, Hankinson O. Two murine homologs of the Drosophila single-minded protein that interact with the mouse aryl hydrocarbon receptor nuclear translocator protein. J Biol Chem 1997;272:4451-7.

335. Sonnenfeld M, Ward M, Nystrom G, Mosher J, Stahl S, Crews S. The Drosophila tango gene encodes a bHLH-PAS protein that is orthologous to mammalian Arnt and controls CNS midline and tracheal development. Development 1997;124:4571-82.

336. Kwak HI, Gustafson T, Metz RP, Laffin B, Schedin P, Porter WW. Inhibition of breast cancer growth and invasion by single-minded 2s. Carcinogenesis 2007;28:259-66.

337. Goshu E, Jin H, Fasnacht R, Sepenski M, Michaud JL, Fan CM. Sim2 mutants have developmental defects not overlapping with those of Sim1 mutants. Mol Cell Biol 2002;22:4147-57.

338. Shamblott MJ, Bugg EM, Lawler AM, Gearhart JD. Craniofacial abnormalities resulting from targeted disruption of the murine Sim2 gene. Dev Dyn 2002;224:373-80.

339. Blavier L, Lazaryev A, Groffen J, Heisterkamp N, DeClerck YA, Kaartinen V. TGF-beta3-induced palatogenesis requires matrix metalloproteinases. Mol Biol Cell 2001;12:1457-66.

340. Brown NL, Yarram SJ, Mansell JP, Sandy JR. Matrix metalloproteinases have a role in palatogenesis. J Dent Res 2002;81:826-30.

341. Letra A, Silva RA, Menezes R, et al. MMP gene polymorphisms as contributors for cleft lip/palate: association with MMP3 but not MMP1. Arch Oral Biol 2007;52:954-60.

342. Morris-Wiman J, Du Y, Brinkley L. Occurrence and temporal variation in matrix metalloproteinases and their inhibitors during murine secondary palatal morphogenesis. J Craniofac Genet Dev Biol 1999;19:201-12.

343. Satge D, Sasco AJ, Chompret A, et al. A 22-year French experience with solid tumors in children with Down syndrome. Pediatr Hematol Oncol 2003;20:517-29.

344. Satge D, Sasco AJ, Pujol H, Rethore MO. [Breast cancer in women with trisomy 21]. Bull Acad Natl Med 2001;185:1239-52; discussion 52-4.

345. Satge D, Sommelet D, Geneix A, Nishi M, Malet P, Vekemans M. A tumor profile in Down syndrome. Am J Med Genet 1998;78:207-16.

346. Sullivan SG, Hussain R, Glasson EJ, Bittles AH. The profile and incidence of cancer in Down syndrome. J Intellect Disabil Res 2007;51:228-31.

347. Hasle H. Pattern of malignant disorders in individuals with Down's syndrome. Lancet Oncol 2001;2:429-36.

348. Hasle H, Clemmensen IH, Mikkelsen M. [Incidence of cancer in individuals with Down syndrome]. Tidsskr Nor Laegeforen 2000;120:2878-81.

349. Hasle H, Clemmensen IH, Mikkelsen M. [Occurrence of cancer in individuals with Down syndrome]. Ugeskr Laeger 2000;162:4535-9.

350. Hasle H, Clemmensen IH, Mikkelsen M. Risks of leukaemia and solid tumours in individuals with Down's syndrome. Lancet 2000;355:165-9.

351. Sussan TE, Yang A, Li F, Ostrowski MC, Reeves RH. Trisomy represses Apc(Min)-mediated tumours in mouse models of Down's syndrome. Nature 2008;451:73-5.

352. Swanton C, Downward J. Unraveling the complexity of endocrine resistance in breast cancer by functional genomics. Cancer Cell 2008;13:83-5.

353. Sapi E, Flick MB, Rodov S, Kacinski BM. Ets-2 transdominant mutant abolishes anchorage-independent growth and macrophage colony-stimulating factor-stimulated invasion by BT20 breast carcinoma cells. Cancer Res 1998;58:1027-33.

354. Buggy Y, Maguire TM, McDermott E, Hill AD, O'Higgins N, Duffy MJ. Ets2 transcription factor in normal and neoplastic human breast tissue. Eur J Cancer 2006;42:485-91.

355. Baker KM, Wei G, Schaffner AE, Ostrowski MC. Ets-2 and components of mammalian SWI/SNF form a repressor complex that negatively regulates the BRCA1 promoter. J Biol Chem 2003;278:17876-84.

356. Halvorsen OJ, Rostad K, Oyan AM, et al. Increased expression of SIM2-s protein is a novel marker of aggressive prostate cancer. Clin Cancer Res 2007;13:892-7.

357. Aleman MJ, DeYoung MP, Tress M, Keating P, Perry GW, Narayanan R. Inhibition of Single Minded 2 gene expression mediates tumor-selective apoptosis and differentiation in human colon cancer cells. Proc Natl Acad Sci USA 2005;102:12765-70.

358. DeYoung MP, Tress M, Narayanan R. Down's syndrome-associated Single Minded 2 gene as a pancreatic cancer drug therapy target. Cancer Lett 2003;200:25-31.

359. DeYoung MP, Tress M, Narayanan R. Identification of Down's syndrome critical locus gene SIM2-s as a drug therapy target for solid tumors. Proc Natl Acad Sci USA 2003;100:4760-5.

360. Young AP, Schlisio S, Minamishima YA, et al. VHL loss actuates a HIF-independent senescence programme mediated by Rb and p400. Nat Cell Biol 2008;10:361-9.

361. Nakopoulou L, Mylona E, Papadaki I, et al. Study of phospho-beta-catenin subcellular distribution in invasive breast carcinomas in relation to their phenotype and the clinical outcome. Mod Pathol 2006;19:556-63.

362. Kwak HI, Gustafson T, Metz RP, Laffin B, Schedin P, Porter WW. Inhibition of breast cancer growth and invasion by single-minded 2s. Carcinogenesis 2007; 28(2):259-66.

363. Radisky DC, Levy DD, Littlepage LE, et al. Rac1b and reactive oxygen species mediate MMP-3-induced EMT and genomic instability. Nature 2005;436:123-7.

364. De Craene B, van Roy F, Berx G. Unraveling signalling cascades for the Snail family of transcription factors. Cell Signal 2005;17:535-47.

365. Peinado H, Olmeda D, Cano A. Snail, Zeb and bHLH factors in tumour progression: an alliance against the epithelial phenotype? Nat Rev Cancer 2007;7:415-28.

366. Peinado H, Marin F, Cubillo E, et al. Snail and E47 repressors of E-cadherin induce distinct invasive and angiogenic properties in vivo. J Cell Sci 2004;117:2827-39.

367. Cote M, Miller AD, Liu SL. Human RON receptor tyrosine kinase induces complete epithelial-to-mesenchymal transition but causes cellular senescence. Biochem Biophys Res Commun 2007;360:219-25.

368. Niimi H, Pardali K, Vanlandewijck M, Heldin CH, Moustakas A. Notch signaling is necessary for epithelial growth arrest by TGF-beta. J Cell Biol 2007;176:695-707.

369. Debnath J, Brugge JS. Modelling glandular epithelial cancers in three-dimensional cultures. Nat Rev Cancer 2005;5:675-88.

370. Debnath J, Muthuswamy SK, Brugge JS. Morphogenesis and oncogenesis of MCF-10A mammary epithelial acini grown in three-dimensional basement membrane cultures. Methods 2003;30:256-68.

371. Debnath J, Mills KR, Collins NL, Reginato MJ, Muthuswamy SK, Brugge JS. The role of apoptosis in creating and maintaining luminal space within normal and oncogene-expressing mammary acini. Cell 2002;111:29-40.

372. Reginato MJ, Mills KR, Paulus JK, et al. Integrins and EGFR coordinately regulate the pro-apoptotic protein Bim to prevent anoikis. Nat Cell Biol 2003;5:733-40.

373. Mailleux AA, Overholtzer M, Brugge JS. Lumen formation during mammary epithelial morphogenesis: insights from in vitro and in vivo models. Cell Cycle 2008;7:57-62.

374. Shackleton M, Vaillant F, Simpson KJ, et al. Generation of a functional mammary gland from a single stem cell. Nature 2006;439:84-8.

375. Fillmore CM, Kuperwasser C. Human breast cancer cell lines contain stem-like cells that self-renew, give rise to phenotypically diverse progeny and survive chemotherapy. Breast Cancer Res 2008;10:R25.

376. Yong Yi S, Jun Nan K. Tumor-initiating stem cells in liver cancer. Cancer Biol Ther 2008;7 Epub ahead of print. PMID: 18285703.

377. Wright MH, Calcagno AM, Salcido CD, Carlson MD, Ambudkar SV, Varticovski L. Brca1 breast tumors contain distinct CD44+/CD24- and CD133+ cells with cancer stem cell characteristics. Breast Cancer Res 2008;10:R10.

378. Cho RW, Wang X, Diehn M, et al. Isolation and molecular characterization of cancer stem cells in MMTV-Wnt-1 murine breast tumors. Stem Cells 2008;26:364-71.

379. Kim CF, Jackson EL, Woolfenden AE, et al. Identification of bronchioalveolar stem cells in normal lung and lung cancer. Cell 2005;121:823-35.

380. Rukstalis JM, Habener JF. Snail2, a mediator of epithelial-mesenchymal transitions, expressed in progenitor cells of the developing endocrine pancreas. Gene Expr Patterns 2007;7:471-9.

381. Phillips TM, McBride WH, Pajonk F. The response of CD24(-/low)/CD44+ breast cancer-initiating cells to radiation. J Natl Cancer Inst 2006;98:1777-85.

382. Woodward WA, Chen MS, Behbod F, Alfaro MP, Buchholz TA, Rosen JM. WNT/beta-catenin mediates radiation resistance of mouse mammary progenitor cells. Proc Natl Acad Sci USA 2007;104:618-23.

383. Scharenberg CW, Harkey MA, Torok-Storb B. The ABCG2 transporter is an efficient Hoechst 33342 efflux pump and is preferentially expressed by immature human hematopoietic progenitors. Blood 2002;99:507-12.

384. Troester MA, Herschkowitz JI, Oh DS, et al. Gene expression patterns associated with p53 status in breast cancer. BMC Cancer 2006;6:276.

385. Okui M, Yamaki A, Takayanagi A, Kudoh J, Shimizu N, Shimizu Y. Transcription factor single-minded 2 (SIM2) is ubiquitinated by the RING-IBR-RING-type E3 ubiquitin ligases. Exp Cell Res 2005;309:220-8.

386. Beasley SA, Hristova VA, Shaw GS. Structure of the Parkin in-between-ring domain provides insights for E3-ligase dysfunction in autosomal recessive Parkinson's disease. Proc Natl Acad Sci USA 2007;104:3095-100.

387. Schmid T, Zhou J, Brune B. HIF-1 and p53: communication of transcription factors under hypoxia. J Cell Mol Med 2004;8:423-31.

388. Zhang HG, Wang J, Yang X, Hsu HC, Mountz JD. Regulation of apoptosis proteins in cancer cells by ubiquitin. Oncogene 2004;23:2009-15.

389. Brooks CL, Gu W. Ubiquitination, phosphorylation and acetylation: the molecular basis for p53 regulation. Curr Opin Cell Biol 2003;15:164-71.

390. Corn PG, McDonald ER, 3rd, Herman JG, El-Deiry WS. Tat-binding protein-1, a component of the 26S proteasome, contributes to the E3 ubiquitin ligase function of the von Hippel-Lindau protein. Nat Genet 2003;35:229-37.

391. Kapitsinou PP, Haase VH. The VHL tumor suppressor and HIF: insights from genetic studies in mice. Cell Death Differ 2008;15:650-9.

392. Baum B, Settleman J, Quinlan MP. Transitions between epithelial and mesenchymal states in development and disease. Semin Cell Dev Biol 2008;19:294-308.

393. Hay ED, Zuk A. Transformations between epithelium and mesenchyme: normal, pathological, and experimentally induced. Am J Kidney Dis 1995;26:678-90.

394. Perigny M, Bairati I, Harvey I, et al. Role of immunohistochemical overexpression of matrix metalloproteinases MMP-2 and MMP-11 in the prognosis of death by ovarian cancer. Am J Clin Pathol 2008;129:226-31.

395. Jinga DC, Blidaru A, Condrea I, et al. MMP-9 and MMP-2 gelatinases and TIMP-1 and TIMP-2 inhibitors in breast cancer: correlations with prognostic factors. J Cell Mol Med 2006;10:499-510.

396. Tetu B, Brisson J, Wang CS, et al. The influence of MMP-14, TIMP-2 and MMP-2 expression on breast cancer prognosis. Breast Cancer Res 2006;8:R28.

397. Talvensaari-Mattila A, Paakko P, Turpeenniemi-Hujanen T. Matrix metalloproteinase-2 (MMP-2) is associated with survival in breast carcinoma. Br J Cancer 2003;89:1270-5.

398. Blons H, Gad S, Zinzindohoue F, et al. Matrix metalloproteinase 3 polymorphism: a predictive factor of response to neoadjuvant chemotherapy in head and neck squamous cell carcinoma. Clin Cancer Res 2004;10:2594-9.

399. Lievre A, Milet J, Carayol J, et al. Genetic polymorphisms of MMP1, MMP3 and MMP7 gene promoter and risk of colorectal adenoma. BMC Cancer 2006;6:270.

400. Leinonen T, Pirinen R, Bohm J, Johansson R, Kosma VM. Increased expression of matrix metalloproteinase-2 (MMP-2) predicts tumour recurrence and unfavourable outcome in non-small cell lung cancer. Histol Histopathol 2008;23:693-700.

401. Dean RA, Butler GS, Hamma-Kourbali Y, et al. Identification of candidate angiogenic inhibitors processed by matrix metalloproteinase 2 (MMP-2) in cell-based proteomic screens: disruption of vascular endothelial growth factor (VEGF)/heparin affin regulatory peptide (pleiotrophin) and VEGF/Connective tissue growth factor angiogenic inhibitory complexes by MMP-2 proteolysis. Mol Cell Biol 2007;27:8454-65.

402. Li HC, Cao DC, Liu Y, et al. Prognostic value of matrix metalloproteinases (MMP-2 and MMP-9) in patients with lymph node-negative breast carcinoma. Breast Cancer Res Treat 2004;88:75-85.

403. Mendes O, Kim HT, Lungu G, Stoica G. MMP2 role in breast cancer brain metastasis development and its regulation by TIMP2 and ERK1/2. Clin Exp Metastasis 2007;24:341-51.

404. Han YP, Tuan TL, Wu H, Hughes M, Garner WL. TNF-alpha stimulates activation of pro-MMP2 in human skin through NF-(kappa)B mediated induction of MT1-MMP. J Cell Sci 2001;114:131-9.

405. Kheradmand F, Rishi K, Werb Z. Signaling through the EGF receptor controls lung morphogenesis in part by regulating MT1-MMP-mediated activation of gelatinase A/MMP2. J Cell Sci 2002;115:839-48.

406. Wong RP, Tsang WP, Chau PY, Co NN, Tsang TY, Kwok TT. p53-R273H gains new function in induction of drug resistance through down-regulation of procaspase-3. Mol Cancer Ther 2007;6:1054-61.

407. Corn PG, El-Deiry WS. Microarray analysis of p53-dependent gene expression in response to hypoxia and DNA damage. Cancer Biol Ther 2007;6:1858-66.

408. Eaton JL, Glasgow E. The zebrafish bHLH PAS transcriptional regulator, single-minded 1 (sim1), is required for isotocin cell development. Dev Dyn 2006;235:2071-82.

409. Goshu E, Jin H, Lovejoy J, Marion JF, Michaud JL, Fan CM. Sim2 contributes to neuroendocrine hormone gene expression in the anterior hypothalamus. Mol Endocrinol 2004;18:1251-62.

410. Nambu JR, Franks RG, Hu S, Crews ST. The single-minded gene of Drosophila is required for the expression of genes important for the development of CNS midline cells. Cell 1990;63:63-75.

411. Murray SA, Oram KF, Gridley T. Multiple functions of Snail family genes during palate development in mice. Development 2007;134:1789-97.

VITA

Name: Brian Laffin

Address: Texas A&M College of Veterinary Medicine, VMA Bldg Rm 107, College Station, TX 77843-4458

Email Address: blaffin@cvm.tamu.edu

Education: B.S., Biochemistry, Texas A&M University, 2001
Ph.D., Toxicology, Texas A&M University, 2008

Honors:

Fall '05	TAMU Academic Excellence Award
Spring '06	1st place, oral presentation, Texas A&M University Faculty of Toxicology Research Symposium
Spring '06	1st place, oral presentation, Texas A&M University Student Research Week
Fall '06	Charles J. Koerth Memorial Scholarship
Spring '07	1st place, poster presentation, Gordon Research Conference on Mammary Gland Biology, Salve Regina University, RI,

Publications:

Laffin B, Wellberg E, Kwak HI, Burghardt RC, Metz RP, Gustafson T, Schedin P, Porter WW. Loss of singleminded-2s in the mouse mammary gland induces an epithelial-mesenchymal transition associated with up-regulation of slug and matrix metalloprotease 2. Mol Cell Biol. 2008 Mar;28(6):1936-46.

Kwak, H.I., Gustafson, T., Metz, R.P., Laffin, B., Schedin, P., and Porter, W.W. Inhibition of breast cancer growth and invasion by single-minded 2s. Carcinogenesis 2007; *28*: 259-266.

Metz, R.P., Kwak, H., Gustafson, T., Laffin, B., and Porter, W.W. Differential transcriptional regulation by mouse single-minded 2s. J Biol Chem 2006;*281*: 10839-10848.

Metz RP, Qu X, Laffin B, Earnest D, and Porter WW. Circadian Clock and Cell Cycle Gene Expression In Mouse Mammary Epithelial Cells and in the Developing Mouse Mammary Gland. Dev Dyn. 2006 Jan;235(1):263-71.